

THE EFFECT OF SHOT PEENING
ON THE INITIATION OF FATIGUE
CRACKS BY FRETTING.

G. Leadbeater B.Sc. (Honours)

Thesis submitted to the University of Nottingham
for the Degree of Doctor of Philosophy.

May 1983



BEST COPY AVAILABLE.

VARIABLE PRINT QUALITY

TEXT CUT OFF IN THE
ORIGINAL

CONTENTS.

Page

Abstract.

<u>Chapter One - Introduction</u>	1
1.1 Fretting and Fretting Fatigue.	1
1.2 Shot Peening.	2
1.3 Al-Cu-Mg Alloys.	3
<u>Chapter Two - Literature Review</u>	5
2.1 Fretting - A Brief History.	5
2.2 Effect of Variable Factors on Fretting.	12
2.2.1 Environment.	13
2.2.2 Temperature.	14
2.2.3 Relative Slip Amplitude.	15
2.2.4 Cyclic Frequency.	16
2.2.5 Contact Pressure.	16
2.2.6 Mechanical State of Contacting Surfaces.	17
2.2.7 Surface Finish.	18
2.3 Fretting Fatigue - A Brief History.	18
2.4 Effect of Variable Factors on Fretting Fatigue.	23
2.4.1 Environment.	23
2.4.2 Temperature.	25
2.4.3 Relative Amplitude and Direction of Slip.	26
2.4.4 Cyclic Frequency.	27
2.4.5 Contact Pressure.	28
2.4.6 Mechanical State of Contacting Surfaces.	28

2.4.7 Surface Finish.	31
2.5 Prevention of Fretting and Fretting Fatigue.	31
2.5.1 Design.	31
2.5.2 Lubrication.	32
2.5.3 Sacrificial Inserts.	32
2.5.4 Surface Coatings.	33
2.5.5 Mechanical Surface Treatments.	34

Chapter Three - Shot Peening 35

3.1 Characteristics of Shot Peening.	35
3.1.1 Types of Equipment and Shot Materials.	35
3.1.2 Shot Peening Control and Measurement.	36
3.1.3 Shot Peening Specifications.	37
3.2 Effect of Shot Peening on Fatigue, Fretting Fatigue, and Fretting.	39
3.2.1 Plain Fatigue.	39
3.2.2 Relaxation of Residual Stress due to Fatigue.	43
3.2.3 Fretting and Fretting Fatigue.	44

Chapter Four - Experimental Procedure 47

4.1 Materials and Treatments.	47
4.1.1 Heat Treatment.	47
4.1.2 Surface Treatment.	47
4.2 Plain Fatigue and Fretting Fatigue Tests.	48
4.2.1 Specimens.	48
4.2.2 Testing Equipment.	49
4.2.3 Testing Procedure.	50
4.3 Plain Fretting Tests.	51

4.3.1	Specimens.	51
4.3.2	Equipment.	52
	(i) The Oscillating Movement System.	52
	(ii) The Oscillating Control System.	53
	(iii) Friction and Normal Contact Force Measurement.	54
4.3.3	Calibration of Equipment.	54
4.3.4	Test Procedure.	54
4.4	Surface Analysis.	55
4.4.1	Residual Stress Analysis by X-Rays.	55
	4.4.1.1 Summary of Method.	55
	4.4.1.2 Equipment.	57
	4.4.1.3 Specimen Preparation.	57
	4.4.1.4 Test Procedure.	58
4.4.2	Work Hardening Analysis.	59
	4.4.2.1 Microhardness Traverses.	59
	4.4.2.2 Testing of 'Stretched' Specimens.	60
4.4.3	Surface Roughness Analysis.	60
	4.4.3.1 Talysurf Traces.	60
	4.4.3.2 Microscopy.	61
4.5	Post Testing Analysis.	61
	4.5.1 X-Ray Residual Stress Analysis.	61
	4.5.2 Optical Microscopy.	62
	4.5.3 S.E.M. Analysis.	62
	4.5.4 Talysurf Traces.	63
4.6	Summary of Experimental Procedure.	63
 <u>Chapter Five - Results</u>		 64
5.1	Plain Fatigue and Fretting Fatigue Results.	64

5.2 Plain Fretting Test Results.	64
5.3 Surface Analysis.	65
5.3.1 Residual Stress Analysis by X-Rays.	65
5.3.2 Work Hardening Analysis.	66
5.3.2.1 Microhardness Traverses.	66
5.3.2.2 Testing of 'Stretched' Specimens.	66
5.3.3 Surface Roughness Analysis.	67
5.3.3.1 Talysurf Traces.	67
5.3.3.2 Microscopy.	68
5.4 Post Testing Analysis.	68
5.4.1 Residual Stress Analysis by X-Rays.	68
5.4.2 Optical Microscopy.	69
5.4.3 S.E.M. Analysis.	70
5.4.4 Talysurf Traces.	74
<u>Chapter Six - Discussion</u>	75
6.1 Effect of Fretting on Fatigue.	75
6.2 Effect of Shot Peening.	75
(i) On Material Surface.	75
(ii) On Fatigue Strengths.	77
6.3 Residual Stress Stability.	79
6.4 Crack Morphology.	81
6.5 Fretting Damage.	83
6.6 Conclusion and Future Work.	85
Acknowledgements.	88
References.	89
Appendices.	101
FIGURES, TABLES AND PLATES.	

ABSTRACT

Plain fatigue and fretting fatigue studies have been carried out on an Al - 4% Cu - 1% Mg alloy in various heat treated conditions. It has been determined that shot peening the surface results in substantial improvements in plain fatigue and fretting fatigue strengths. The major cause of the improvement of these properties is the presence of compressive stresses that are induced in the surface by the shot peening process. Surface roughening and work hardening of the surface are also caused by the shot peening process but these have little or no effect on the fretting fatigue properties.

The magnitude of the compressive stresses at the peened surface are around 200 - 250MPa and these result in the nucleation of subsurface cracks that run parallel to the surface during the fretting process. Debris with a characteristic spherical shape is produced on the faces of the subsurface cracks. Subsequent delamination allows the spherical debris to reach the specimen surface causing a reduction in the friction between the fretting members.

C H A P T E R O N E

INTRODUCTION

The thesis is concerned with the fretting fatigue behaviour of shot peened age-hardening Al - Cu - Mg alloys. This chapter defines the three areas of fretting fatigue, shot peening and age-hardenable Al - Cu - Mg alloys.

1.1 Fretting and Fretting Fatigue.

Fretting is defined as the relative oscillatory tangential movement between two contacting surfaces. This movement is termed 'slip'. If damage is caused to the surfaces and debris produced, this phenomenon is sometimes described as 'fretting corrosion'.

It is often necessary to clarify the difference between fretting and wear, in which the relative movement involved is in one direction and over a greater distance. In fretting the amplitude of slip is commonly between $25\mu\text{m}$ and $70\mu\text{m}$ but may be even less. During the wear process, any debris formed can escape from the contacting surfaces, but during fretting the debris is, for the most part, entrapped and thus can contribute to further damage.

The main significance of fretting as an engineering problem is it's association with fatigue. Fretting can be produced under the same conditions that cause fatigue i.e. cyclic stressing, thus it can be said that in these situations, the cyclic strain resulting from fatigue produces fretting. The synergistic effect of fretting and fatigue is known as 'fretting fatigue'.

The endurance of materials and components in fretting fatigue

is substantially lower than in plain fatigue, this being due to the early initiation of the fatigue cracks from the fretted areas. The occurrence of fretting alone can lead to loss of fit between components, poor lubrication due to the debris formation, and even seizure. The occurrence of fretting fatigue will probably lead to the early catastrophic failure of one of the components.

1.2 Shot Peening.

Shot peening is a cold working process used primarily to reduce failure of machine and structural parts by fatigue. It is also effective for improving impact strength and resistance to stress corrosion cracking.

The process is one of bombarding the component with relatively hard particles, or 'shot', which induce a work hardened, compressively stressed layer in the surface. The modern day process is conducted in special machines under fully-controlled conditions. However, Baldauf (1) shows that shot peening is an ancient art. He quotes the story of Damascus and his famous singing swords that would not break, due probably to the fact that the blades were 'shot peened' with ball peen hammers to make them tougher before battle. History also shows that the early makers of body armour found that they could improve the quality of their product by cold working. The process, however, was somewhat different from today; that is the armour makers would have their serfs fill the inside of the armour with round stones, and roll them around the courtyard for days or even weeks!

The modern version of shot peening was 'discovered' during the 1930's, when it was found that components exhibited an improved fatigue life after shot blast cleaning. The main investigators were

J.O. Almen and J. Straub, and they first applied the shot peening process commercially in the early days of World War II. It had been found that tank tread pins were breaking too easily and hence the treads were failing. Shot peening was applied to the problem and eventually cured the trouble, resulting in time and money being saved. It also proved that shot peening was a very worthwhile process.

During the 1940's the shot peening process was examined in great detail. It was determined what exactly happened to the material during peening, why the process worked, how to perform it efficiently and how to monitor it. These aspects will be discussed in the proceeding chapters.

1.3 Aluminium - Copper Alloys.

Aluminium - Copper alloys are heat treatable alloys which are very widely used in the aerospace industry. These alloys are more expensive than the work-hardenable alloys such as Al - Mn and Al - Mg alloys, due to the additional costs of heat-treatment, higher in-plant scrap generation and lower volume. However the savings in weight of the final product, made possible by the higher strength, far outweigh these higher costs.

The three most widely used wrought aluminium-copper alloys are (using The Aluminium Association designation system):- Alloy 2017, commonly called duralumin, containing 4 per cent copper, and widely used for rivets in aircraft construction; Alloy 2014, having a higher percentage (4.4) of copper and other alloying elements, principally 0.2 - 0.8% Mg, 0.5 - 0.9% Si. This alloy is used for heavy-duty forgings, aircraft fittings and truck frames; and Alloy 2024, containing 4.5 percent copper, 1.5 percent magnesium and 0.5 percent silicon, used

in aircraft structures, rivets, hardware, truck wheels and screw-machine products.

In the present work the alloy that has been used is from the 2014 specification from hereon termed 'Al -4% Cu - 1% Mg.

CHAPTER TWO

FRETTING AND FRETTING FATIGUE

2.1

Fretting - A Brief History.

The first reference to fretting in scientific history was made in 1911 in a paper by Eden, Rose and Cunningham (2). While performing some standard fatigue tests on steel specimens using a Wöhler machine, they often experienced great difficulty in removing the broken specimen from its holder. Considerable quantities of 'red dust' were observed especially after heavily loaded long term tests. They believed that this 'corrosion' was due to the varying stresses between the specimen and its holder. To investigate further they set up lubricated specimens and found that a similar phenomenon occurred with these, so showing that the 'corrosion' was not due solely to the presence of moisture.

It wasn't until sixteen years later that Tomlinson et al (3,4) performed the first experimental study into this 'new' phenomenon. They produced the slip, required for fretting, between a ball bearing and a flat steel surface, which resulted in large quantities of red oxide debris. These results lead them to propose a mechanism of 'molecular attrition' to describe the fretting process, suggesting that the cohesion between molecules as they touched caused them to be detached from the surfaces and subsequently oxidised.

In 1930 Fink (5) used the term 'wear oxidation' to describe the damage produced on metals while studying their wear properties under slightly imperfect rolling conditions. He suggested that this new phenomenon was of much importance during the fatigue of metals

due to the fact that the surfaces of fatigue fractures are in most cases oxidised.

These early reports on fretting effectively reviewed the occurrence of fretting and its general appearance, and on the whole were in agreement. Following papers which discussed the basic mechanisms of fretting tended to disagree as to whether fretting was a predominantly mechanical, physical or chemical phenomenon.

Tomlinson (3,4) had first hit on the idea that fretting was caused by a 'molecular attrition' process and Godfrey et al (6,7) also concluded that the loosening of finely divided material was due to an adhesion process. He also stated that in addition to this physical process, a chemical action was involved, as, when this finely divided material escaped from the contact area it was readily oxidised. However, the fact that fretting readily occurred between noble metals relegated oxidation as a cause to a secondary factor.

Uhlig (8) postulated that both a chemical factor, along with a mechanical factor, was involved in the mechanism of fretting. He said that an asperity on one surface rubbing on the other surface produces clean metal, which either automatically oxidises or absorbs a layer of gas. The next asperity then wipes the oxide away or causes the metal and absorbed gas to combine. Uhlig also produced the first quantitative expression for fretting damage, viz:

$$W(\text{total}) = (K_0 L^{\frac{1}{2}} - K_1 L) \frac{C}{f} + K_2 \epsilon LC$$

Where: W = specimen weight loss.

L = load.

C = number of cycles.

f = frequency.

ϵ = slip distance.

K_0, K_1, K_2 = constants.

This equation predicts that fretting weight loss is a linear function with number of cycles, a parabolic function with applied load and a hyperbolic function with frequency. It also brings to notice that fretting is dependent on many variables. Earlier tests by Feng and Uhlig (9) on mild steel had shown that variables such as temperature and humidity were of major importance during fretting and Uhlig (8) suggests that the different mechanisms i.e. chemical and mechanical, involved bear unique relationships to each separate variable, e.g. the chemical factor of fretting is predominant at low frequencies, but is overshadowed by mechanical wear at high frequencies.

Feng and Rightwire (10) were in favour of a predominantly mechanical process during fretting. They suggested that if asperities in contact carry enough load, plastic deformation can take place, producing a mechanical interlocking effect. Subsequent relative slip would cause the shearing of the interlocking peaks, thus producing wear particles. This then leads to an abrasive action effect. They later suggest a four-stage process as a mechanism for fretting as shown in Figure 2.1.

Stages:

OA - Initial stage where the rapid rise and bending of the curve are caused by metal transfer and wear.

AB - Transition stage where the change in wear action from shear-

ing to abrasion causes a second upturn in the curve.

BC - Declining stage where the decreasing effectiveness of the abrasive action causes continued decline in the rate of fretting weight loss.

CD - Steady State characterized by a constant rate of fretting damage.

Some agreement with this theory was provided by Halliday and Hirst (11) who proposed the formation of intermetallic junctions on contact and suggested that when the junctions rupture, loose metallic fragments are formed leading to the scoring of the contacting surfaces. Eventually, the formation of loose oxide debris reaches a point where rolling takes place between the surfaces and the coefficient of friction is lowered. Metal to metal contact is prevented and a mild wear mechanism then sets in, hence the steady state proposed by Feng and Rightmire (10).

In a review of fretting corrosion Waterhouse (12) states that the contribution of chemical and mechanical processes to fretting damage depends largely on the type of environment present. He states that in the absence of oxygen or water-vapour, fretting damage would be essentially a mechanical process. The mechanism proposed is one of metal removal from the surfaces in a finely divided form by a mechanical grinding action or by the formation of welds at points of contact followed by tearing. He also predicts that this mechanism is valid for fretting of non-metallic materials.

If fretting takes place in the presence of oxygen or water

vapour the chemical factor is introduced. Two mechanisms are proposed here, the first one being similar to the afore-mentioned except that after the metal particles are removed they are immediately oxidised producing an 'abrasive powder' which continues the damaging action. The second mechanism is one where the metal is already oxidised but the fretting action repeatedly removes the oxide layer, thus creating debris and an exposed surface of virgin metal ready to be oxidised and continue the process.

These early theories on fretting are a mixture of agreement and conjecture. Agreement is reached on the occurrence, appearance and the need for adequate prevention of fretting, but conjecture appears when discussing the contributions of chemical and mechanical aspects to fretting. Even the term 'fretting corrosion' has met with opposition from Feng (9,13) as it implies a chemical nature to the process. However these disagreements led to research taking a broader front as it had become evident that fretting was dependent on several variable factors such as environment, temperature, frequency, etc. It is convenient, therefore, to review the literature by considering each individual factor, and this will be done later in this section.

A later paper by Hurricks (14) concisely reviews the mechanisms of fretting previously suggested, and stated that the process can be divided into three stages, i.e. initial adhesion and metal transfer, production of debris, and finally, a steady state wear condition.

In the first stage of initial adhesion and metal transfer, it is suggested that any protective oxide film on the metal surface is broken down and metal to metal contact is established, which leads to adhesion. This idea again involves other variables, such as oxide

and metal hardness. The strength of this adhesion then dictates the degree of metal transfer and hence subsequent damage. The second stage, one of debris formation, involves initially virgin metal debris, later oxidising to form the final debris product, and leading to a reduction in metal to metal contact. The third stage, the steady state, comes about by the general disintegration of the zones affected in the initial stages of the fretting. Hurricks does suggest here that abrasion is not significant, and that a local fatigue mechanism causes most of the damage at this stage.

Hurricks also mentions other important considerations involved in the mechanism of fretting, such as local temperature increases and work hardening effects, for example, in any sliding process, plastic deformation takes place and there is extensive dislocation movement at and below the surface. He also points out that this plastic deformation will have a considerable effect on the chemical and diffusion processes in metals.

Considering the idea of local temperature increases during fretting, Wright (15) remarked that local temperature rises did not occur, stating that during fretting tests of mild steel on polymethacrylate, which has a melting point of 80°C , no softening of the polymer occurred. However, Waterhouse (16) suggests that, as these two materials are incompatible, no welding between the surfaces is possible, hence no severe working of the surfaces occurs, which would in fact be the major cause of the temperature increase. He goes on to state that, in fretting fatigue tests of mild steel on mild steel, strong adhesion occurred between the surfaces and the fretting debris included $\alpha - \text{Fe}_2\text{O}_3$, an oxide that transforms from $\gamma - \text{Fe}_2\text{O}_3$ in the temperature region of 500°C , strongly suggesting a large temperature rise during

the fretting process. However, it was noted here that the high pressure involved in fretting could affect the transition temperature of the oxide debris. More conclusive evidence, though, in this work was that the ferrite in the test materials underwent some recrystallization; a process which also occurs at about 500°C, but would not be affected by the contact pressure of fretting.

More recently, Sproles and Duquette (17), have questioned the evidence used in proposing these local temperature increases, and work done by themselves incorporating interface potential measurements to record temperature changes, showed that the maximum temperature increase at the fretting interface was 18°C.

Concerning the plastic deformation and dislocation movement below the surface during a sliding process, Suh (18) put forward a new and somewhat controversial theory for the mechanism of wear, called 'the delamination theory of wear'. The theory proposes four stages of wear, viz: dislocation build-up below a dislocation-free surface; dislocation pile-up at a finite distance from the surface leading to void formation; coalescence of voids into long narrow cracks; finally the long narrow crack reaching a critical length and the material between the crack length and surface shearing, thus producing a sheet-like particle of wear debris. Applying this theory to fretting, Waterhouse and Taylor (19) showed that, on three different materials, the morphology of the fretting debris, that is, oxide coated on thick metal plates, was consistent with the delamination theory. An important point raised here was the fact that environment would have little effect on initiation of a subsurface crack, but could affect its propagation after breaking the surface.

In a later paper Waterhouse (20) states that, early in the

fretting process macroscopic adhesion takes place between the two surfaces. Eventually this adhesion falls off, as described by Hurricks (14), and then material removal takes place by delamination in accordance with Suh's theory. Waterhouse goes on to state, however, that the delamination process contributed only to the production of debris, confirming that the subsurface cracks propagate only to the surface, not into the bulk of the material.

Sproles and Duquette (21), in fretting experiments on an annealed steel, observed a mixture of metallic flakes and oxide fretting debris. They proposed a mechanism by which fretting cold works the surface early on, thus removing the ductility and producing brittle cracks which go on to isolate metal flakes from the bulk of the specimen, in combination with a delamination process. This is shown schematically in Figure 2.2. They discount the adhesion and metal transfer mechanisms as unable to explain the shape of the flake-like metallic debris. In the case of the oxide debris, they express agreement with the mechanism of oxidation and subsequent removal by asperity scraping, as proposed by Uhlig (8), as this can account for the observations of probable oxide particle agglomeration with embedded metallic debris.

On the whole, there is substantial disagreement concerning the basic mechanisms of fretting. However, this is not too surprising when considering the variables involved, which clearly lead to variation in the conditions under which experiments in this field are performed. Thus, as stated earlier, it is convenient to discuss fretting in relation to some of these variables.

2.2 Effect of Variables on Fretting.

2.2.1 Environment.

In a normal environment the most important agents that affect fretting are oxygen and water vapour (humidity). The effect of oxygen on fretting reiterates the chemical nature of the process mentioned earlier, and the role of oxidation has been investigated by several researchers.

Work done by Sakmann and Rightmire (22) showed that fretting in air and pure oxygen produced the same amount of damage, whereas if the fretting was conducted in an inert atmosphere or in a vacuum the damage was much reduced. From this they resolved that the damage produced by oxide particles was greater than if produced by metal transfer or by metallic debris.

Feng and Rightmire (10) fretted steel specimens in dry air, carbon dioxide and helium to assess how different atmospheres affected their 'four stage' theory of fretting. They found that when comparing the dry air and carbon dioxide tests, the initial stages of the latter tests were prolonged due to a lack of suppression of metal transfer. This they said was due to the fact that in dry air an oxide layer forms quickly thus reducing metal transfer, whereas in carbon dioxide only an absorbed layer of the gas is acquired by the fretting surfaces, which is much less effective in preventing metal transfer. The damage produced in the helium atmosphere seemed like another step down in that practically no gas was absorbed onto the contacting surfaces, and so metal transfer was more profuse than in carbon dioxide. This led to a suppression of the second stage of fretting, showing that the damage produced in the helium was entirely due to metal transfer. This was further supported by observations that depressed areas on one

surface corresponded to elevated areas on the mating surface and the weight loss was very low, showing that only small amounts of loose wear had been produced.

The effect of humidity on fretting has been discussed by Wright (15), and he states that "the changes occurring in fretting with a variation in the humidity probably arise through the absorption or capillary condensation of the water vapour onto the metal and oxide surfaces". It was proposed, therefore, that this absorbed layer of water behaved as a lubricant and was effective in removing oxide debris from the contact area and thus reducing the severity of the damage. This was supported by observations at low humidity, which showed that the oxide detritus had not been removed, and pits had been formed.

Feng and Uhlig (9) also found that on mild steel, the fretting damage decreased as the humidity increased. However, tests were not performed at 100 per cent relative humidity because of rusting of the test specimens and subsequent error in weight loss determinations.

2.2.2 Temperature.

The effect of temperature on fretting has been difficult to isolate from the effect of humidity, as these two variables tend to affect each other.

Almen (23) first noticed that damage due to fretting was worse in winter than in summer and this was later verified by Feng and Uhlig (9) who found that the fretting damage was greater as temperatures fell below 0°C , whereas at a temperature of 50°C the fretting damage was only about 50 per cent of that at 0°C , and after the run in, about 65 per cent. Waterhouse (24) states that the sudden decrease in damage which occurs between 0°C and room temperature is likely to

be associated with the effectiveness of absorbed moisture as a lubricant.

Obviously at very high temperatures the role of humidity disappears and then the fretting damage becomes dependent upon the type of oxide film produced, e.g. spinel type oxides are capable of being transformed into a 'glaze' oxide which is very protective.

2.2.3 Relative Slip Amplitude.

Feng and Uhlig (9) first reported that specimen weight loss was a linear function of slip amplitude through a range of 0 - 250 μm . However, Halliday and Hirst (11) found that for 10^6 cycles, there was a linear relationship between wear volume and slip amplitude, S, upto $S \approx 75 \mu\text{m}$, above which the wear rate increased rapidly. This type of relationship was confirmed by Ohmae and Tsukizoe (25) in tests over 10^5 cycles on a low carbon steel and pure iron, as shown in Figure 2.3. Ohmae and Tsukizoe (25) go on to say that the mechanism of fretting at amplitudes lower than 70 μm is different from that occurring at $S \approx 70 \mu\text{m}$. They suggest, in both cases, a three stage mechanism of plastic deformation of asperities leading to a mechanical type wear including adhesion, culminating in oxidative wear and abrasive wear. They suggest that where the amplitude is less than 70 μm , the oxidative wear predominates in the final stage resulting in a mild wear process, whereas at amplitudes greater than 70 μm , the oxidative wear and abrasive wear occur simultaneously, hence the increased wear volume.

The definition of fretting includes no limits to the amplitude of slip, except to say that the contacting surfaces are nominally at rest. O'Connor (26) states that fretting damage is visible at amplitudes as low as 0.1 μm , but does not state an upper limit. However,

at high amplitudes a wear form called 'reciprocal sliding' takes place. Ohmae and Tsukizoe (25) therefore have suggested that the transition from fretting to reciprocal sliding occurs at about $300\mu\text{m}$. They also suggest that when the amplitude of slip is less than $70\mu\text{m}$ the process should be called 'fretting corrosion' and above $70\mu\text{m}$ (thus $70\mu\text{m} - 300\mu\text{m}$) the term 'fretting wear' is more appropriate.

2.2.4 Cyclic Frequency.

The effect of cyclic frequency on fretting is reviewed (24, p.115) to be dependent itself on the environment in which the fretting takes place. Lower frequencies appear to produce more fretting damage in corrosive environments, implying that the corrosive medium has more time to act on the fretted surface between cycles. However, in high frequency tests, the effect is negligible.

2.2.5 Contact Pressure.

When the contact pressure is increased during fretting, the tendency is to reduce the amplitude of slip, and as a result cause some reduction in fretting damage. It is not possible though to prevent fretting completely by this method.

However, if the amplitude is kept constant then the general tendency, found by several researchers (9, 15), is that any increase in contact pressure causes an increase in fretting damage. As there will exist a specific value for clamping pressure at which it is no longer possible to maintain constant slip amplitude, then the damage caused by the increase in clamping pressure passes through a maximum and then decreases, as found by Uhlig et al (27).

2.2.6 Mechanical State of the Contacting Surfaces.

The mechanical state of the contacting surfaces essentially means the hardness and state of stress of the surface layers in contact.

Waterhouse (24, p.119) states that hardness affects fretting in two ways. First of all high hardness implies a higher fatigue strength of the material, which means that the local high strain fatigue action of fretting has a less damaging effect. Secondly, high hardness means a greater resistance to any abrasive action in fretting by hard oxide debris.

The harder the material, the lower the adhesion between the contacting surfaces. This is confirmed by Mokhtar (28), who also states that any increase in hardness by heat treatment, alloying or shot peening also lowers frictional resistance, thus lowering adhesion. However, such treatments are effectively meta-stable states and it is reported by Bethune and Waterhouse (29) that adhesion is inversely proportional to the hardness of the material in its equilibrium state. It is suggested that the high strain fatiguing due to fretting is sufficient to restore the surface layers to their equilibrium state, thus any artificial hardening, such as work hardening or age hardening will be removed by fretting. Tests done on an age hardened Al - 4% Cu alloy showed that a softened layer of material was formed under the fretted region, as shown in Figure 2.4 (29). The depth of this layer was found to be dependent on the number of fretting cycles.

Concerning the state of stress of the surface of a metal in relation to fretting, it is well established that a compressive residual stress in the surface improves the fatigue resistance. Thus most of the studies relating to this topic have been done in conjunction with

fretting fatigue, and so are discussed in detail in the next section.

2.2.7 Surface Finish.

Waterhouse (24, p.122) states that generally the smoother the surface then the more serious the fretting damage. He states that on rough surfaces the asperities will at first be plastically deformed, but will not be worn away completely due to work hardening. Thus some of the sharper asperities are able to 'absorb' some of the tangential movement due to fretting, by elastic deformation. Also, debris formed on a rough surface is easily entrapped in the spaces between asperities, and so becomes redundant in the fretting process.

2.3 Fretting Fatigue.

The combined action of fretting and fatigue, known as fretting fatigue, is probably the most common situation in which fretting occurs in practice. As Walker (30) says, 'The main significance of fretting to the engineer is its association with fatigue,... The link between fretting and fatigue is a double one. Not only does fretting cause fatigue, but it is itself produced by the same conditions of fluctuating load that can produce fatigue directly. Thus, paradoxically, fretting incites fatigue under conditions where fatigue is likely to occur anyway'.

The first published information relating fretting to fatigue was by Warlow-Davies (31), who performed fatigue tests on pre-fretted specimens of a medium carbon steel and a high tensile alloy steel. Results showed a 13 per cent reduction in fatigue strength due to the fretted surface for the medium carbon steel, and an 18 per cent reduction for the alloy steel. However, these tests were not strictly

fretting fatigue tests as the two processes were not occurring simultaneously.

Fenner et al (32) reported several annoying fretting fatigue failures occurring during the course of laboratory fatigue testing. These results were troublesome because the tests were of the plain fatigue type, but the fretting fatigue occurring between the grips and the specimen led to premature failure in the wrong place!

Examples such as these showed undoubtedly that fretting had a substantial effect on the fatigue life of materials, and this lead to specific research into the area of fretting fatigue.

Fenner and Field (33, 34) concluded that the early formation of damage due to fretting was caused by surface fatigue strains induced by the relative displacement of contacting asperities at microwelds. This causes the initiation of shallow cracks inclined to the surface, which later coalesce to form pits, with the release of debris. They state that if the applied fatigue stresses are high enough then these inclined cracks will propagate and lead to failure. This mechanism is in agreement with that of Bethune and Waterhouse (29) who showed that adhesion and local welding occurs where like metals fret, and they suggested that the initiation of fatigue cracks is associated with the local high strain fatigue at these welds, which leads to their rupture.

Waterhouse and Taylor (35) said that fretting fatigue cracks were initiated at the boundary between slip and non-slip in the contact region, suggesting that if slip is ensured over all of the contact region, then crack initiation would be prevented.

Hoepfner and Goss (36) reviewed the mechanisms of fretting fatigue, observing that the major effect of fretting is to act to decrease the period required to initiate a crack. They also developed

their own model for the mechanism of fretting fatigue, which is shown schematically in Figure 2.5. It suggests the coming together of asperities under normal load, which are subsequently deformed and broken, producing debris and eventually initiating fatigue cracks. It also suggests that high strain fatigue between asperities could be an important factor. This model was proposed in conjunction with the idea of a 'fretting fatigue envelope' i.e. an area on the S - N curve outside which fretting has no effect on fatigue life. This is shown schematically in Figure 2.6, in which to the left of line A the removal of the fretting device results in no (or possibly less) degradation of fatigue life, and line B represents the termination of the fretting fatigue experiment in either failure, or a point in the test at which it no longer matters whether the fretting device is connected or not.

This idea was further investigated by Wharton et al (37), who proposed a 'fretting fatigue limit', which is the number of fretting cycles required to initiate a propagating fatigue crack. Hence, they were able to determine the minimum number of fretting cycles which would ultimately result in failure, and could calculate the number of fatigue cycles required to actually propagate the fatal crack to failure. From their results they proposed a five-stage sequence of events in fretting fatigue, viz:-

- (1) Events preceding the nucleation of a crack.
- (2) Crack nucleation.
- (3) Growth of a microcrack.
- (4) Growth of a macrocrack.
- (5) Final failure.

They suggested that the fretting, being a localized action on the surface nucleates a crack in the first few thousand cycles, in which

it grows oblique to the surface as it is influenced by the alternating stress produced by the fretting action. Then the crack passes out of the region influenced by fretting and so changes direction to propagate perpendicular to the cyclic stressing, through to final failure. The mechanism suggested earlier (35) on initiation from slip/non-slip boundaries is adhered to here and is shown in Figure 2.7.

However, this mechanism was questioned by Alic et al (38, 39) following analysis of fretting fatigue tests on an aluminium alloy. They stated that cracks initiate first from locations of highest local stress, and that these locations may indeed coincide with slip/non-slip boundaries in certain cases. Their experiments showed that cracks which led to failure initiated at the boundary of fretted/unfretted regions, and they presumed that this is really where the highest stresses and strains exist. Another notable observation from this work was the smearing of metal in some places within the fretted areas, suggesting large plastic strains.

From metallographic analysis of fretting fatigue test specimens, Hoepfner and Goss (40) concluded that large numbers of secondary cracks are produced in the fretted areas. They state that the major effect of fretting is the production of surface damage which accelerates the initiation stage of fatigue, and they add that once cracks have been initiated, surface oxide debris produced by fretting is forced into them resulting in an apparent widening of the initial crack.

By using optical microscopy and electrical resistance measurements, Endo and Goto (41) investigated the initiation and propagation of fretting fatigue cracks in a 0.34% carbon steel. They were able to plot curves of crack depth versus number of fretting cycles during the fatigue tests, as shown in Figure 2.8. These show two straight lines

denoting the initiation and propagation stages interrupted at knee point, and also the final period of life. Other analysis showed that the fretting fatigue damage was saturated in the first 20 - 25% of total life. It was clear from this that the crack growth rate is much higher in the initiation stage, that is, under the influence of fretting. Other tests showed that the depth at which the direction of crack growth changed coincided with the knee point of crack growth rate, and that this depth was greater if the cyclic stress or tangential force was higher. They concluded that the knee point was the maximum depth at which the tangential forces of fretting contribute to the propagation of the crack and that this point also coincides with 20 - 25% of fatigue life.

Alic and Hawley (42) showed agreement with these results on early crack growth rates, in work on an aluminium alloy. They found that fretting fatigue cracks grow much faster, particularly in their early stages, than would be expected based on cyclic fatigue stresses and alloy characteristics alone. Two reasons were given for this observation, viz:-

- (1) The influences of the high stresses created by fretting in the near surface region, and
- (2) The general tendency of very short fatigue cracks to grow faster than long cracks under otherwise comparable conditions.

Alic and Hawley state that their cracks were of the type growing obliquely to the surface to a length of approximately $100\mu\text{m}$, as in (41), before changing to a direction perpendicular to the surface. In their fracture mechanics analysis on this they suggest, however, that the fretting can affect the crack growth to a depth in the range $100\mu\text{m}$ - $1,000\mu\text{m}$. Also similar results were obtained by the author et al (43)

on an age hardened Al - 4%Cu - 1%Mg alloy, and are summarized in Figure 2.9. In this case the fretting fatigue cracks grew at an angle of 45 degrees to the surface to depths of about 500 μ m before changing direction, but then, amongst other test variations, a much higher clamping pressure was used here compared with the previous works (41, 42).

In a recent paper, Hoepfner and Gates (44) reviewed several of the aspects of fretting fatigue mentioned so far. They also listed several of the variables which, as with plain fretting, have a direct effect on the outcome of fretting fatigue. They state that each occurrence of fretting fatigue must be dealt with as a separate problem and consideration must be given to the conditions operating each time. Therefore it is important to discuss fretting fatigue in the light of these variable conditions.

2.4 Effect of Variables on Fretting Fatigue.

2.4.1 Environment.

The effect of the environment on the mechanism of fretting fatigue has always been questionable. Initially investigators were concerned with the effect of oxygen and the effect of water vapour.

Fenner and Field (34) performed fretting fatigue tests on an Al - 4%Cu - 1%Mg alloy to study the effects of variation in environment. Using vacuum as a standard, the results showed that the presence of oxygen lowered the fretting fatigue strength.

Endo and Goto (45) performed tests to see how environmental variations affected the fretting fatigue of an Al - Zn - Mg alloy, and found that water vapour, not oxygen, influenced fretting fatigue crack

initiation. They observed that in humid air, the initiation phase of cracking proceeded to a depth of 250 - 300 μm , whereas in dry air the initiation phase of cracking continued to a depth of only 100 μm . This was found to be due to the material below the fretted surface being softened to a depth of about 400 μm in humid air, but remaining hard in dry air. Further research by the same workers showed that the softening was caused by a decrease in the concentration of the alloying elements near the fretting surface. No such decrease was found in the tests done in dry air and it was concluded that the decrease in concentration in alloying elements in humid air was due to a reaction between water vapour and the freshly created surface, the mechanism of which was not clearly understood.

Poon and Hoepfner (46, 47) performed tests on Al - Zn - Mg type alloys (7075 - T6) to compare the fretting fatigue performance in laboratory air to that in vacuum.

Results of these tests showed that the specimens tested in vacuum had lives 10 - 20 times longer than those in laboratory air. They concluded therefore, that the presence of a laboratory environment introduces a chemical factor into the fretting fatigue process which plays a dominant role in reducing the fatigue life of the alloy. The observed mechanism here is that, during fretting fatigue in a laboratory environment, corrosion pits are formed on the fretted surface, which subsequently become packed with oxide debris. The debris cannot escape due to the contact pressure between the surfaces. Cracks were seen to initiate from the bottoms of these pits as the volume of debris increased and pushed the sides of the pit apart. In the tests done under vacuum there was no evidence of corrosion pits, and therefore it was concluded that crack initiation was due to some other

mechanism. However, these results were in contrast to the results from two earlier papers by Nishioka and Hirakawa (48) and Reeves and Hoepfner (49), concerning work on steels. Nishioka and Hirakawa had shown that the majority of cracks in a fretted area bore no relation to the positioning of corrosion pits and Reeves and Hoepfner had found that the mechanical damage incurred during the fretting process was predominant over the chemical damage due to oxide formation.

Hoepfner does state later though (50) that, in some materials, for example, titanium alloys, the corrosion product does play an important role, whereas for other materials such as low carbon steels, there is no strong dependence on corrosion product.

2.4.2 Temperature.

A great deal of work has been done on the effect of temperature on fretting wear, rather than on fretting fatigue, and this has been summarized by Hoepfner and Gates (50). However, as mentioned earlier (section 2.2.2) at high temperature it is possible that the fretting wear product consists of a 'glaze' oxide, which acts as a protective coating.

Concerning fretting fatigue, work done by Hamdy and Waterhouse (51) on a nickel-based alloy showed that, in the temperature range 280° - 540°C, fretting fatigue strength was improved 130 per cent, restoring it to its room temperature plain fatigue value. This improvement was found to be due to a 'glaze' oxide formation. However, later work (52) showed that this 'glazing' property depends on the material, as tests on the alloy Ti - 6Al - 4V resulted in a lowering of fretting fatigue strength in the temperature range 200° - 600°C and no 'glaze' formation was detected.

2.4.3 Relative Amplitude and Direction of Slip.

In general for lower values of slip, fretting fatigue strength decreases with increased relative slip amplitude. This was first shown by Fenner and Field (33) on an Al - 4%Cu - 1%Mg alloy. However, there is a maximum slip amplitude above which no further reduction in fretting fatigue strength occurs. Waterhouse (24, p.145) states that at zero mean stress, fretting fatigue damage increases as the amplitude of slip increases up to a value of $8\mu\text{m}$, above which the damage is constant. However, with a mean cyclic stress the most damaging slip amplitude is in the range $9\mu\text{m}$ to $14\mu\text{m}$. Yeh and Sinclair (53) state that at a slip amplitude of $15\mu\text{m}$ the fatigue stress required to initiate cracks is at a minimum, hence the material is at its weakest stage. Above this value the crack initiation increases because wear processes dominate at large slip amplitudes and fretting cracks are quickly worn away.

Nishioka and Hirakawa (54) developed a quantitative expression to describe the relationship between slip amplitude and fretting fatigue strength, viz:

$$\sigma_{fwl} = \sigma_{wl} - 2\mu p_o \left[1 - \exp(-S/K) \right]$$

Where;

σ_{fwl} = the stress required to initiate a fatigue crack under fretting conditions,

σ_{wl} = the plain fatigue strength,

μ = the coefficient of friction,

p_o = the contact pressure,

S = the slip amplitude, and

K = a constant.

However, as stated by Waterhouse (55), this expression implies an increase in plain fatigue strength will result in an increase in fretting fatigue strength, but this is not always the case.

The effects of direction of slip on fretting fatigue were shown by Collins and Tovey (55) using pre-fretted fatigue tests on 4340 steel. They showed that specimens pre-fretted with a slip direction parallel to the subsequent fatigue cycling exhibited a 76 per cent reduction in fatigue strength after 10^6 cycles, whereas specimens pre-fretted perpendicular to the fatigue stress were reduced in strength by only 41 per cent. Similar kinds of results are reviewed by Waterhouse (24, p.149) on an Al - 4%Cu alloy, and he states that cracks formed by fretting perpendicular to the cyclic stress are in a plane parallel to the stress and it is not until they 'curl' round that they are propagated by the cyclic stress.

2.4.4 Cyclic Frequency.

It was found by Endo et al (56) that, on a carbon steel, the fretting fatigue strength decreases at low frequencies. It is explained by Endo and Goto (57) that the damage due to fretting fatigue is partially dependent on tangential stress, which itself is dependent on frequency because fretting friction is significantly affected by the oxidation of the contact surfaces. They go on to say that when the frequency is lower, the tangential force increases more rapidly, reaching a maximum value in fewer cycles, hence crack initiation is earlier, thus lowering the fretting fatigue strength.

2.4.5 Contact Pressure.

Changes in contact pressure in fretting fatigue only have a noticeable effect below a certain saturation value. Waterhouse (24, p.137) states that fretting fatigue strength falls rapidly as contact pressure is increased, up to a value of 70MPa, above which the strength remains more or less constant.

Nishioka and Hirakawa (58) reported that fretting fatigue strength based on the initiation of cracks decreases linearly with increasing contact pressure, stating no limit. However, they also reported that the fretting fatigue strength based on fracture decreased gradually with increasing contact pressure up to a value of 20MPa, above which the strength remained constant.

The effect of contact pressure also varies in relation to the material. Goss and Hoepfner (59) showed that variable contact pressure was a major factor in fretting fatigue tests on a Ti - 6Al - 4V alloy, but had little effect on similar tests on the 7075 - T6 aluminium alloy. This difference in behaviour was rationalized on the basis of the role of microstructure and microscopic toughness during the fretting process.

2.4.6 Mechanical State of the Contacting Surfaces.

Again the mechanical state of the contacting surfaces represents the hardness and the state of stress of the material surfaces.

The effect of hardness on fretting fatigue involves several additional considerations. For example, is the actual fatigue specimen harder than the fretting pad or vice versa? How is the difference in hardness achieved? By heat treatment, work hardening or a combination of materials with different hardnesses?

Considering the first question, Nichioka and Hirakawa (58) found that an increase in hardness of the fatigue specimen did not significantly affect the fretting fatigue strength except when large differences were involved. It was explained that at high hardness differences, the determining factor was wear resistance.

Waterhouse (24, p.151), using aluminium alloy pads on mild steel, showed that the fretting fatigue strength was reduced as the hardness of the pad was increased, as shown in Figure 2.10. Similar kinds of results were found on a titanium alloy by Liu et al (60) using a selection of different materials for the fretting pads. Adhesion was found to be a major factor here because with certain combinations of materials very strong adhesion can develop. Waterhouse (24, p.154) also shows that using similar materials of differing hardness due to work hardening, produces contrasting results as shown in Figure 2.11. This effect is explained again by the fact that adhesion decreased with increasing hardness.

Another consideration that has to be made is the effect of fretting fatigue on the hardness, especially when any increase in hardness is due to work hardening or heat treatment. Waterhouse (24, p.154) states that where fretting is involved, work hardening does not necessarily improve fretting fatigue strength because it is a metastable state. Similarly for the case of a heat treated Al - 4%Cu alloy, he states that a higher fretting fatigue strength is found for the annealed form than for the age hardened form.

The effect of the state of stress of the material surface on fretting fatigue involves either residual stress in the surface or a mean stress applied during fatigue cycling.

A slight variation on the latter point was reported by Collins

and Marco (61), who pre-fretted a series of specimens of 4340 steel while under axial compression, and another series of specimens while under tensile load, as shown schematically in Figure 2.12. The specimens were then tested in fatigue and it was found that the specimens pre-fretted under compression were weaker in subsequent fatigue than those specimens that were pre-fretted under tension. The explanation is also shown in Figure 2.12, in that for the compressed specimens, during fretting, cracks are initiated, which after the removal of the compressive load are left with a local tensile stress at their tip, thus leading to easy propagation during fatigue cycling. The reverse is true for the tensile loaded specimens.

Nishioka and Hirakawa (62) stated that the influence of a residual stress on ordinary fatigue strength is, in principle, similar to that of an externally applied static stress, thus a residual stress may also be regarded as a mean stress in the case of fretting fatigue. Their results showed that the fretting fatigue strength with respect to fracture was decreased by a tensile mean stress, but increased by a compressive mean stress. They stated that this is the same trend as in plain fatigue, i.e. crack propagation is affected by mean stress but initiation is not, thus they said that the fretting fatigue strength based on crack initiation is unaffected by mean stress.

Kantimathi and Alic (63) performed fretting fatigue tests on an aluminium alloy during which tensile overloads or compressive underloads were applied. It was found that for low fatigue stresses, the tensile overloads significantly improved the fretting fatigue life, whereas compressive overloads showed no great effect. This was explained by the property of long crack retardation during the tensile overload. However, it was not possible to assess whether or not crack

retardation took place on the shorter cracks produced by fretting.

2.4.7 Surface Finish.

In plain fatigue a rough surface is generally a weaker surface due to a high proportion of stress concentrations. However, in fretting fatigue an extra stress concentration is 'provided' by the fretting, thus the deleterious effect of a rough surface is diminished. In fact in the mechanism of fretting fatigue proposed by Hoepfner and Goss (36), a rougher surface would perhaps be beneficial by 'absorbing' some of the tangential force as suggested by Waterhouse (24, p.122) during plain fatigue.

It has been shown that fretting and fretting fatigue are dependent on many variables, and that many of the variables themselves are affected by each other, thus it is impossible to isolate each one. It must therefore be emphasised that each fretting fatigue occurrence must be treated as a separate problem.

One thing which is undoubtedly clear is that fretting and fretting fatigue are a major engineering problem, and much effort has been made towards preventing and eliminating them.

2.5 Prevention of Fretting and Fretting Fatigue.

2.5.1 Design.

The occurrence of fretting and fretting fatigue requires contacting surfaces, therefore prevention by design must avoid, if possible, the contact of surfaces which are likely to undergo some relative movement or vibration. When this is not possible, a stress relieving facility must be employed, such as grooves or recesses situated in

positions of high stress concentration, for example, at the edge of contacting areas. Bowers et al (64) found that the configuration shown in Figure 2.13 developed a much better fretting fatigue strength than one with a plane surface.

It has been stated earlier that certain materials are more susceptible to fretting and fretting fatigue damage than others, and that certain combinations of materials do not produce good fretting fatigue results. Therefore a suitable choice of materials is an important design factor.

2.5.2 Lubrication.

The use of greases and liquid lubricants has only met with limited success. Improvements in fretting fatigue strength have reached values of only a few percent, basically because the lubricant is squeezed out from between the contacting surfaces soon after the onset of cyclic motion. Solid lubricants such as molybdenum disulphide and graphite have proved more beneficial, creating improvements of up to 20% in fretting fatigue strength.

Waterhouse and Allery (65) showed that the use of a combination of solid lubricant powders and grease did not improve the fretting fatigue strength of steel to any significant degree, and in some cases the solid powders caused an increase in adhesion between the two surfaces by facilitating the removal of the original oxide layer.

2.5.3 Sacrificial Inserts.

The application of soft material sacrificial inserts between contacting surfaces is quite common in some industrial processes, for example, polythene inserts in automobile leaf springs. The purpose of

the inserts is to totally separate the contacting surfaces. Bowers et al (64) showed that inserts of $75\mu\text{m}$ thick sheets of terylene produced significant improvements in the fretting fatigue strength of aluminium alloys.

The disadvantages involved with this method are that the inserts must be replaced periodically and that they can only be used on surfaces of simple geometry.

2.5.4 Surface Coatings.

Non-metallic coatings, such as P.T.F.E. (Teflon), have had limited success under **low** contact pressures ($\sim 7\text{MPa}$), but under high contact pressures the coating is soon worn away.

Metallic coatings are of two types: electrodeposited and metal sprayed. Generally the performance of either type in improving fretting fatigue strength is dependent on such factors as thickness, hardness, internal stress and internal integrity of the coating.

Waterhouse et al (66) showed significant improvements in the fretting fatigue strength of mild steel using electrodeposited coatings of silver and copper. Similarly, Jones and Lee (67) found that electrodeposited nickel with a compressive internal stress produced improvements in the fretting fatigue strength of mild steel of up to 58.5 per cent.

In the case of metal sprayed coatings, for example, Al - 1%Zn coatings, it has been found that the wear rate is reduced, but because these coatings contain many flaws and surface cracks, which soon propagate into the base metal, no real improvement in fatigue strength is obtained. However, molybdenum sprayed coatings have given better results in improving fretting fatigue strength (68).

2.5.5 Mechanical Surface Treatments.

Mechanical methods are now employed to produce a residual compressive stress in the surface of components which will undergo fatigue or fretting fatigue. The two most common methods are shot peening and surface rolling.

Shot peening forms a major part of the present work and will therefore be discussed in Chapter Three. Surface rolling is a process which produces similar results to shot peening, i.e. residual compressive stress and work hardening in the surface, but it is more expensive. It is used when extra depth of the compressive stress is required. Fretting fatigue tests done by Sachs and Horger (69) showed that on surface rolled specimens, the deleterious effect of fretting on fatigue is almost completely removed.

3.1. Characteristics of Shot Peening.

3.1.1 Types of Equipment and Shot Materials.

Whitney (70) briefly describes the main aspects of shot peening in industry. The equipment used is mainly of two types, i.e.,

- (1) the Airless or Wheel Blast system, and
- (2) the Airblast system.

In the Airless or Wheel Blast system, the particles that is propelled by a high speed rotating wheel against the part being treated. The main advantages of this method are constant shot velocity and suitability for use in the production industry and to a high rate of

CHAPTER THREE

SHOT PEENING

Shot peening is a cold-working process performed under highly controlled conditions in which the metal component being treated is bombarded by a stream of hard rounded media or 'shot'. This bombardment is performed with sufficient velocity so that the shot indents the metal surface. The indentations result from the plastic yielding of the impacted metal, which in effect 'seeks' to expand. However, the underlying material deforms elastically and then recovers and the surface layers are thus residually stressed in compression.

In order to maintain equilibrium, however, this compressive stress must be balanced, and this results in a tensile stress within the material immediately below the compressed layer, as shown in Figure 3.1.

3.1 Characteristics of Shot Peening.

3.1.1 Types of Equipment and Shot Materials.

Whinney (70) briefly describes the main aspects of shot peening in industry. The equipment used is mainly of two types, i.e.,

- (1) the Airless or Wheel Blast system, and
- (2) the Airblast system.

In the Airless or Wheel Blast system, the metallic shot is propelled by a high speed rotating wheel against the part being peened. The main advantages of this method are constant shot velocity and suitability for use in the production industry due to a high rate of

shot flow, which can be achieved very economically.

The Airblast system has two available processes; a direct pressure method is the most efficient, producing a higher shot velocity, and it is the only process with the capability of peening into deep holes. In this method the shot is contained in a pressure vessel and is allowed to fall, under gravity, into a compressed air blast line.

A method described by Montemarano and Wells (71) called 'rotary brush peening' is adaptable as a portable, manual or automatic method of controlled shot peening. The shot is uniformly distributed and bonded to nylon cloth flaps mounted on a rigid hub. The hub can be fixed on to any conventional hand grinder and rotated at speed so that the peening takes place as the shot hits the work piece. In effect, each nylon flap acts as a miniature peen hammer, controlled by the grinding machine. The impact force is dependent on the type of shot, brush diameter and rotational speed.

The material most widely used for shot is cast-steel, although cast iron is sometimes used for economy, despite being less efficient. Glass beads are used when the operation is predominantly for surface cleaning, although where specimen sections are thin or iron contamination is strictly prohibited, glass beads are preferred. More unusual materials have included walnut shells, ceramic media and even ball bearings in certain applications.

3.1.2 Shot Peening Control and Measurement.

Almen (72) describes the (his) standard procedure for the control and measurement of shot peening. Simply it consists of a standard steel strip, rigidly bolted to a heavy hardened steel base, as shown in Figure 3.2. The strip is then peened on its exposed side

only. When subsequently removed from its base, it is found that the compressive stress induced by the peening results in a convex curvature of the strip on its peened side. This curvature, generally called the 'arc height', is measured by micrometer, and its value is a measure of the shot peening intensity.

Originally, two thicknesses of strip were standardized to meet the requirements of light and severe peening. These were designated A and C, being 1.33mm and 2.38mm respectively in thickness as shown in Figure 3.3. Baldauf (1) states that the additional strip, designated N, has also been standardized and has a thickness of 0.79mm, but is seldom used. The length and width of the strips are always the same, being 76mm and 19mm respectively.

Arc height values of peening intensity are always stated as a range to allow for tolerances in the operation. Baldauf (1) gives a typical specification of arc height (commonly given in inches) as 0.018" - 0.022" (0.46 - 0.56mm) on an A strip. If a reading on an A strip is less than 0.004" (0.1mm) then an N strip should be used, which would give a reading of about three times that of the A strip. If the range is above 0.022" (0.56mm) on an A strip, then a C strip is used, giving values of about 0.3 times that of the A strip.

The use of the Almen strip provides a degree of quantitative control for shot peening, but further specifications are required for precise quality control.

3.1.3 Shot Peening Specifications.

- (i) Coverage: The uniformity, magnitude and depth of the stressed layer produced by shot peening is known as coverage. The most common coverage specification is 98 per cent, which according to Baldauf, literally

means that 98 per cent of the metal surface must be covered by shot craters or 'dimples'. In effect, this necessitates that the metal part remains in the blast zone long enough to acquire a uniform compressive residual stress, otherwise the part could still fail prematurely in service.

Coverage is frequently only checked by visual examination, but a 'rule of thumb' has been adopted by industry (73); an initial strip is peened under prevailing conditions and the arc height is measured. A second strip is then peened under the same conditions, except that the exposure time is doubled, and then the arc height is measured. If the second reading is less than 10 per cent greater than the first reading, as in Figure 3.4, then 98 per cent coverage is assumed on the first strip.

Modern methods, however, have been developed to aid visual examination of the actual peened component (73). Liquids, which when dry form an elastic film, are applied to the component to be peened. This film requires break up by the peening, for removal from the surface. Thus after peening, the part is examined for film remaining, the amount of which is calibrated to percentage coverage on predetermined standards.

- (ii) Shot Size and Quality: In general the shot size selected is the maximum size that will not damage the part to be peened. This, then is dependent on section thickness, surface irregularities, fillet size, abrasion desired and the manner of eventual loading of the part. Baldauf (1) states that although shot size is often determined by experimental work, certain 'rules of thumb' are still used in industry. Typical shot sizes, used on A strip intensity, range from 0.5 - 1.0mm.

In discussing shot quality, Almen (72) states that six factors are important, namely; size range, shot hardness, impact fatigue strength, shape, soundness and mass. In general the shot should be as hard as or harder than the work piece, otherwise the shot will lose energy due to deformation. The impact fatigue strength of commercial shot is quite low, thus, the rate of fracture is high. This emphasizes then, the need for efficient separation equipment to maintain acceptable grades in the shape of shot, as shown in Figure 3.5. Badly shaped media produces harmful surface effects and also affects the uniformity of peening. Soundness of shot is important in that hollow shot, which is quite common, will fracture more easily leading to early elimination from the process. The mass of the shot is obviously dependent on the shot material which has been discussed earlier.

- (iii) Shot_Velocity: Almen (72) states that shot velocity is dependent on shot size, hardness, mass and the direction of the shot's path relative to the work piece. Concerning the direction of the shot's path it has been found that the energy of the shot that is absorbed by the work varies approximately with the sine of the angle between the plane of the work and shot direction. This means that any change in the direction, for example due to work piece shape variations, requires a change in the shot velocity, to maintain uniformity of peening.

3.2 Effect of Shot Peening on Fatigue, Fretting Fatigue and Fretting.

3.2.1 Plain Fatigue.

It is well established that the shot peening of surfaces of

metals improves the fatigue life. In fact the primary use of shot peening in industry is for this purpose, although it is used also to prevent stress corrosion cracking of metal parts.

As pointed out by Almen (74), the surfaces of structural materials are much weaker in fatigue than are subsurface materials. He also explains the two theories as to why shot peening does improve fatigue life, viz:-

- (i) The compressive residual stress induced by shot peening inhibits fatigue fractures because they can only develop from tensile stresses.
- (ii) Shot peening strengthens the surface layer by work hardening.

Stulen et al (75), stated that there are differences in opinion as to why shot peening is capable of improving fatigue properties, i.e., is the residual compressive stress the major factor? They reported also that variations in peening conditions could affect the final fatigue improvements obtained.

Viglione (76) stated that the improvements due to shot peening varied with the type of fatigue cycling. He stated that shot peening improves the fatigue strength in bending or torsion, where the stress is at a maximum at the surface of a part subjected to axial loading.

Coombs et al (77) showed that the residual compressive stress produced in the surface by shot peening has the effect of increasing the intrinsic fatigue strength of the surface. They went on to investigate the effects of the different characteristics of shot peening i.e., shot velocity, energy and size, on the improvement in fatigue strength showing that each condition exhibited a saturation or optimum value. Also, by a process of material removal from the peened surface prior to fatigue testing they were able to investigate the depth of greatest effect of shot peening and how this varied with peening conditions. Results showed that no

matter which peening condition was varied, maximum fatigue life was found on specimens with 0.004 - 0.007 inches (0.1 - 0.18mm) removed from the surface by polishing, as shown in Figure 3.6, for variations in total energy of shot peening.

These results showed that the maximum improvement in fatigue life produced by shot peening is obtained basically when the surface is machined or 'smoothed' after peening, as shown in Figure 3.7. Another major observation from this paper was the surface damage caused by peening. It was found that softer materials could be 'overpeened' leading to surface damage and cracking which can form initiation points for fatigue cracks.

Arnold (78) states that the compressively stressed surface on a peened part is highly effective in preventing premature failure during fatigue. This is because the compressive stresses reduce the fibre stresses under load, and block the formation of fatigue cracks. He also points out that a component, of which the surface has been damaged prior to peening, does not have this impaired surface removed by the peening, but the process does compensate for the damage by improving surface quality. The surface defects still exist, but are 'submerged' in a compressive layer $250\mu\text{m} - 750\mu\text{m}$ in depth.

Graf and Verpoort (79) stated that in precipitation hardened alloys, slip bands can act as preferred initiation sites for fatigue cracks. They showed that during fatigue cycling, high slip steps are formed due to the inhomogeneous distribution of plastic deformation, which is determined by the interaction of moving dislocations with precipitate particles. It was then established that by homogenising the distribution of plastic deformation, i.e. by shot peening, a very fine slip distribution, and thus, low slip steps, was produced. Therefore the probability of producing a slip step of critical height to

initiate a fatigue crack is reduced. They also recognised the further advantages of shot peening for improving fatigue life, i.e. a local increase in yield stress and residual stress in the surface layers.

Morgan and Brine (80) investigated the use of shot peening as a means of preventing the severe loss in fatigue strength in aluminium alloy L.65 when plated with chromium. They found that chromium plating 'merely converts a plain test-piece into a notched one', due to different levels of internal stress between the coating and substrate, or the fact that cracks in the chromium plate propagate into the aluminium base metal. A compressively stressed layer induced into the substrate by shot peening was found to neutralize the tensile stress concentration at the root of the crack thus enabling the aluminium to sustain a higher applied stress without failure. As a result, the 60 per cent reduction in fatigue strength of the aluminium alloy due to the plating was completely eliminated.

A further related paper by Morgan and Mayhew (81) showed that shot peening had a similar effect on chromium plated titanium alloys. Two further observations made here concerning shot peening were; that overpeening could produce fatigue damage and also mask flaws such as fine cracks, thus pointing out that shot peening has to be carefully controlled; and that shot peening followed by heat treatment leads to some relief of the residual stress. Residual stress of surfaces also undergoes some relief or 'fading' due to fatigue cycling. Thus not only does residual surface stress affect fatigue, but also fatigue affects residual stress.

3.2.2 Residual Stress Relaxation due to Fatigue.

Investigations (82) into the effect of surface residual stresses on fatigue life showed compressive residual stresses improve fatigue life, but tensile residual stresses are detrimental. The stability of the residual stress during fatigue cycling was also considered and it was found that residual stresses hardly change when fatigue loading is near the fatigue limit, but, relaxation or 'fading' was noticed at cycling stresses above the fatigue limit. However in these tests the residual stresses were simulated by mean stresses which were assumed to be analogous. It was also found that softer materials were more susceptible to this fading.

By using the x-ray diffractometer technique for surface residual stress measurement, Esquivel and Evans (83) investigated this stress relaxation. They found that fatigue cycling did reduce the residual compressive stress induced by shot peening, and that this fading was directly related to the residual stress/depth profile, concluding that a large stress gradient was more susceptible to relaxation. This relaxation, they found, occurred early in the fatigue cycling process, after about 2.8×10^4 cycles. However, they did state that the precise mechanism for this phenomenon was not fully clear.

Boggs and Byrne (84) investigated the residual stress relaxation due to fatigue in two nickel-cobalt alloys using the x-ray diffractometer method. They found that fading of stress was a function of cycling, stating that the greatest relaxation was produced in the first 100 cycles. They also found that the work hardened layer produced by shot peening was not affected by the cycling. They concluded that residual stress fading due to fatigue was a dynamic

recovery process. They noted that alloys with a high stacking fault energy, and which therefore undergo easier dislocation movement, are more susceptible to this fading.

Leverant et al (85) conducted tests to measure residual stress relaxation on the alloy Ti - 6Al - 4V, at room and elevated temperatures. It was found that the residual stress decayed at all ranges of temperature, and that this decay was directly attributable to fatigue cycling. Further, tests done with imposed mean stresses, also showed residual stress relaxation, but in the case of the compressive mean stress, the relaxation was much more severe. From this it was concluded that the compressive mean stress superimposed on the residual compressive stress resulted in a total surface stress that exceeded the yield stress, thus providing the plastic deformation required for cyclic shakedown.

A consequence of fading is pointed out by Fuchs (86), who states that the often quoted analogy between mean stress and residual stress must be viewed with caution as, when fatigue tests are performed, particularly at cyclic stresses above the yield stress, the residual stress may disappear or be redistributed, whereas a mean stress will persist throughout the test.

3.2.3 Fretting and Fretting Fatigue.

Only a limited amount of work has been reported on the effect of shot peening on fretting and fretting fatigue compared to the effect on plain fatigue.

Liu et al (60) found in tests on a titanium alloy, that shot peening improved the fretting fatigue strength because the process cold worked the surface, raising the stress needed to initiate and

propagate cracks.

Bowers et al (64) found, using an aluminium alloy, that shot peening vastly improved the fretting fatigue strength. They stated that the fatigue damage produced by the rubbing of the specimen against a fretting pad would not propagate as long as the stress remained compressive. Metallographic examination showed evidence of cracks in the fretted region which had not propagated and failure often occurred away from the fretting pad, indicating that the shot peening had at least raised the fretting fatigue strength up to the plain fatigue strength. They explained that this effect was due to the inability of the cracks to penetrate the subsurface layer of compressive stress. Further they did state that the surface damage caused by peening results in a lower fatigue strength for the as-peened state when compared with that of the peened and polished state.

In tests on steels, Waterhouse and Saunders (87) found that shot peening improved the fretting fatigue strength of an austenitic stainless steel by almost 100%, whereas similar tests on a mild steel showed an improvement of only 22%. In both cases this improvement resulted in fretting fatigue strengths equivalent to or higher than the plain fatigue strength without peening. The greater degree of improvement on the stainless steel was said to be due to the high ductility and work hardenability of these steels, allowing a greater and deeper compressively stressed and work hardened layer, than in the mild steel. A further point made here was that a polished peened surface produces better fatigue results, as a peened surface contains many stress raisers.

A fretted surface undergoing fatigue is often said to be analogous to a notched specimen (24, p.135) under similar circumstances.

Indeed, fretting has also been compared to stress corrosion (64). Fuchs (88) shows schematically how a crack from a notch is arrested by a compressive residual stress, as shown in Figure 3.8. This emphasizes that a crack will not propagate as long as a compressive stress acts on it. In a later paper (86) he states that all crack-prone surfaces can have their fatigue strengths raised to that of smooth surfaces if a compressive residual stress is induced.

In the case of stress corrosion or corrosion fatigue, it was concluded by Baxa et al (89) that the residual compressive stress produced by peening resulted in a decrease in early (micro) fatigue crack propagation rates.

From this review of the literature in plain fatigue strength improvement by shot peening it can be said with confidence that the major factor is the compressive residual stress as opposed to the work hardening effect. The position with fretting fatigue is not so clear: with fretting a wear phenomenon is involved and as hardness has a direct influence on wear, the work hardening effect produced by shot peening may play an important role.

The mechanical properties of three stress-aging conditions are shown in Table 4.3. The treatments were selected to show the behaviour of the hardest, 'active' and softest form of the alloy. Heat treatment was carried out in an air-circulation furnace after final specimen machining.

4.1.2 Surface Treatment

In this work three types of surface treatment have been investigated, viz:

- (1) Unpeened - After heat treatment the specimen gauge lengths were polished

CHAPTER FOUR

EXPERIMENTAL PROCEDURE

The outline of the experiments performed in this work is shown in Figure 4.1. Basically the plan consists of three sections, namely; the mechanical testing; surface analysis; and post testing procedures.

4.1 Materials and Treatments.

The material used throughout this work was an aluminium based alloy, Al - 4%Cu - 1%Mg, of which the exact composition is shown in Table 4.1.

4.1.1 Heat Treatment.

This alloy, as mentioned previously, is an age hardenable alloy and as such was tested in three different heat treated forms as described in Table 4.2.

The mechanical properties of these three aging conditions are shown in Table 4.3. The treatments were selected to show the behaviour of the hardest, 'medium' and softest form of the alloy. Heat treatment was carried out in an air-circulation furnace after final specimen machining.

4.1.2 Surface Treatment.

In this work three types of surface treatment have been investigated, viz;

- (i) Unpeened - after heat treatment the specimen gauge lengths were polished

using successively finer grade silicon carbide papers, using water as lubricant, with a final polish of 00 grade emery paper.

- (ii) Shot peened (smooth) - after heat treatment the specimen gauge lengths were shot peened. After peening the rough dimpled surface was removed by polishing as above to a finish of 00 emery paper. It was ensured that polishing was taken no further than the base of the surface dimples.
- (iii) Shot peened (rough) - after heat treatment the specimen gauge lengths were shot peened, and the rough dimpled surface was not treated further.

All the polishing was done slowly by hand to ensure that there were no increases in temperature and that the surface properties were unaffected by the polishing.

The shot peening intensity was determined on a type A Almen test strip. The archeight was in the range 0.012 - 0.016 A. The average shot size used was 0.84mm.

4.2 Plain Fatigue and Fretting Fatigue Tests.

4.2.1 Specimens.

The design of the specimens used for the plain fatigue and fretting fatigue tests is shown in Figure 4.2. Essentially the specimens were 35.5cm long and 9.5mm in diameter with two machined flats (gauge length) in the centre. The flats were 28.5mm long and 6.35mm apart, with a 50mm radius machined at the end to reduce any stress concentration due to a sudden change in cross sectional area. The positioning of the flats ensured that they were within the constant bending moment region of the fatigue machine.

The fretting bridges are shown schematically in Figure 4.3 (a). They were 19.05mm in length and 6.35mm wide. Each bridge had two

fretting feet measuring 2.4mm x 6.35mm on the base, and a counter sunk notch on top to facilitate the fitting of the proving ring (see section 4.2.2).

Prior to the testing all the specimens were hand polished as previously described, except the shot peened (rough) specimens, and all specimens were degreased in inhibisol.

in Appendix B.

4.2.2 Testing Equipment.

All the plain fatigue and fretting fatigue tests were performed on a four point loading rotating-bending machine. The fatigue specimen was held by four bearings, of which the outer two were fixed rigidly to the machine, while the inner two were constructed to subject the specimen gauge length to a bending moment. This is shown schematically in Figure 4.4, and the machine as a whole is shown in Plate 1a.

While subject to the bending moment, the fatigue action was produced by rotating the specimen by means of a vee-belt drive and pulley system connected at one end via a drive shaft and rubber coupling. The system was powered by a 186.5 watt electric motor, at a speed of 1450r.p.m. At the opposite end, the specimen was connected to a counter mechanism, which recorded the number of revolutions, hence the fatigue cycles. The machine was fitted with a microswitch cut-out system located under one of the central bearing housings. The action was such that when the specimen failed, the applied load caused the broken end to fall, and an attachment on the bearing housing operated an electrical contact which cut the power to the motor. The machine thus ceased rotation and the number of fatigue cycles could be read off from the counter.

The fretting action was produced by fitting fretting bridges

to the specimen gauge length by means of a proving ring, as shown in Figure 4.3 (b) and (c) and Plate 1b. The fact that the bridges themselves were not directly subjected to the applied load, lead to relative movement between the bridges and the specimen. The calculation of the bending stress in the specimen is shown in Appendix A, and the determination of the amplitude of slip produced by this mechanism is shown in Appendix B.

4.2.3 Testing Procedure.

Plain fatigue and fretting fatigue tests were carried out on all the heat treatment and surface treatment combinations previously described (with one exception; fully annealed, shot peened - rough) to obtain sufficient data to construct S - N curves.

During testing the specimen was held in the bearings by means of tapered collets, which were positioned and tightened on the specimen in a jig prior to loading onto the fatigue machine. All plain fatigue and fretting fatigue tests were carried out on the one machine, and all tests were continued until the failure of the specimen or until a run out value of 10^7 cycles had been reached.

All the tests were carried out under normal laboratory conditions. Temperature and relative humidity were recorded but not controlled. The average temperature was 22°C and the average relative humidity was 64%. In all the fretting fatigue tests a contact pressure of 32MPa was used. This was determined by previously calibrating the proving ring on a Mayes tensile testing machine, for load applied against change in diameter of the proving ring as shown in Appendix C.

In each test the heat treatments of the specimens and bridges were matched. However, no bridges were shot peened, and so their surface

finish was always the same i.e. unpeened, polished to 00 grade emery paper, and degreased in inhibicol.

After the test was completed, the specimens were removed from the machine, usually by cutting well away from the gauge length. In the case of the fretting fatigue tests the bridges and proving ring were carefully removed. All specimens were retained for subsequent examination.

4.3 Plain Fretting Tests.

4.3.1 Specimens.

The specimens used for the plain fretting tests were the spherical rider and stationary flat type, the dimensions of which are shown in Figure 4.5. The specimens were machined from what had previously been untested fatigue specimens of the type described in section 4.2.1. The stationary flat was machined from the gauge length section, and was 50mm long by 9mm wide with a thickness of 3mm. Two holes 40mm apart were introduced to enable attachment to the fretting machine. The spherical rider was manufactured from a non-machined section of the fatigue specimen, having a diameter of 9.5mm and radius at the rider tip of 100mm. The total length was 30mm, of which part comprised an M6 size screw thread for fitting to the fretting machine.

In the case of the shot peened specimens, the peening was done on the fatigue specimen prior to the manufacture of the rider and flat from it. As in the fretting fatigue tests the heat treatments of the rider and flat were matched in each test. For testing the shot peened surfaces, only the flat was subjected to peening. Except for the tests on the shot peened rough surface, all the specimens were

polished to 00 grade emery paper and degreased in inhibisol prior to testing.

4.3.2 Testing Equipment.

Plain fretting tests were performed on a sphere-on-flat testing machine as described by Overs (90) and adapted by Hamdy (91). This equipment enabled the occurrence of plain fretting between the spherical rider and the flat specimen, with the added facility of measuring and recording the friction force and normal contact force simultaneously.

The principle elements of this equipment are shown schematically in Figure 4.6 and also Plate 2. These are:-

- (i) The oscillating movement system,
- (ii) The oscillating movement control and measuring arrangement, and
- (iii) The friction and normal contact force measuring and recording equipment.

(i) The Oscillating Movement System - (Plain Fretting Machine).

This system is shown in detail schematically in Figure 4.7. Its function was to produce oscillatory tangential relative movement between the rider and flat specimens. Essentially it consisted of an S - shaped transmission shaft, to which the rider was fixed at one end. The other end was connected to the driving spindle of a Goodman's electromagnetic vibration generator, model 390 A. A power amplifier with a built in, low distortion oscillator was used to drive the vibration generator and so produce the oscillatory motion of the driving spindle, which was transmitted via the transmission shaft to the rider.

The transmission shaft was shaped so that the point of application of the tangential friction force between the rider and the flat

specimen was in line with the main centre line of the shaft and the driving spindle. The shaft itself was hollow, as it had sometimes been used for high temperature work, requiring cooling water to be circulated inside it. At the reduced shaft wall thickness in this portion, the strain gauges were attached. These were used for the detection of frictional and normal forces. Eight strain gauges were used.

The vibration generator was supported on a horizontal hinged support which could be tilted in the vertical plane by using an adjusting screw and nut mechanism, thus enabling easy and accurate positioning. A steel plate was attached to the transmission shaft to present a gap between the shaft and the fixed probe.

(ii) The Oscillating Movement and Control System.

The vibration generator was driven by a Ling Altec 5 VA power oscillator, enabling control of slip amplitude and frequency of the fretting motion. A Wayne Kerr vibration meter, model B731B was used for the measurement of the slip amplitude.

When the probe connected to the vibration meter was brought into proximity with the steel plate attached to the transmission shaft, the capacitance so formed was displaced in terms of distance and peak to peak vibration amplitude on the two meters of the instrument.

(iii) Friction and Normal Contact Force Measuring and Recording Equipment.

Eight strain gauges, bonded to the outer surface of the transmission shaft, were used to detect the frictional and normal contact forces produced at the fretting site. The arrangement of the strain gauges, both in position and electrical connection enabled the measurement of frictional force and normal contact load simultaneously and

independently at the fretting site. The output signals from the strain gauge measuring equipment were amplified using a multichannel amplifier, and fed into a U - V recorder; a direct recording Visicorder oscillograph, model 2106.

4.3.3 Calibration of Equipment.

It must be stated here that for the original work on this equipment many calibrations were performed by Hamdy (91) to ensure accuracy, validity and reproducibility of the results from it. In subsequent work, including this research, these original calibrations have been taken as valid, and so, with one exception, have not been repeated. The one exception; the calibration of the relationship between frictional force and normal contact load, was repeated using spring balances, the arrangement of which is shown in Appendix D.

4.3.4 Testing Procedure.

Plain fretting tests were conducted on the age hardened and naturally aged forms of the alloy in all the surface treatments previously described.

After preparation as described in section 4.3.1, the rider was fixed securely onto the transmission shaft with a locking nut, and the flat was positioned on the holder using two screws. The rider was then carefully lowered onto the flat using the tilting mechanism, until the required normal contact pressure was reached, indicated on the U - V recorder. The friction force arrangement was then set, and the machine started. After the required number of cycles the machine was stopped, the specimens carefully removed and retained for subsequent examination.

All the tests were performed under the same conditions, i.e;

Frequency	= 25Hz.
Slip Amplitude	= 30 μm .
Number of Cycles	= 2×10^6 .
Contact Pressure	= 32MPa (maximum).
Average Temperature	= 22°C.
Average Relative Humidity	= 64%.

These conditions were chosen so as to be as close as possible to the conditions of a high cycle fretting fatigue test.

4.4 Surface Analysis.

In order to assess the effect of surface treatment on fatigue crack initiation due to fretting it was important to analyse the surface properties both before and after testing. As shot peening was used as the special surface treatment, tests were done to examine the effects of residual compressive stress, work hardening and surface roughness.

4.4.1 Residual Stress Measurement by X-Rays.

The measurement of residual stress in surfaces by X-rays was first outlined by Norton and Rosenthal (92) and is described in detail by Hilley et al (93). This method, known as the 'two exposure' method relies upon the elastic strain being measured in terms of changes that occur in the lattice spacing (d) in the specimen surface. When changes in d occur this affects the diffraction angle θ and since strain is related to stress, the stress can be calculated from measurements of changes in θ .

The technique requires two X-ray exposure runs, one at an

angle of incidence (ψ) of 0° to the surface normal, and one at another angle, usually 45° , ($\psi 45$) as shown in Figure 4.8. Then from the standard equation relating stress to strain;

$$S = \left(\frac{E}{1 + \nu} \right) \left(\frac{1}{\sin^2 \psi} \right) \cdot \frac{d\psi - d\psi_0}{d\psi_0} \quad \dots(4.1)$$

Where;

S = Residual Stress.

E = Young's Modulus.

ν = Poissons Ratio.

$d\psi$ = d Spacing at ψ° to Surface Normal.

$d\psi_0$ = d Spacing at 0° to Surface Normal.

Which for convenience simplifies to;

$$S = \left[\frac{E}{1 + \nu} \cdot \frac{1}{\sin^2 \psi} \cdot \frac{\cot \theta_0}{2} \cdot \frac{\pi}{180} \right] \cdot 2(\theta_1 - \theta_\psi) \dots(4.2)$$

Where;

θ_0 = Diffraction Angle of a Stress Free Surface.

θ_1 = Diffraction Angle at Incidence 0° .

θ_ψ = Diffraction Angle at Incidence ψ° .

The quantity in the square brackets in equation (4.2) is a constant called the stress factor, K .

$$\text{Thus; } S = K \cdot 2(\Delta \theta) \quad \dots(4.3)$$

producing S as a function of the shift of diffraction angle between the two exposures.

4.4.1.2 X-Ray Equipment.

X-ray tests in this work were performed using the back reflection film technique. The X-ray generator and camera used were of the Seimens Kristalloflex 4 Diffractometer system. The camera construction with the specimen inserted is shown in Plate 3. This camera was so constructed to enable the positioning of the specimen such that the exposure of X-rays from any angle was incident at the same point on the specimen. This was done by adjustments with the microscope and goniometer head.

4.4.1.3 Specimen Preparation for Stress Depth Profiles.

Since a large part of the thesis is concerned with the propagation of fatigue cracks from a fretted surface, it was necessary to determine how the residual compressive stress from the peening operation varied with distance from the surface. This meant that the residual stress had to be measured at various depths from the original surface by means of systematically removing surface layers and then taking a stress measurement. This was done by recording the initial thickness of the specimen by micrometer, immersing in a chemical polishing solution for layer removal, and then checking the thickness again. After the appropriate amount of material had been removed an X-ray measurement was taken. The procedure was repeated until the residual compressive stress had been reduced to zero.

The polishing solution used was 20% NaOH in water at 50°C, which provided a removal rate of approximately 10 μ m per minute. The resulting surface using this solution, however, was coated with a black scale, but this was removed by an instantaneous dip into a 50% HNO₃ aqueous solution.

4.4.1.4 Test_Procedure.

In all the X-ray tests done in this work the same procedure was used, i.e. the back reflection film method.

Prior to mounting in the camera, the specimen surface was smeared with a silver powder/petroleum gel mixture as a standard for accurate film to specimen distance measurement. The specimen was then placed in position in the camera as shown in Plate 3. The exact positioning of the specimen was done by trial and error; rotating the goniometer stage through -45° - $+45^{\circ}$ while viewing the specimen through the cross wires of the adjusting microscope. The microscope was then removed and the camera fitted onto the X-ray generator for exposure. For each exposure the same conditions were used, viz;

Cu K_{α} radiation.

Wavelength = 1.54178\AA .

Voltage = 40 KV.

Exposure time = 90 mins.

Diffraction plane (hkl) = (422)

Diffraction angle 2θ = 137.6° .

Current = 20 mA.

After exposure the film was removed and developed. As previously described, two exposures of each specimen were required. In all cases the incident angles ψ were 0° and 45° . After developing, the films were processed using a photo microdensitometer to obtain the diffraction ring diameters and subsequently the difference in diffraction angle peak $\Delta 2\theta$. This quantity was then applied to equation 4.3 using

a K value previously determined at 162.2 MPa/deg 2θ , thus obtaining the value of the residual stress.

In the case of the stress/depth profiles, the actual results obtained for stress had to be corrected to allow for the stress change due to surface layer removal. This procedure was done by computer programme, based on the theory proposed by Moore et al (94), the readouts of which are shown in Appendix E.

4.4.2 Work Hardening Analysis.

4.4.2.1 Microhardness Traverses.

In order to determine the degree and depth of work hardening produced by shot peening, microhardness traverses were obtained for all the specimen treatments.

This was done by producing sections from samples of untested fatigue specimens for all the treatments studied. The sections were then mounted in cold setting resin, with a support specimen at the side. The sections were polished to 1 μ m grade diamond surface finish. The purpose of the support specimen was to ensure that the edge of the specimen under investigation did not develop a rounded surface due to preferential removal of surrounding resin. This would have resulted in non uniform indentations when measuring the microhardness.

The microhardness traverses were performed on a Vickers microscope with microhardness attachment comprising a diamond pyramid microhardness indenter.

One problem encountered here was that due to the fact that the diamond indenter obviously had a finite width, it was impossible to obtain hardness readings at the very edge. The smallest depth at

which accurate measurements could be made was $\sim 50 - 100 \mu\text{m}$, and so extrapolation was used for the immediate surface regions.

4.4.2.2 Testing of Stretched Specimens.

Although it is well established that residual compressive stress due to shot peening is the major factor in improving plain fatigue strength, the contribution of work hardening cannot be dismissed, especially where fretting fatigue is involved. Therefore tests were done on specimens on which attempts had been made to remove the residual compressive stress, while leaving the work hardening unaffected. This was done by introducing a degree of plastic deformation into the specimen in the form of a stretching operation.

The stretching was done on an Instron tensile testing machine with extensometer attachment. Degrees of 0.5 per cent and 1.0 per cent plastic deformation were introduced into a series of as-peened age hardened specimens. The stretching was done on as-peened specimens so that subsequent polishing removed any damage made by the extensometer knife edges.

After stretching the specimens were analysed for residual compressive stress and work hardening, and then tested in plain fatigue and fretting fatigue by the methods already described.

4.4.3 Surface Roughness Analysis.

4.4.3.1 Talysurf Measurements.

Talysurf measurements were made using 'Talysurf 4' equipment, to assess the surface roughening produced by the shot peening treatment. This enabled also the Centre Line Average (C.L.A.) to be recorded.

4.4.3.2 Microscopy.

Both optical microscopy, using a Reichert Nr 265133 model optical microscope, and scanning electron microscopy (S.E.M.), using a Cambridge 600 Stereoscan, were performed to examine directly the surface morphologies produced by shot peening. Optical microscopy was used to examine sections through the peened surfaces, and S.E.M. was performed directly on the treated surfaces.

4.5 Post Testing Analysis.

After testing under conditions of plain fatigue, fretting fatigue and plain fretting, further analysis was performed on selected specimens to obtain information on the influence of shot peening on the fretting and fatigue properties of the material.

4.5.1 X-Ray Residual Stress Analysis.

X-ray residual stress analysis, using the technique previously described, was performed on tested fretting fatigue specimens in areas of fretting fatigue; i.e. on the fretting scar; and in areas of plain fatigue: i.e. away from the fretting scar, to establish whether or not fretting fatigue or plain fatigue resulted in the following:

- (i) Induced residual stress - primarily in the unpeened specimens; or
- (ii) Residual stress relaxation in the shot peened specimens.

The measurements were performed in directions both parallel and perpendicular to the axis of the fatigue stress and fretting direction. It was found that the difference in stress value resulting from the measurements in the two directions was negligible.

Prior to the measurements on the fretting fatigue scars, the specimens were immersed very briefly in a 50% HNO_3 aqueous solution to remove the fretting debris, which had earlier been found to adversely affect the X-ray photograph. Preliminary tests were done on dummy specimens to ensure that this immersion did not affect the residual stress situation.

4.5.2 Optical Microscopy.

Optical microscopy was used to examine sections through fretting fatigue scars. The specimens for examination were sectioned longitudinally, i.e. parallel to the fretting direction, through the fretting fatigue scar, thus exposing the material directly underneath the scar. The sections were mounted in cold setting resin and polished to 1 μm diamond grade for examination in the unetched condition.

4.5.3 S.E.M. Analysis.

Extensive S.E.M. analysis, using the Cambridge 600 Stereoscan and Jeol 35C microscopes, was undertaken to examine certain features of the tested specimens, viz:

- (i) Fretted surfaces; the fretted surface regions of both the fretting fatigue and plain fretted specimens were examined. This was done to examine the morphologies of the fretted surfaces and to study the effect of the shot peening treatment on these morphologies.
- (ii) Fretting fatigue sections; sections through fretting fatigue specimens similar to those used for optical microscopy, except without the mounting resin, were observed. These specimens were prepared in some cases by careful sectioning and polishing, and in other cases by simply

removing the mounting material from one of the optical microscopy specimens. This type of specimen enabled the examination of the fretting scar and subsurface material simultaneously.

Prior to S.E.M. examination all the specimens were ultrasonically cleaned in inhibisol and then coated with a thin evaporated carbon film.

4.5.4 Talysurf Traces.

Talysurf traces were made on the fretted regions of selected fretting fatigue and plain fretted specimens in all the surface treatments used. This enabled comparison of surface roughness before and after testing.

4.5.5 Summary of Experimental Procedure.

A summary of the experimental work undertaken here is shown in Table 4.4. This table shows the tests and analyses done on each particular specimen treatment (marked by ●).

5.2 Plain Fretting Tests

The quantitative results of the plain fretting tests are in the form of coefficient of friction (μ) measurements, plotted against the number of fretting cycles, to show how the friction force varied during the test. Figures 5.10 and 5.11 show these plots for the two

CHAPTER FIVE

RESULTS

The results of the experimental work are presented in the same format as used in the previous chapter.

5.1 Plain Fatigue and Fretting Fatigue Test Results.

Results of the plain fatigue and fretting fatigue tests are presented in the form of S - N curves. These are shown in Figures 5.1 to 5.7. To facilitate the assessment of how the shot peening has affected the plain fatigue and fretting fatigue strengths, the curves are replotted in Figures 5.8 and 5.9 in compilation for each heat treatment. To summarize these results, Table 5.1 has been constructed to show, in percentages, the reductions in fatigue strength due to fretting, and the subsequent improvements produced by shot peening. Examination of these results shows the age hardened alloy to be much more susceptible to both the reduction in fatigue strength due to fretting, and the improvement afforded by shot peening, than the other heat treated forms. A notable observation also is that in all cases the shot peening improved the fretting fatigue strengths to levels equal to or above the plain fatigue strength of the unpeened material.

5.2 Plain Fretting Tests.

The quantitative results of the plain fretting tests are in the form of coefficient of friction (μ) measurements, plotted against the number of fretting cycles, to show how the friction force varied during the test. Figures 5.10 and 5.11 show these plots for the age

hardened and naturally aged alloy, in all three forms of surface treatment.

In general, the patterns of the friction behaviour of the two heat treatments were similar, varying only in degree. The unpeened alloys showed a steady increase in μ which levelled off at a value of approximately 1.6 after $\sim 2 \times 10^5$ cycles. For the shot peened (smooth) alloys, after initial increases up to ~ 1.5 , μ decreased. A similar trend was found for the shot peened (rough) forms, but the rates of change were much more abrupt, especially for the age hardened alloy. On average, the final μ values of the shot peened treatments were 30 - 40% lower than the unpeened ones.

5.3 Surface Analysis.

5.3.1 Residual Stress Analysis.

In the case of the pre-testing residual stress analysis, the results are presented as residual stress/depth profiles. Figure 5.12 shows the profiles for the age hardened and naturally aged alloy, in the unpeened and shot peened (smooth) forms. The results reported here have been corrected for stress relief due to surface layer removal, as explained in the previous chapter. These results show that the naturally aged material developed a slightly higher residual stress due to shot peening. For both heat treatments, maximum stress was reached 100 - 200 μm from the surface with values of 230 - 250 MPa. The approximate depth of penetration of compressive stress was 650 μm .

The unpeened alloys showed surface stresses of 100 - 150 MPa, but significant stresses were not detected at depths greater than 50 μm .

For the fully annealed material, stress/depth profiles were

not obtained, but surface stress was measured giving values 59 MPa and 5 MPa for the shot peened and unpeened conditions respectively. This would imply a maximum residual stress in the subsurface of the shot peened material of around 75 MPa.

5.3.2 Work_Hardening_Analysis.

5.3.2.1 Microhardness Traverses.

Results from the microhardness tests are presented as hardness/depth profiles for all the treatments used, and are shown in Figure 5.13. The plots show that for the age hardened alloy, the bulk material hardness was 140 VHN, but the shot peening increased the subsurface hardness to a measurement value of 240 VHN, extrapolated to ~ 280 VHN at the surface. For this alloy treatment the depth of the work hardened layer was approximately $1,000\mu\text{m}$.

In the case of the naturally aged alloy, the bulk material hardness was 125 VHN, and the maximum measured subsurface value was 220 VHN, extrapolated to around 260 VHN for the immediate surface value. The depth of the work hardened layer for this treatment was $\sim 1.4\text{mm}$.

The fully annealed alloy produced much lower results, the bulk material having a hardness of 61 VHN, rising to 105 VHN in the subsurface. The depth of the work hardened layer was approximately $350\mu\text{m}$.

5.3.2.2 Testing of 'Stretched' Specimens.

The results of the plain fatigue and fretting fatigue tests on the age hardened alloy stretched 0.5% and 1.0%, are presented as S - N curves in Figure 5.14. Also plotted here for comparison are the

equivalent curves for the unpeened alloy and the shot peened (smooth) alloy.

Comparing these curves shows the stretching action to have almost completely removed the beneficial effect of the shot peening. Both degrees of plastic deformation give similar values, showing that the plain fatigue and fretting fatigue lives of the stretched specimens were comparable with those of the unpeened specimens.

Microhardness traverses on similarly stretched specimens confirmed that the work hardening was unaffected by the stretching operation, producing results similar to those shown for shot peened specimens in Figure 5.13. Residual stress measurements gave values of 49 MPa and 44 MPa for the 0.5% and 1.0% specimens respectively. These measurements having been taken at the surface, implied that more than 75 per cent of the residual stress was removed by the stretching procedure.

5.3.3 Surface Roughness Analysis.

5.3.3.1 Talysurf Traces.

Typical talysurf traces for the polished finish and shot peened (rough) finish are shown in Figure 5.15. These plots clearly illustrate the much rougher as-peened surface, especially considering that the polished specimen trace has double the vertical magnification of the other. The roughness span of the as-peened surface shown here is $\sim 60 \mu\text{m}$ as compared with $\sim 5 \mu\text{m}$ for the polished surface. More accurate data was obtained by measurement from ten specimens of each surface finish and this gave the following results:

C.L.A for polished finish = $0.13 \mu\text{m}$.

C.L.A for as-peened finish = $6.56 \mu\text{m}$.

Thus the as-peened material is approximately 50 times more rough.

5.3.3.2 Microscopy.

Micrographs from S.E.M. observation of the shot peened (rough) surfaces are shown in Plate 4. Dimples formed by the peening operation are approximately $200\mu\text{m}$ maximum in diameter. The higher magnifications show further peening damage, where it was apparent that 'folding' or layering of material had taken place.

Optical micrographs (a) and (b) in Plate 5 confirm this observation showing definite material layering. Plate 5 (c) shows a shot peened (smooth) specimen section, which still appears to have some subsurface damage, even after polishing.

5.4 Post Testing Analysis.

5.4.1 Residual Stress Analysis by X-Rays.

The results from the X-ray residual stress analysis on the tested alloys shown in Figures 5.16 and 5.17, as plots of residual compressive stress against number of fatigue cycles.

Figure 5.16 shows that for the unpeened age hardened alloy, any residual stress in the immediate surface had been detected in the pre-fatigue test material was soon reduced. In the case of plain fatigue cycling the stress, after falling to $\sim 50\text{ MPa}$ after 10^4 cycles was unaffected by further stress cycles. However, for fretting fatigue a definite increase in residual stress was observed at a fatigue life $> 10^5$ cycles after initially falling in a similar manner to that during plain fatigue cycling.

For the shot peened age hardened alloy, residual stress

relaxation was observed in both plain fatigue and fretting fatigue. However, the degree of relaxation caused by fretting fatigue was much higher at equivalent numbers of cycles; a reduction of approximately 75 per cent of the original surface stress was caused by fretting fatigue cycling, but only 25 per cent fading was caused by plain fatigue cycling.

A similar pattern of results was found for the naturally aged specimens, except that on the unpeened material the fretting fatigue cycling showed a much lower tendency to induce any residual stress.

5.4.2 Optical Microscopy.

The results from optical metallography can be divided into two general groups, i.e. observations of sections through the fretted areas of the unpeened alloy treatments, and of the shot peened ones.

Plate 6 shows a series of micrographs of the unpeened naturally aged alloy. The microcracks seen are typical of fretting cracks, initiating at approximately 45° to the surface and eventually moving to 90° , i.e. at right angles to the direction of the alternating stress. Plate 7 (a) and (b) show micrographs of the shot peened (smooth) naturally aged alloy. Here it is clearly seen that the microcracks travel for some distance parallel to the surface, before diverting to the more usual 45° and 90° paths. In 7 (c), which was a run out age hardened specimen, the microcracks all appear to have been arrested at a depth of $< 40 \mu\text{m}$, and in one case, the crack has been redirected toward the surface.

Plate 8 shows a selection of micrographs from the age hardened alloy of both unpeened and shot peened (smooth) finishes. Again the unpeened specimens showed the typical fretting fatigue cracks,

whereas, in the peened specimens the cracks initiated at much shallower angles. 8 (d) also shows evidence of delamination at the surface.

Plate 9 shows a comparison between the cracks found in the unpeened and shot peened (smooth) fully annealed alloy. Again the angle of initiation of the cracks in the shot peened form were at a much lower angle to the surface, but the depth at which the cracks changed direction was much nearer to the surface than for the other heat treatments. Plate 12 shows a series of micrographs of a shot peened

(smooth) Measurements of angles to the surface of initiated fretting fatigue cracks on a series of ten miscellaneous specimens of both unpeened and shot peened (smooth) finishes showed average values of 48° and 29° respectively.

Plate 10 shows a further kind of damage observed on the fully annealed material. 10 (a) shows the subsurface damage produced by shot peening prior to testing, and 10 (b) and (c) show the type of fretting fatigue damage that probably occurred in these regions. It would seem that the volume of material that has been damaged by the shot peening has been lifted out and a crack has propagated from the resulting pit.

5.4.3 S.E.M. Analysis.

(i) Sections;

Results of the S.E.M analysis are presented first of all by micrographs of the sections through the fretting scars on selected fretting fatigue specimens. From these it was possible to observe the initiation of cracks from the surface through to the subsurface material.

Plate 11 shows micrographs of an unpeened naturally aged

specimen. 11 (a) and (b) show an oblique view to give an indication of the surface roughness, while (c) and (d) show a more direct observation of the scar and section through it. From these it can be seen that the initiation of the cracks occurred close to the fretted/unfretted boundary, and that the initiation region extends along the length of this boundary. Also, there is evidence of delamination in the fretting scar shown in Figure 11 (d).

Plate 12 shows a series of micrographs of a shot peened (smooth) naturally aged specimen. These show clearly a 'lip' formed at the crack initiation region, arising from the low angle of inclination of the crack to the surface. However, this 'lip' was shorter here than those observed by optical microscopy, even allowing for the oblique viewing.

Plate 13 shows a series of micrographs of a shot peened age hardened specimen, taken at the edge of the fretting scar. 13 (a) clearly shows that the crack ran the length of the fretting/non-fretting boundary, and also that the fretting scar had many areas of delamination. 13 (b) shows the crack initiation region, unfortunately masked slightly by debris, but clearly the crack has propagated at a shallow angle to the surface for a short distance. An interesting feature here was the first evidence of subsurface cavity formation at the depth of about $5 - 10\mu\text{m}$ as shown in 13 (b) and (c).

Further, more convincing evidence of this subsurface cavity formation is shown in Plate 14. This shows a series of micrographs of a shot peened naturally aged specimen taken near the centre of the fretting scar. Clearly a cavity had formed, approximately $10\mu\text{m}$ below the fretting surface and had opened up slightly. From the ends of the cavity, cracks were evident moving parallel to the surface. 14 (c)

shows debris to be contained within the cavity and to have a characteristic spherical shape, 1 - 2 μm in diameter.

Plate 15 presents micrographs again of a shot peened (smooth) naturally aged specimen, showing large areas of delamination, with one particular layer approximately 10 μm in thickness. Debris was also detected under this delaminated layer. It must be pointed out that cavity formation and delamination of this degree were not detected in any of the unpeened specimens.

A further kind of damage detected only on shot peened specimens is shown in Plate 16. In this case the specimen was a naturally aged specimen with a shot peened (rough) finish. It appeared that the crack had initiated and was subsequently packed with fretting debris. Plate 17 shows a similar effect on a naturally aged shot peened (smooth) specimen, except that one of the crack sides and the initiation region were not clearly discernible.

(ii) Fretting Scars (Fretting Fatigue Specimens).

Plate 18 shows a comparison of two typical fretting scars. 18 (a) is from a naturally aged unpeened specimen showing the two edges of the scar with a crack running the length of the scar near the fretted/non-fretted boundary. 18 (b) shows the scar of a shot peened (smooth) age hardened specimen. Although no crack was evident here, there was a greater proportion of delamination areas, and also an unusual 'fish bone' configuration made up of parallel ridges in the central region of the scar.

Plate 19 shows examples of the fretting debris found on the unpeened specimens. 19 (a) and (b) show the general surface distress, but 19 (c) and (d) show another unusual feature, where the oxide film

had broken up along lines parallel to the fretting direction. Plate 20 shows further examples of the damage on a naturally aged unpeened specimen. Smearing of material and debris break-up are evident in 20 (a) and (b), and also cracking of the oxide film in 20 (c).

Plate 21 shows micrographs of the typical fretting debris found on shot peened specimens, in this case from a naturally aged shot peened (rough) sample. Extensive delamination is evident in 21 (a) and the higher magnifications of 21 (b) and (c) show cavities exposed when delamination plates are dislodged from the fretting surface. These cavities are approximately $10\mu\text{m}$ into the surface and contain spherical debris, $1 - 2\mu\text{m}$ in diameter. Plate 22 shows further damage on the same specimen, where the 'fish bone' configuration was again observed.

Plate 23 shows fretting debris on an age hardened shot peened (smooth) specimen. Again exposed cavities were found containing spherical debris of similar size to that previously observed.

(iii) Fretting Scars (Plain Fretting Specimens).

Plate 24 shows micrographs of fretting debris on a naturally aged unpeened specimen. 24 (a) and (b) clearly show that material has been caused to smear over the surface. 24 (c) and (d) show also that some delamination has taken place, and a cavity has been exposed. However, no spherical debris was detected in the cavity. Plate 25 shows similar observations made on an age hardened unpeened specimen.

Plate 26 presents the typical damage produced in plain fretting on shot peened (smooth) surfaces. In this case the specimen was naturally aged, showing much more delamination and less smearing, when compared with the unpeened specimens. Exposed cavities were found to include spherical debris as shown in 26 (b) and (c).

Plate 27 shows micrographs from an age hardened shot peened (smooth) specimen, which had a high proportion of delamination, with plates up to $200\mu\text{m}$ in size having been produced.

Finally, Plate 28 shows typical plain fretting damage produced on the shot peened (rough) surfaces. Clearly the fretting resulted in some levelling of the rough surface, and has even caused some delamination on these levelled areas, as shown in 28 (c).

A general observation from the plain fretting tests was that the fretting scars on the peened specimens were 2 - 3 times larger in area than on the unpeened specimens, even though all testing conditions were similar.

5.4.4 Talysurf Traces.

Talysurf traces taken from the plain fretting scars of the three treatments tested are shown in Figure 5.18 with arrows marking the scar boundaries. The most striking point again is the difference in size of the scar on the unpeened specimen to those of the shot peened ones. The shot peened (smooth) specimen scar is not only larger, but much rougher; an observation consistent with the S.E.M. analysis. For the shot peened (rough) specimen some slight flattening of the 'peaks' within the scar boundaries can be detected, and this is also consistent with S.E.M. observations.

CHAPTER SIX

DISCUSSION

6.1 The Effect of Fretting on Fatigue.

The detrimental effect of fretting on fatigue strength has been shown clearly in all the fretting fatigue tests performed. It was also evident that the age hardened material in the unpeened state was much more susceptible to the effect of fretting. However, as fretting influences the fatigue strength in a similar way to the effects produced by a notch, this observation on the age hardened alloy is not surprising as high strength precipitation hardened materials have a high notch sensitivity.

Overall, of the three heat treatments tested in this work, the naturally aged condition proved to be the stronger in both plain fatigue and fretting fatigue.

6.2 The Effect of Shot Peening.

(i) On the Material Surface.

The analysis of the shot peened surfaces was carried out to show the extent of the three main conditions produced by shot peening.

Considering the results from the microhardness traverses it was clearly shown that the naturally aged material had a higher propensity for work hardening. This is due to its higher ductility as shown by its elongation in Table 4.3. Although the final hardness of the work hardened layer of this material was not as high as the age hardened material due to its lower initial hardness, the actual hardening

increment that took place was higher, approximately 80%, as compared with the age hardened form, $\sim 70\%$. The depth of the work hardened layer, also, was much greater for the naturally aged condition, thus emphasizing this point.

These results lead to an explanation of the data for the residual stress/depth profiles. As the residual stress produced by shot peening is the result of the elastic recovery of the material surrounding the plastically deformed areas, then for a higher degree of plastic deformation, a greater residual compressive stress is to be expected. This was indeed the case for the present work, with the naturally aged material showing a higher residual compressive stress and a greater depth of penetration when compared to the age hardened material.

The results for the fully annealed material are not so simply explained. Although the hardening increment produced by the shot peening was around 80%, in line with its ductility if compared with the naturally aged material, the depth of the work hardened layer was not so great. The surface residual stress measurement on the fully annealed material implied a maximum subsurface stress approximately equal to the yield stress for this condition, as did the results on the naturally aged material.

The reason for the smaller depth of the work hardened layer in the fully annealed material is probably associated with recovery or recrystallisation that is known to take place in aluminium that has been subjected to plastic deformation at or near ambient temperature (95). In the aged materials, the shot peening produces a high uniform dislocation density in the surface regions. These dislocations are stable even at very large plastic deformations as they are pinned in

position by the fine θ' precipitates, and hence the work hardening is maintained at high levels at the peened surface.

In the case of the fully annealed material, where a soft matrix surrounds large precipitates, heavy plastic deformation will produce dislocations, but these will not be stable since they are not pinned by small θ' precipitates. In this case dynamic recovery will take place during peening and reduce the degree of work hardening. The result is a limited depth of hardening by the peening of the annealed alloy.

The surface roughness analysis showed that the type of damage produced by shot peening is one that would be expected to be very sensitive to fatigue cycling. Particularly the areas of folded material could be expected to act as stress concentration points.

(ii) On_Fatigue_Strengths.

Shot peening is well established as a major industrial process for the improvement in fatigue strength, thus the improvements in plain fatigue strength found in this work were to be expected. The improvements to the two aged treatments were of the same order, although the slightly higher percentage for the age hardened alloy was at first surprising in view of the fact that, from surface analysis, the naturally aged alloy was more susceptible to the effects of shot peening.

Generally, however, these results were found to be consistent with an observation by Starker et al (96) who observed that the influence of residual stresses on the fatigue strength strongly depends on the ultimate tensile strength and that no distinct correlation exists between surface residual stresses and the improvement of the fatigue strength. However, they stated further that soft annealed materials

show no improvement in fatigue strength with residual compressive stress, but results in this work on the fully annealed alloy did show a small, but definite, improvement. This result, though is still in agreement with the general statement of the U.T.S. dependency of fatigue strength improvement.

In the case of fretting fatigue, again improvements in strength were found in all alloy conditions. The most notable observation, though, is the vast improvement found for the age hardened treatment. It seems that the shot peening has had a dual effect on the age hardened material, i.e. not only has it improved the fretting fatigue strength, but in doing so, has apparently reduced some of its notch sensitivity, hence sensitivity to fretting, because the improved level is approximately the same as the equivalent result for the naturally aged alloy.

Results from the tests done to assess the effects of surface roughness on the fatigue lives showed no significant differences. This suggests that the beneficial effects due to the residual compressive stress or work hardening produced by shot peening compensate for the defects that the process also creates. This is well described by Was and Pelloux (97) who state, '...the fatigue life of shot peened parts is a compromise between lower surface tensile stress and a greater number of fatigue crack initiation sites'.

In order to assess the separate contributions of work hardened surface layers and residual surface stresses to the improvements in fatigue strengths, the tests on the stretched specimens were performed, and the results showed that when a major proportion of the residual compressive stress is removed, the improvement in fatigue strength is lost. Thus the major factor is the residual compressive

stress. The action of the compressive stresses, particularly in the cases involving fretting, is to close up cracks initiated at the surface and to inhibit their propagation. Also, as the work hardening alone did not appear to produce any improvement in fretting fatigue strength it can be said that the wear characteristic of fretting is not an important factor involved in the early initiation of fatigue cracks by fretting. This adds weight to the theory that fretting initiates cracks due to local high alternating shear stresses, rather than by general surface damage.

6.3 Residual Stress Stability.

Having confirmed that the residual compressive stress is the major factor involved in improving fretting fatigue strengths by shot peening, it was necessary to investigate the stability of these stresses, bearing in mind that residual stresses are known to fade with fatigue cycling, and that fretting does introduce several other characteristics which may affect the magnitude of these stresses.

Results from the X-ray analysis on the tested specimens showed that fretting fatigue produced a higher degree of residual stress fading than did plain fatigue for equivalent numbers of fatigue cycles. Fading as a result of fatigue cycling, is generally regarded as being due to a shakedown process. The question arises then as to why fretting accelerates this process of fading. One possible explanation is that fretting produces localized heating; enough to produce local softening, annealing and stress relief. However, localized heating produced by fretting of metallic specimens is probably quite small and in the present case unlikely to be $\sim 150^{\circ}\text{C}$, which would be required for effective stress relief. Secondly the idea of the wear produced by fretting

causing the removal of stressed layers cannot be applied here because the results of the residual stress/depth profiles showed that at depths just below the surface the residual stress increased, and the material worn away by fretting and even subsequent debris removal in this work was negligible compared to that which would be needed to reach depths of lower residual stress suggested by the analysis of the tested specimens. Indeed, in the tests performed here, a higher degree of wear was found on specimens analysed after lower numbers of fretting fatigue cycles, and these gave higher residual stress readings.

The most favourable theory, then, suggests that fretting accelerates the shakedown processes produced by fatigue cycling. However, in considering the theory proposed by Leverant et al (85) that stress fading can be facilitated by a mean compressive stress being superimposed on the residual compressive stress, one must consider the possibility that fretting induces some compressive stress itself. By examining the residual stress results for the unpeened fretting fatigue tested specimens, it seems that this feature is possible, especially on the age hardened alloy. Also, it was found by Endo and Goto (45) that fretting could induce a residual compressive stress, up to the point where small cracks are initiated. In this work, though, it was not confirmed whether or not the specimens, which recorded the induced residual stress from fretting contained any microcracks, although it is thought likely that they did.

The most favourable theory then on the accelerated residual stress fading due to fretting fatigue is one involving the local stressing effects of the fretting action, which accelerates the shakedown process already occurring.

In the alloys studied in the present work, the stacking fault

energy is high and so under suitable stresses, dislocation movement and dislocation annihilation is relatively easy. In the shot peened surfaces of the aged alloys the density of tangled dislocations is very high on account of the severe plastic deformation that takes place during shot peening. During plain fatigue cycling these dislocations undergo rearrangement by cross slip processes and this will result in a reduction of the residual stresses at the surface. However, in those regions influenced by the fretting action the additional shear stresses acting at the surface will cause the movement and rearrangement of dislocations to be accelerated, therefore speeding up the fading of the residual stresses.

6.4 Crack Morphology.

Usually, in unpeened materials, fretting fatigue cracks initiate at the surface and grow at an angle of $\sim 45^\circ$ due to the high shear stresses caused by fretting. However, in the shot peened specimens it has been shown that initiation takes place in the subsurface regions, at a depth of about $10\mu\text{m}$ (Plate 14).

Once a crack has nucleated in the subsurface it will propagate parallel to the surface, since shear stresses induced by fretting will not be transmitted easily across the crack. Therefore, the shear stresses will be localized at the crack tip which will therefore propagate parallel to the surface. Propagation in a direction normal to the surface will be prevented, initially at least, by the residual compressive stresses.

At a later stage of the fretting fatigue process, cracks will propagate either inward or towards the surface from the subsurface flow. The former will eventually lead to failure. The latter process

causes the delamination that was frequently observed (Plate 15).

~~two point~~ Subsurface initiation in shot peened surfaces has been detected by Starker et al (96) and Was and Pelloux (97). Both of these papers however reported that the subsurface initiation occurred at depths much greater ($200 - 400\mu\text{m}$) than that of the present work. It was suggested that the subsurface initiation was due to the residual tensile stress under the compressively stressed layer. However, this explanation does not hold for this work due to the much smaller depth involved. Starker et al (94) did note, however, that the exact positions of crack initiation coincided with the locations of intermetallic inclusions, and it was reported earlier from the present work (43) that during plain fatigue tests on the age hardened alloy, crack initiation occurred at intermetallic inclusions of Al - Fe - Mn - Si and Al - Mg - Cu immediately below the surface. Thus, it is possible that during the fretting fatigue of the shot peened alloy a similar mechanism of crack nucleation can take place, then propagating in the manner stated earlier.

6.5 ~~Discussion~~ A further consideration is the possibility of subsurface crack initiation at points of subsurface damage caused by shot peening, such as that shown in Plate 5 (c) and 10 (a). This type of damage was observed in the aged alloys at depths of around $10\mu\text{m}$ and therefore it is quite possible that these are acting as nucleation sites for cracks. Also, it was found that in the fully annealed material the depth to which peening damage extended was greater, a feature which is to be expected due to the annealed material being of lower strength and higher ductility. As a result, the fretting fatigue damage produced on the fully annealed shot peened material was more severe (Plate 10). This also correlates with the fretting fatigue test results on the fully annealed material which showed a smaller improvement due to shot peening

than did the aged materials. Thus when shot peening annealed materials, two points must be considered; the residual stress induced by shot peening does not greatly improve the fatigue strength; and the increased damage produced by the shot peening of annealed material may well abrogate the effects desired of the treatment.

The other type of damage shown in Plates 16 and 17 suggests that once a crack has initiated and propagated to the surface, further propagation into the bulk material is sufficiently retarded by the residual compressive stress, that packing of the crack with fretting debris is possible. Another possibility here, however, is that the debris is produced by the crack faces rubbing together, similar to a Mode II type fatigue action induced by the shear stresses of the fretting action. This **explanation** would seem more appropriate for the observations in Plate 17 in which one of the crack faces appears to have sustained severe damage.

6.5 Fretting Debris.

The characteristic feature, not found in the hitherto mentioned reports, was the presence of small spherical particles within the subsurface cracks in the surface of the peened material. The production of spherical particles in tribological situations has often been reported (98 - 102), and several different mechanisms have been proposed to explain their formation.

However, none of the observations reported in the literature coincided exactly with the observations in the present work on fretting fatigue. Consequently, plain fretting tests were carried out to investigate these particles more fully. It was found that, on the shot peened surfaces, after approximately 10^4 cycles the coefficient of

friction (μ) was reduced. This implied that approximately 10^4 cycles is required to produce the spherical debris, and thereafter the rolling action of this debris produces a dramatic decrease in friction.

The spherical particles are probably produced by a burnishing action, and in this respect Rabinowicz (100) has proposed that for fretting:-

$$d \leq K_b x$$

Where,

d = Maximum diameter of the particle.

K_b = Wear coefficient for burnishing - typically 10^{-6} .

x = Total sliding distance.

Applying this to the present work, where $d = 2\mu\text{m}$, and using $30\mu\text{m}$ as the amplitude of movement (thus in one cycle the total sliding distance is $120\mu\text{m}$), it is found that spherical particles will be formed after $\sim 1.6 \times 10^4$ cycles. This correlates very well with the point at which μ begins to fall on the shot peened alloys.

However, there are limitations which must be considered when applying this criterion to the present work; for example the fact that the particles are formed in a subsurface crack may not be fully described by this criterion. Nevertheless, the actual observation of spherical particles produced by fretting on shot peened surfaces, and the practical implication that a 'self lubricating' situation can develop is a definite stimulus for further investigation.

The other notable observation from the plain fretting tests was that the fretting scars on the shot peened surfaces were much larger. This can be explained by considering the geometry of the specimens used;

for the tests on the shot peened surfaces, only the flat was shot peened, thus the work hardened surface would not wear as quickly as the softer hemispherical rider. As the test progressed the tip of the rider would become flattened, thus creating a larger contact surface and hence a larger fretting scar. In the tests on the unpeened surfaces, there would be no preferential wear of the rider because the two surfaces were of similar hardness, thus the relative increase in contact area would be smaller.

The fretting debris on unpeened specimens generally consisted of the broken oxide layer, and smeared material. The smearing was predominant because the unpeened surfaces had not been plastically deformed prior to testing, and so retained their ductility. However, the surfaces of the shot peened material were work hardened and therefore much less ductile. Consequently, the surface tended to crack and break up more easily, thus producing the much rougher surface as depicted in the post testing talysurf traces.

6.6 Conclusions and Future Work.

1. Fretting causes substantial reductions in fatigue strength of the Al - 4%Cu - 1%Mg alloy, particularly in the age hardened condition.
2. A major improvement in fretting fatigue properties is produced by shot peening. This improvement arises from the induced residual compressive stress at the surface.
3. The work hardening of the surface layers produced by the shot peening does not play a major role in the improvement of fretting fatigue

strength. The surface roughening does not produce a detrimental effect on the fretting fatigue properties provided that these defects are contained within the zone of influence of the compressive stresses at the surface.

4. For the shot peened conditions used in this work, the residual compressive stresses are in the range 200 - 250 MPa at the surface. Fading of these stresses occurs due to fatigue cycling and is most rapid under fretting conditions.
5. Fretting fatigue crack initiation is at the surface in the unpeened material, but in the shot peened samples, subsurface cracks nucleate and initially grow parallel to the surface.
6. Spherical debris is produced on the faces of the subsurface cracks. Delamination subsequently takes place and allows the spherical debris to reach the surface. The debris causes a reduction of friction between the fretting members and hence a reduction of the fretting stresses.

Future Work.

1. Residual stress/depth profiles on shot peened surfaces which have undergone fretting fatigue testing, to investigate the depth of influence (of stress relaxation) of the fretting action.
2. More detailed studies on the residual compressive stresses induced by fretting.

3. T.E.M. analysis of shot peened surfaces, affected by both plain fatigue and fretting fatigue to examine the dislocation arrangement, and thus shed more light on the actual mechanisms involved in the interaction of these processes.
4. Investigations into the possible application of using the spherical wear debris as a means of reducing the magnitude of the fretting stresses.

A C K N O W L E D G E M E N T S

I would like to express my sincere gratitude to my supervisors, Dr. B. Noble and Dr. R.B. Waterhouse, for their guidance, encouragement and patience throughout the course of this work.

Thanks are also due to Professor J.S.L l. Leach, Head of the Department of Metallurgy and Materials Science, for the provision of laboratory facilities, The Ministry of Defence (Procurement Executive) for financial support, and to P.J.E. Forsyth, C.J. Peel and B. Evans for many helpful discussions about the work.

Thanks are also extended to the technical staff of the Department for their help and co-operation, especially to Mr. M. Brown.

Throughout the course of this work, I have been fortunate enough to have made many friends within the Department. I would like to express my thanks to these few people for their encouragement, help and most of all for their sincere friendship; in particular, to Feri Nedjat-Haiem, Mike Overs, Richard Taylor, (C.R.) and more recently to Keven Harlow.

I would also like to express my heartfelt thanks to my family for their encouragement, support and trust throughout my University studies.

Finally, I am indebted to Mrs. Stephanie Bazrafshan for the excellent typing of the manuscript.

R E F E R E N C E S

- (1) Baldauf, F.K. 'Shot Peening - An Added Dimension', S.A.E. Technical Paper Series No. 790513.
- (2) Eden, E.M., Rose, W.N. and Cunningham, F.L. 'The Endurance of Metals'. Proc. Inst. Mech. Engrs. , 4, 1911, p.839.
- (3) Tomlinson, G.A., 'The Rusting of Steel Surfaces in Contact', Proc. Royal Soc. Series A, 115, 1927, p.472.
- (4) Tomlinson, G.A., Thorpe, P.L. and Gough, M.J., 'An Investigation of the Fretting Corrosion of Closely Fitting Surfaces'. Proc. Inst. Mech. Engrs. 141, 1939, p.223.
- (5) Fink, M., 'Wear Oxidation, A New Component of Wear'. Transactions A.S.S.T., 18, 1930, p.1026.
- (6) Godfrey, D., 'Investigation of Fretting by Microscopic Observation', N.A.C.A. Report 1009, 1951.
- (7) Godfrey, D., Bailey, J.M., 'Coefficient of Friction and Damage to Contact Area During the Early Stages of Fretting - I (Glass, Copper or Steel against Copper)'. N.A.C.A. YN 3011, 1953.
- (8) Uhlig, H.H., 'Mechanism of Fretting Corrosion', J. Applied Mech., 21, 1954, p.401.

- (9) Feng, I.M., Uhlig, H.H., 'Fretting Corrosion of Mild Steel in Air and in Nitrogen', J. Applied Mech., 21, 1954, p.395.
- (10) Feng, I.M., and Rightmire, B.G., 'An Experimental Study of Fretting', Proc. Inst. Mech. Engrs., 170, 1956, p.1055.
- (11) Halliday, J.S., and Hirst, W., 'The Fretting Corrosion of Mild Steel', Proc. Royal Soc. (London), Series A., 236, 1956, p.411.
- (12) Waterhouse, R.B., 'Fretting Corrosion'. Proc Inst. Mech. Engrs. 169, 1956, p.1157.
- (13) Feng, I.M., Communications Proc. Inst. Mech. Engrs. 169, 1956, p.1165.
- (14) Hurricks, P.L., 'The Mechanism of Fretting - A Review'. Wear 15, 1970, p.389.
- (15) Wright, K.H.R., 'An Investigation of Fretting Corrosion'. Proc. Inst. Mech. Engrs. 1B, 1952, p.556.
- (16) Waterhouse, R.B., 'Influence of Local Temperature Increases on the Fretting Corrosion of Mild Steel'. J. Iron Steel Inst. 197, 1961, p.301.
- (17) Sproles, Jr., E.S., and Duquette, D.J., 'Interface Temperature Measurements in the Fretting of a Medium Carbon Steel', Wear, 47, 1978, p.387.
- (18) Suh, N.P., 'The Delamination Theory of Wear'. Wear, 25, 1973, p.111.

- (19) Waterhouse, R.B., and Taylor, D.E. 'Fretting Debris and the Delamination Theory of Wear'. *Wear*, 29, 1974, p.337.
- (20) Waterhouse, R.B. 'The Role of Adhesion and Delamination in the Fretting Wear of Metallic Materials'. *Wear*, 45, 1977, p.355.
- (21) Sproles, Jr., E.S., and Duquette, D.J., 'The Mechanism of Material Removal in Fretting'. *Wear*, 49, 1978, p.339.
- (22) Sakmann, B.W., and Rightmire, R.G., 'Investigation of Fretting Corrosion under Several Conditions of Oxidation'. N.A.C.A. T.N. 1492, 1948.
1941, p.32.
- (23) Almén, J.O., *Mech. Engineering*, 59, 1937, p.415.
- (24) Waterhouse, R.B., 'Fretting Corrosion'. Pergamon Press, Oxford, 1972.
Reprints: I. Mech. Engrs. London, 1976, p.386.
- (25) Ohmae, N., and Tsukizoe, T., 'The Effect of Slip Amplitude on Fretting'. *Wear*, 27, 1974, p.281.
1974, p.475.
- (26) O'Connor, J.J., 'The Role of Elastic Stress Analysis in the Interpretation of Fretting Fatigue Failures'. *Fretting Fatigue* (Edit. R.B. Waterhouse) Applied Science Publishers Ltd., 1981, p.23.
1980, p.124.
- (27) Uhlig, H.H., Tierney, W.D., and McClellan, A., 'Test Equipment for Evaluating Fretting Corrosion'. A.S.T.M. Spec. Tech. Publ. No.144, 1953, p.71.
1972, p.38.

- (28) Mokhtar, M.O.A., 'The Effect of Hardness on the Frictional Behaviour of Metals'. Wear, 78, 1982, p.297.
- (29) Bethune, B., and Waterhouse, R.B., 'Adhesion of Metal Surfaces under Fretting Conditions. I. Like Metals in Contact'. Wear, 12, 1968, p.289.
- (30) Walker, P.B., 'Fretting in the Light of Aircraft Experience'. J. Royal Aeronautical Soc., 63, 1959, p.293.
- (31) Warlow-Davies, E.J., 'Fretting Corrosion and Fatigue Strength: Brief Results of Preliminary Experiments'. Proc. Inst. Mech. Engrs., 146, 1941, p.32.
- (32) Fenner, A.J., Wright, K.H.R., and Mann, J.Y., 'Fretting Corrosion and it's Influence on Fatigue Failure'. Proc. Int. Conf. on Fatigue of Metals; I. Mech. Engrs. London, 1956, p.386.
- (33) Fenner, A.J., and Field, J.E., 'Fatigue under Fretting Conditions'. Revue de Metallurgie, 55, 5, 1958, p.475.
- (34) Fenner, A.J., and Field, J.E., 'A Study of the Onset of Fatigue Damage due to Fretting'. Trans. N.E. Coast Inst. Engrs. Shipbuilders. 76, 1960, p.184.
- (35) Waterhouse, R.B., and Taylor, D.E., 'The Initiation of Fatigue Cracks in 0.7% Carbon Steel by Fretting'. Wear, 17, 1971, p.139.

- (36) Hoepfner, D.W., and Goss, G.L., 'Mechanisms of Fretting Fatigue'. Lockheed California Company, Rep. No. LR 24367, Dec. 1970.
- (37) Wharton, M.H., Taylor, D.E., and Waterhouse, R.B., 'Metallurgical Factors in the Fretting Fatigue Behaviour of 70/30 Brass and 0.7% Carbon Steel'. Wear, 23, 1973, p.251.
- (38) Alic, J.A., and Kantimathi, A., 'Fretting Fatigue with Reference to Aircraft Structures'. 1979 S.A.E. Business Aircraft Meeting. S.A.E. Pap. 790612. 1979.
- (39) Alic, J.A., Hawley, A.L., and Urey, J.M., 'Formation of Fretting Fatigue Cracks in 7075 - T7351 Aluminium Alloy'. Wear, 56, 1979, p.351.
- (40) Hoepfner, D.W., and Goss, G.L., 'Metallographic Analysis of Fretting Fatigue Damage in Ti - 6Al - 4V MA and 7075 - T6 Aluminium'. Wear, 27, 1974, p.175.
- (41) Endo, K., and Goto, H., 'Initiation and Propagation of Fretting Fatigue Cracks'. Wear, 38, 1976, p.311.
- (42) Alic, J.A. and Hawley, A.L., 'On the Early Growth of Fretting Fatigue Cracks'. Wear, 56, 1979, p.377.
- (43) Leadbeater, G., Kovalevskii, V.V., Noble, B., and Waterhouse, R.B., 'Fractographic Investigation of Fretting-Wear and Fretting Fatigue in Aluminium Alloys'. Fat. Eng. Mat. Struct., 3, 1981, p.237.

- (44) Hoepfner, D.W., and Gates, F.L., 'Fretting Fatigue Considerations in Engineering Design'. Wear, 70, 1981, p.155.
- (45) Endo, K., and Goto, H., 'Effects of Environment on Fretting Fatigue'. Wear, 48, 1978, p.347.
- (46) Poon, C., and Hoepfner, D.W., 'The Effect of Environment on the Mechanism of Fretting Fatigue'. Wear, 52, 1979, p.175.
- (47) Poon, C., and Hoepfner, D.W., 'A Statistically Based Investigation of the Environmental and Cyclic Stress Effects on Fretting Fatigue'. Trans. A.S.M.E., 103, 1981, p.218.
- (48) Nishioka, K., and Hirakawa, K., 'Fundamental Investigations of Fretting Fatigue. Part 3, Some Phenomena and Mechanisms of Surface Cracks'. Bull. J.S.M.E., 12, No.51, 1969, p.397.
- (49) Reeves, R.K., and Hoepfner, D.W., 'Microstructural and Environmental Effects on Fretting Fatigue'. Wear, 47, 1978, p.221.
- (50) Hoepfner, D.W., 'Environmental Effects in Fretting Fatigue'. Fretting Fatigue (Edit. R.B. Waterhouse) Applied Science Publishers Ltd. 1981, p.154.
- (51) Hamdy, M.M., and Waterhouse, R.B., 'The Fretting-Fatigue Behaviour of a Nickel-Based Alloy (Inconel 718) at Elevated Temperatures'. Wear of Materials 1979, A.S.M.E. New York, 1979, p.351.

- (52) Hamdy, M.M., and Waterhouse, R.B., 'The Fretting Fatigue Behaviour of Ti - 6Al - 4V at Temperatures up to 600°C'. Wear, 56, 1979, p.1.
- (53) Yeh, H.L., and Sinclair, G.M., 'A Review of Fretting Fatigue'. Fracture Control Program (F.C.P.), U.S.A., 1973.
- (54) Nishioka, K., and Hirakawa, K., 'Fundamental Investigations of Fretting Fatigue. Part 5, The Effect of Relative Slip Amplitude'. Bull. J.S.M.E., 12, No.52, 1969, p.692.
- (55) Collins, J.A., and Tovey, F.M., 'Fretting Fatigue Mechanisms and the Effect of Direction of Fretting Motion on Fatigue Strength'. Journal of Materials, J.M.L.S.A., 7, No.4, 1972, p.460.
- (56) Endo, K., Goto, H., and Nakamura, T., 'Effects of Cycle Frequency on Fretting Fatigue Life of Carbon Steel'. Bull. J.S.M.E., 12, No.54, 1969, p.1300.
- (57) Endo, K., and Goto, H., 'Reply to Comments on 'Initiation and Propagation of Fretting Fatigue Cracks'. Wear, 43, 1977, p.269.
- (58) Nishioka, K., and Hirakawa, K., 'Fundamental Investigations of Fretting Fatigue. Part 6, Effects of Contact Pressure and Hardness of Materials'. Bull., J.S.M.E., 15, No.80 1972, p.135.
- (59) Goss, G.L., and Hoepfner, D.W., 'Normal Load Effects in Fretting Fatigue of Titanium and Aluminium Alloys'. Wear, 27, 1974, p.153.

- (60) Liu, H.W., Corten, H.T., and Sinclair, G.M., 'Fretting Fatigue Strength of Titanium Alloy RC 130B'. Proc. A.S.T.M., 57, 1957, p.623.
- (61) Collins, J.A., and Marco, S.M., 'The Effect of Stress Direction during Fretting on Subsequent Fatigue Life'. Proc. A.S.T.M., 64, 1964, p.547.
- (62) Nishioka, K., and Hirakawa, K., 'Fundamental Investigations of Fretting Fatigue. Part 4, The Effect of Mean Stress'. Bull., J.S.M.E., 12, No.51, 1969, p.408.
- (63) Kantimathi, A., and Alic, J.A., 'The Effects of Periodic High Loads on Fretting Fatigue'. J. Eng. Mat. Technology, 103, 1981, p.223.
- (64) Bowers, J.E., Finch, N.J., and Goreham, A.R., 'The Prevention of Fretting Fatigue in Aluminium Alloys'. Proc. Instn. Mech. Engrs., 182, Part 1., No.33, 1966, p.703.
- (65) Waterhouse, R.B., and Allery, M., 'The Effect of Powders in Petrolatum on the Adhesion Between Fretted Steel Surfaces'. A.S.L.E. Trans, 2, 1966, p.179.
- (66) Waterhouse, R.B., Brook, P.A., and Lee, G.M.C., 'The Effect of Electro-deposited Metals on the Fatigue Behaviour of Mild Steel under Conditions of Fretting Corrosion'. Wear, 5, 1962, p.235.
- (67) Jones, W.J.D., and Lee, G.M.C., 'The Fretting Fatigue Behaviour of Mild Steel with Electrodeposited Nickel and Ni - Co Alloys with Controlled Internal Stresses'. Wear, 68, 1981, p.71.

- (68) Overs, M.P., Private Communication.
- (69) Sachs, G., and Horger, O.J., 'Fretting Corrosion and Fatigue'. A.S.M.E. Handbook, Metals Engineering Design, 2nd Edit., 1965, p.395.
- (70) Whinney, C.D., 'What You Have Always Wanted to Know About Shot Peening'. Soc. Manufacturing Engrs. Tech. Paper, No.MR79 - 766, 1979.
- (71) Montemarano, T.W., and Wells, M.E., 'Improving the Fatigue Performance of Welded Aluminium Alloys'. Welding Journal, 59, (6), 1980, p.21.
- (72) Almen, J.O., 'Shot Peening'. Kents Handbook for Mechanical Engineers. p.20 - 40.
- (73) Metal Improvement, Inc., 'Shot Peening Applications'. Sixth Edition.
- (74) Almen, J.O., 'Fatigue Weakness of Surfaces'. Product Engineering, Nov. 1950, p.118.
- (75) Stulen, F.B., Cummings, H.N., and Schulte, W.C., 'Preventing Fatigue Failures. Part 4 - Surface Treatment and Environment'. Machine Design, June 1961, p.165.
- (76) Viglione, J., 'How to Prevent Fatigue Failures' Product Engineering, Oct. 1955, p.174.
- (77) Coombs, A.G.H., Sherratt, F., and Pope, J.A., 'An Analysis of the Effects of Shot Peening upon the Fatigue Strength of Hardened and Tempered Spring Steel'. Int. Conf. on Fatigue of Metals, I. Mech. Engrs. 1956, p.227.

- (78) Arnold, E.A., 'Re-Establishing Surface Integrity'. Machinery, June 1971, p.61.
- (79) Graf, M., and Verpoort, C., 'Influence of Microplasticity and Crack Initiation on the Fatigue Behaviour of Precipitation Hardened Alloys'. Strength of Metals and Alloys, 2, 5th Int. Conf. Aachen, W. Germany, 27th - 31st Aug. 1979, p.1207.
- (80) Morgan, C.J., and Brine, F.E., 'The Effect of Chromium Plating on the Fatigue Strength of Aluminium Alloy L 65'. Trans. Inst. Metal Finishing, 47, 1969, p.77.
- (81) Morgan, C.J., and Mayhew, P.R., 'The Effect of Shot Peening on the Fatigue Strength of Chromium Plated Titanium Alloys IMI 314 and IMI 680'. Trans. Inst. Metal Finishing, 50, 1972, p.142.
- (82) S.A.E. Iron and Steel Technical Committee, 'Residual Stresses Resemble Static Stresses'. S.A.E. Journal, Aug. 1962, p.47.
- (83) Esquivel, A.L., and Evans, K.R., 'X-Ray Diffraction Study of Residual Microstresses in Shot-Peened and Fatigued 4130 Steel'. Experimental Mechanics, Nov. 1968, p.496.
- (84) Boggs, B.D., and Byrne, J.G., 'Fatigue Stability of Residual Stress in Shot Peened Alloys'. Met. Trans., 4, Sept. 1973, p.2153.
- (85) Leverant, G.R., Langer, B.S., Yuen, A., and Hopkins, S.W., 'Surface Residual Stress, Surface Topography and Fatigue Behaviour of Ti - 6Al - 4V'. Met. Trans., 10A, Feb. 1979, p.251.

- (86) Fuchs, H.O., 'The Effect of Self Stresses on High Cycle Fatigue'.
J. Testing and Evaluation, July 1982, p.168.
- (87) Waterhouse, R.B., and Saunders, D.A., 'The Effect of Shot Peening on
the Fretting Fatigue Behaviour of an Austenitic Stainless Steel and
a Mild Steel'. Wear, 53, 1979, p.381.
- (88) Fuchs, H.O., 'Regional Tensile Stress as a Measure of the Fatigue
Strength of Notched Parts'. Proc. 1971 Int. Conf. on Mech. Behaviour
of Materials, II, p.478. Soc. Mat. Sci. of Japan, 1972.
- (89) Baxa, M.S., Chang, Y.A., and Burck, L.H., 'Effects of Sodium Chloride
and Shot Peening on Corrosion Fatigue of AlSi 6150 Steel'. Met. Trans.
A, 9A, 1978, p.1141.
- (90) Overs, M.P., 'Fretting Wear of Molybdenum Arc-Sprayed Coatings'.
M. Phil Thesis, 1978, University of Nottingham.
- (91) Hamdy, M.M., 'High Temperature Fretting Fatigue of Nickel and Titanium
Alloys'. PhD. Thesis. 1979, University of Nottingham.
- (92) Norton, J.T., and Rosenthal, D., 'Residual Stress Measurement by
X-Rays'. Proc. Soc. Experimental Stress Analysis, 1943, 1, 2, p.73.
- (93) Hilley, M.E., Larson, J.A., Jatzczak, C.F., and Ricklefs, R.E.,
'Residual Stress Measurement by X-Ray Diffraction'. S.A.E. Information
Report J. 784a (1971).

- (94) Moore, M.G., and Evans, W.P., 'Mathematical Correction for Stress in Removed Layers in X-Ray Diffraction Residual Stress Analysis'. S.A.E. Transactions, 66, 1958, p.340.
- (95) Nuttall, J., and Nutting, J., 'Structure and Properties of Heavily Cold-Worked F.C.C. Metals and Alloys'. Metal Science, Sept. 1978, p.430.
- (96) Starker, P., Wohlfahrt, H., and Macherauch, E., 'Subsurface Crack Initiation during Fatigue as a Result of Residual Stresses'. Fat. Eng. Mat. Struct. 1, 1979, p.319.
- (97) Was, G.S., and Pelloux, R.M., 'The Effect of Shot Peening on the Fatigue Behaviour of Alloy 7075 - T6'. Met. Trans. A. 10A, May 1979, p.656.
- (98) Loy, B., and McCallum, R., 'Mode of Formation of Spherical Particles in Rolling Contact Fatigue'. Wear, 24, 1973, p.219.
- (99) Hurricks, P.L., 'The Occurrence of Spherical Particles in Fretting Wear'. Wear, 27, 1974, p.319.
- (100) Rabinowicz, E., 'The Formation of Spherical Wear Particles'. Wear, 42, 1977, p.149.
- (101) Christensen, C., 'On the Origin of Spherical Particles Found on Fatigue Fracture Surfaces and Ferrograms'. Wear, 53, 1979, p.189.
- (102) Smith, M.C., and Smith, R.A., 'The Formation of Spherical Wear Debris in Mode II Fatigue Cracks'. Wear, 76, 1982, p.105.

Calculation of the Bending Stress in the
Rotation-Bending Fatigue Specimen (A1).

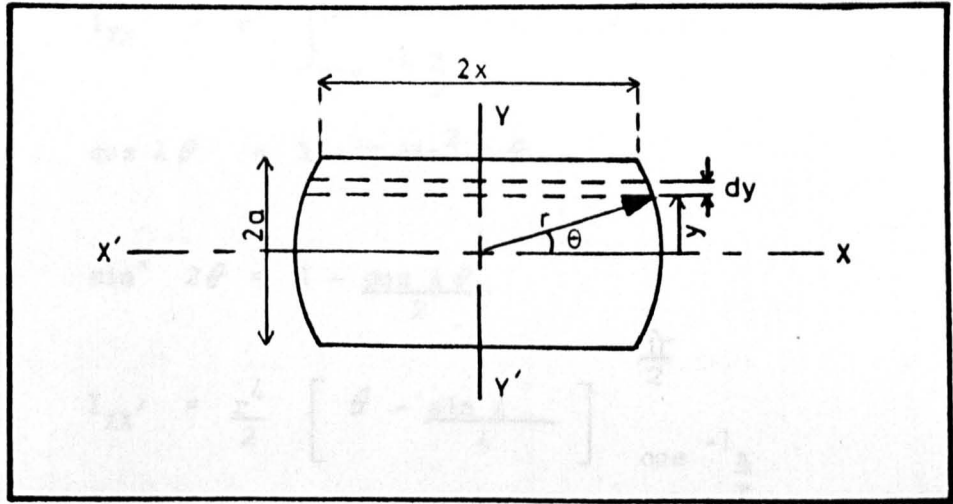


FIG. A1.

To find the second moment of area, $I_{xx'}$ for the section of the specimen as shown in Figure A1.

The area of the elemental strip is $2x \cdot dy$, and it has a second moment of area xx' of $2xy^2 dy$.

Hence, $I_{xx'}$ for the section $= 2 \int_0^a 2xy^2 dy$.

now $x^2 + y^2 = r^2$ or $x = (r^2 - y^2)^{1/2}$

and $I_{xx'} = 4 \int_0^a y^2 (r^2 - y^2)^{1/2} dy$.

Let $y = r \cos \theta$, then $dy = -r \sin \theta d\theta$,

and $(r^2 - y^2)^{1/2} = r(1 - \cos^2 \theta)^{1/2} = r \sin \theta$.

Hence, $I_{xx'} = -4 \int_{\frac{\pi}{2}}^{\cos^{-1} \frac{a}{r}} 2^2 \cos^2 \theta \cdot r^2 \sin^2 \theta d\theta$.

Now $(2 \sin \theta \cos \theta)^2 = (\sin 2\theta)^2.$

then
$$I_{XX'} = r^4 \int_{\cos^{-1} \frac{a}{r}}^{\frac{\pi}{2}} \sin^2 2\theta \cdot d\theta.$$

and $\cos 4\theta = 1 - 2 \sin^2 2\theta.$

$$\sin^2 2\theta = 1 - \frac{\cos 4\theta}{2}$$

$$I_{XX'} = \frac{r^4}{2} \left[\theta - \frac{\sin 4\theta}{4} \right]_{\cos^{-1} \frac{a}{r}}^{\frac{\pi}{2}}$$

Now $\cos^{-1} \frac{a}{r} = \theta$, thus $\cos \theta = \frac{a}{r}$

thus $\sin \theta = \left(1 - \frac{a^2}{r^2}\right)^{1/2}$

$$\sin 4\theta = 4 \sin \theta \cos \theta - 8 \sin^3 \theta \cos \theta.$$

$$= 4 \sin \theta \cos \theta (1 - 2 \sin^2 \theta).$$

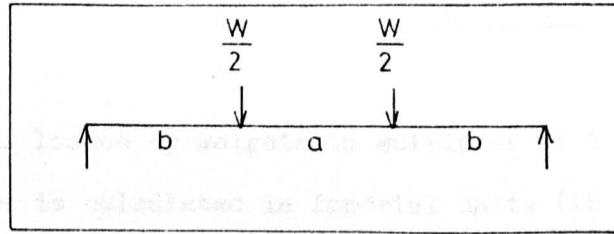
$$= 4 \frac{a}{r} \left(1 - \frac{a^2}{r^2}\right)^{1/2} \cdot \left[1 - 2 \left(1 - \frac{a^2}{r^2}\right)\right]$$

$$= 4 \frac{a}{r} \left(1 - \frac{a^2}{r^2}\right)^{1/2} \cdot \left(2 \frac{a^2}{r^2} - 1\right)$$

Hence,
$$I_{XX'} = \frac{r^4}{2} \left[\frac{\pi}{2} - \cos^{-1} \frac{a}{r} + \left(2 \frac{a^2}{r^2} - 1\right) \cdot \frac{a}{r} \cdot \left(1 - \frac{a^2}{r^2}\right)^{1/2} \right]$$

Particular values used were $r = 0.1875$ in, and $a = 0.125$ in.

This gives $I_{XX'} = \underline{4.17 \times 10^{-4} \text{ in}^4}$



The centre portion of the specimen is under a constant bending moment M ;

$$M = \frac{1}{2} W \cdot b.$$

W , the load, is varied during the experimental work.

From simple bending theory,

$$\frac{M}{I_{XX'}} = \frac{f}{y}$$

Where $I_{XX'}$ = Second moment of area.

f = Maximum bending stress, and

y = Distance from neutral axis to the outer fibres of the specimen.

$$\text{Hence, } f = \frac{My}{I_{XX'}} = \frac{1}{2} \cdot \frac{W \cdot b}{I_{XX'}}$$

The bending stresses for the loads used in the investigation can then be calculated;

e.g. $W = 100 \text{ lb}; \quad b = 3 \text{ in}; \quad y = 0.125 \text{ in}; \quad I_{XX'} = 4.17 \times 10^{-4} \text{ in}^4.$

$$f = \frac{100 \times 3 \times 0.125}{2 \times 4.17 \times 10^{-4}} = 44,964 \text{ lb in}^{-2}$$

$$(11) \text{ Whorl, S.F., "Experiments" } = \underline{310.1 \text{ MPa}}$$

The machine is loaded by weights in multiples of 5 lb. The alternating bending stress is calculated in Imperial units (lb in^{-2}), as above, and then converted to SI units (MPa) using the conversion factor

$$1 \text{ MPa} = 145 \text{ lb in}^{-2}.$$

REFERENCE

- (A1) Wharton, W.H., 'Environmental Effects in the Fretting of Titanium Alloys'. Ph. D Thesis, Nottingham University, 1977.

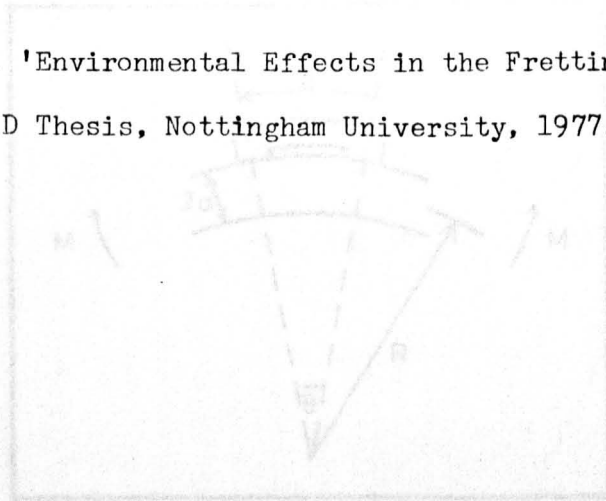


FIG. B1

Slip, δ , is distributed over both feet of the bridge, $\theta = \theta$.

From simple bending theory:

$$R = \frac{I \cdot E}{M}$$

where: I = Second moment of area.

M = Bending moment, and

E = Young's Modulus for the material.

From Figure B1 for $R \gg d$

$$d = R \theta$$

$$\theta = \frac{d}{R} = \frac{d \cdot M}{I \cdot E}$$

For $d = 0.25$ in. the diameter of the specimen = 0.25 in.

and $I = 4.37 \times 10^{-11}$ (Appendix A).

The actual value of slip can then be determined.

A P P E N D I X B

Calculation of Slip of Bridges during Rotating-Bending (A1).

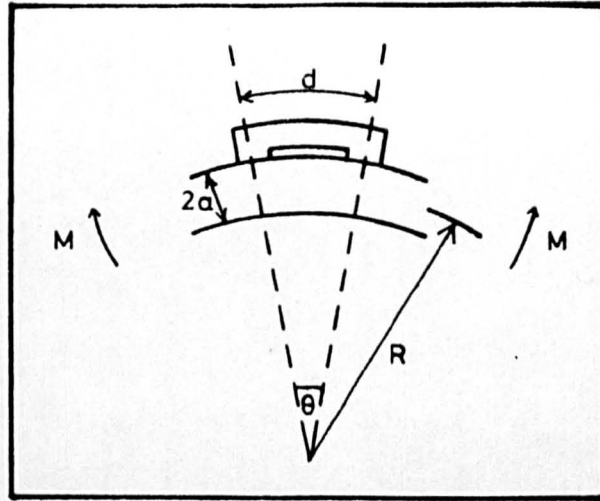


FIG. B.1.

Slip, S , is distributed over both feet of the bridge, $= a \theta$.

From simple bending theory;

$$R = \frac{I \cdot E}{M}$$

Where; I = Second moment of area.

M = Bending moment, and

E = Young's Modulus for the material.

From Figure B1 for $R \gg d$

$$d = R \theta .$$

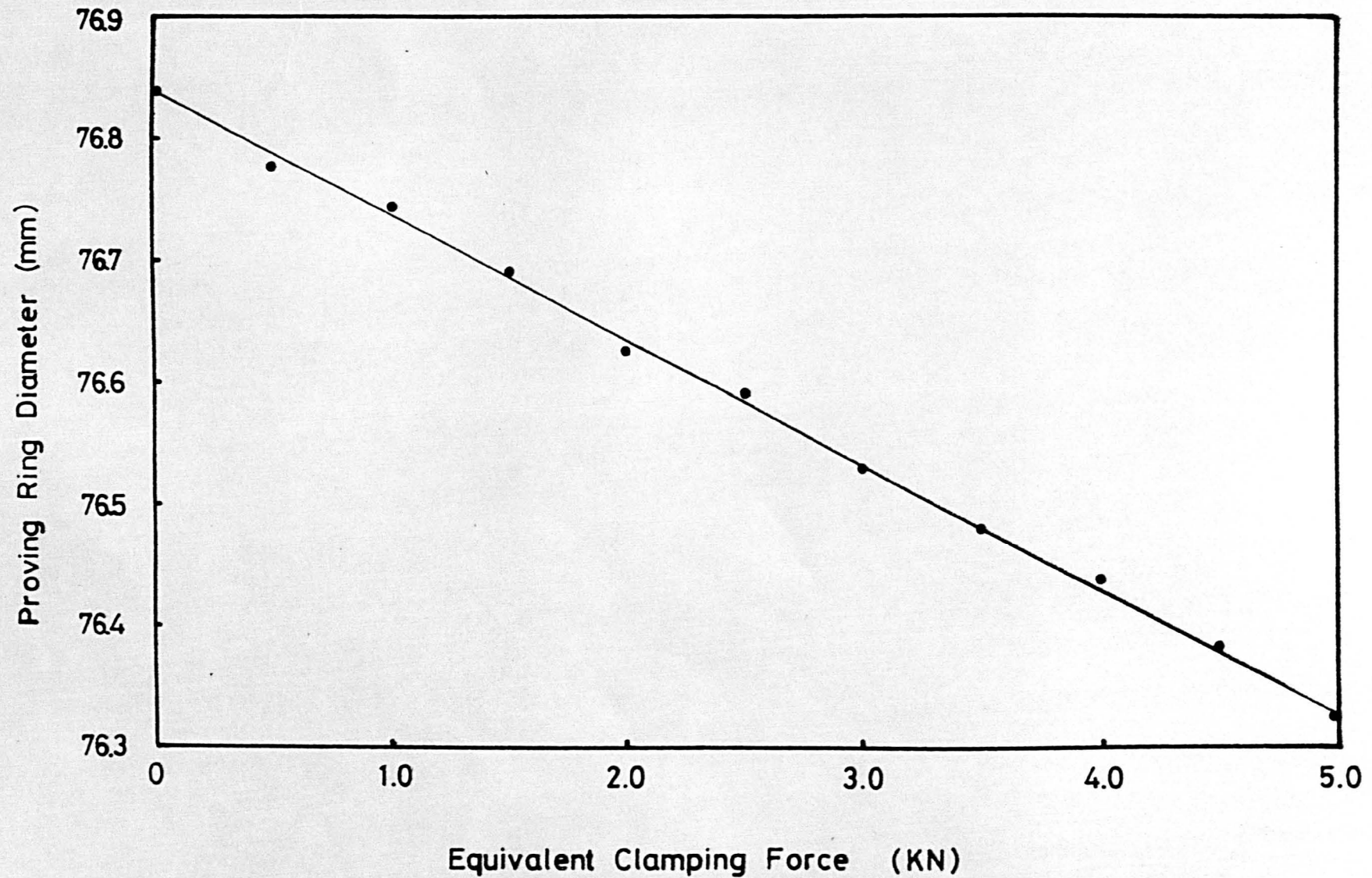
$$\theta = \frac{d}{R} = \frac{d \cdot M}{I \cdot E}$$

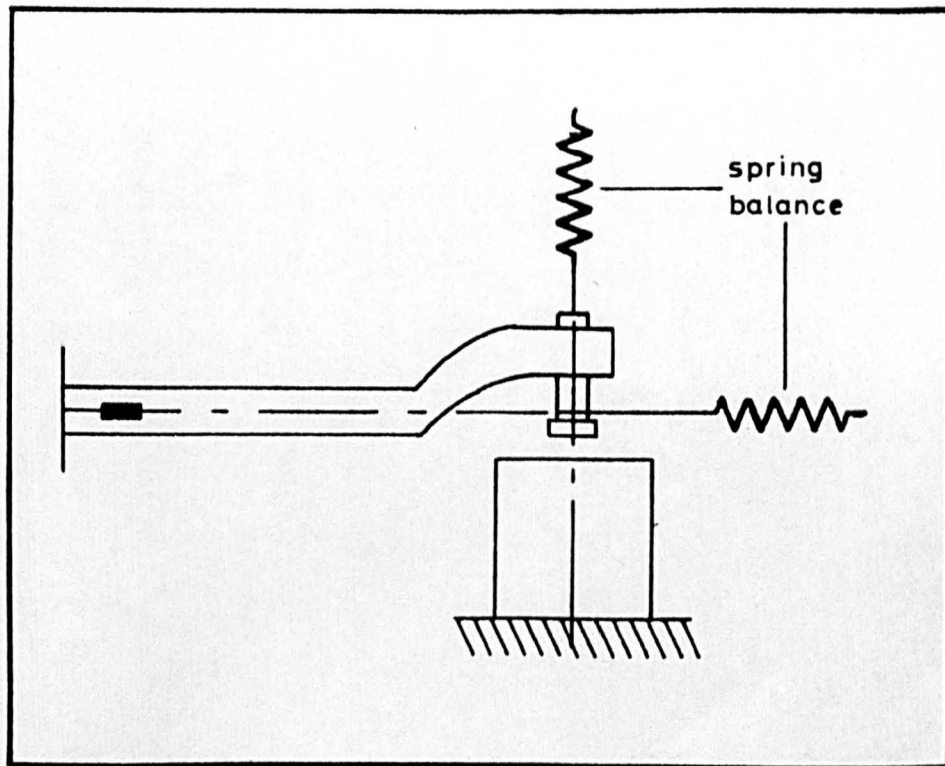
for $2a = 0.25$ in, the diameter of the specimen = 0.375 in,

and $I = 4.17 \times 10^{-4}$. (Appendix A).

The actual value of slip may then be determined.

Calibration Curve for the Proving Ring.





Spring Balance Arrangement for the Calibration of Friction and Normal Forces.

A P P E N D I X E

Stress Relief Computer Readouts (E1).

NOT-PEENING DATA PROCESSING PROGRAMME

SPECIMEN TYPE: AGED AT RM. TEMP

SPECIMEN RADIUS= 4.75 MM

DEPTH(MM)	UNCORRECTED STRESS(N/MM2)	CORRECTED STRESS(N/MM2)	HARDNESS V.H.N.	50/K
0	205	205	270	.400136532
.04	230	226.329393	254	.4695784
.08	236	228.345689	238	.5056314
.12	222	210.406349	227	.5084849
.16	245	229.353347	217	.5570107
.2	243	223.082007	211	.55718613
.24	239	214.826009	205	.5522696
.28	231	202.639161	197	.5420949
.32	220	187.585591	190	.5203122
.36	204	167.740365	188	.4702165
.4	187	147.162055	180	.43086533
.44	163	119.929754	180	.3511330
.48	143	97.077414	177	.28904348
.52	120	71.6030838	174	.2168706
.56	100	49.513678	160 mo	.15328950
.6	80	27.7379398	153 65	.08558671
.64	62	8.41344911	153 63	.02718013
.68	48	-6.6617017	158	-.02222011
.72	34	-21.4709152	156	-.07253442
.76	24	-32.0489857	155	-.10896848
.8	15	-41.4414859	153	-.14274539
.84	8	-48.6752261	151	-.169882735
.88	2	-54.7777393	148	-.19505638
.92	-3	-59.7670796	145	-.217226222

(E1) D.A. Hills, Private Communication.

```

5 OPEN 4,4
10 PRINT#4,"SHOT-PEENING DATA PROCESSING PROGRAMME"
15 PRINT#4,"*****" :PRINT#4
16 PRINT"GIVE SPECIMEN TYPE":INPUT A$:PRINT#4,"SPECIMEN TYPE:";A$
20 PRINT"SPECIMEN RADIUS(MM)=":INPUT R0:PRINT#4,"SPECIMEN RADIUS=";R0" MM"
30 PRINT"INCREMENT OF DEPTH REQUIRED(MM)=":INPUT T
40 PRINT#4,"DEPTH(MM)    UNCORRECTED    CORRECTED    HARDNESS","90/K"
45 PRINT#4,"          STRESS(N/MM2)    STRESS(N/MM2)    V.H.N."
80 I=0:R1=R0:Z1=0:J=0
100 PRINT"DEPTH(MM)=";J*T:PRINT"GIVE STRESS(N/MM2)":INPUT S:PRINT"GIVE HAR
S":INPUT H
115 R=R0-J*T:IF J=0 THEN 130
120 I=I+0.5*T*(Z1/R1+3/R)
130 S1=S-2*I:S0=S1/(1.8975*H):PRINT#4,J*T,S,S1,H,S0
140 R1=R:Z1=S:J=J+1:GOTO 100
160 REM
999 END

```

SHOT-PEENING DATA PROCESSING PROGRAMME

SPECIMEN TYPE:AGED AT 185 C
 SPECIMEN RADIUS= 4.75 MM

DEPTH(MM)	UNCORRECTED STRESS(N/MM2)	CORRECTED STRESS(N/MM2)	HARDNESS V.H.N.	90/K
3	195	195	212	.484749049
.04	216	212.5235	218	.45162004
.08	224	216.770475	238	.4800001
.12	220	208.951198	227	.4851066
.16	215	200.176912	216	.4884031
.2	205	186.501075	214	.45928872
.24	185	163.058079	210	.4062052
.28	165	139.940771	198	.3724751
.32	147	119.136947	200	.3139313
.36	125	94.6706814	195	.2558568
.4	105	72.5662119	190	.20127927
.44	85	50.8118316	198	.14243778
.48	65	29.4140692	186	.08934132
.52	50	13.3323567	182	.03860598
.56	35	-2.47458546	177	-7.3679624
.6	20	-18.0014854	174	-.054522694
.64	10	-28.2915801	171	-.08719253
.68	0	-38.3889037	167	-.121145547
.72	-9	-47.2995737	164	-.151995862
.76	-14	-52.0698928	162	-.16939082
.8	-18	-55.7472634	160	-.183620762

FIGURES
&
TABLES

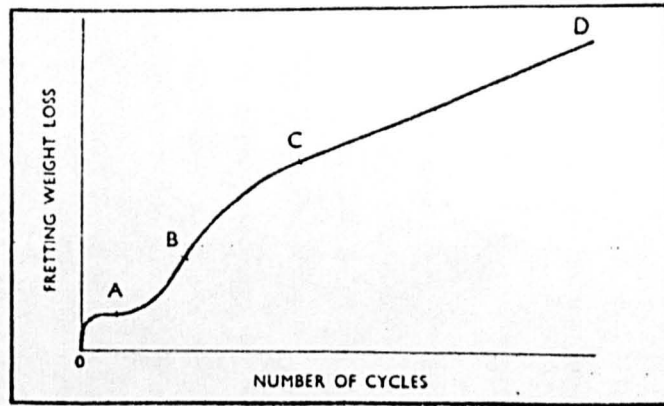


Figure 2.1. Sketch of the Fretting weight-loss against No. of cycles curve illustrating its shape at various stages (after Feng & Rightmire (10))

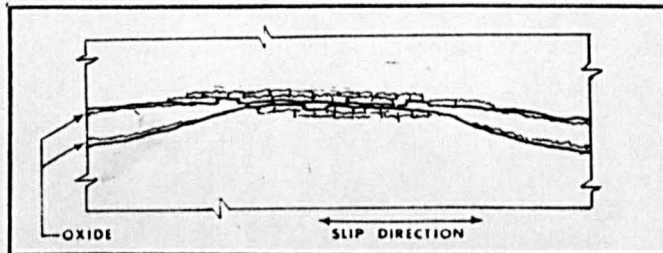


Figure 2.2. Schematic representation of an asperity contact point during fretting. (after Sproles & Duquette (21))

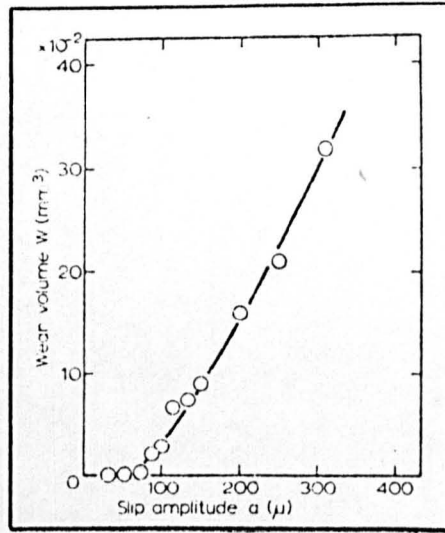


Figure 2.5. Wear volume against slip amplitude after 100,000 cycles. (after Ohmae & Tsukizoe (25))

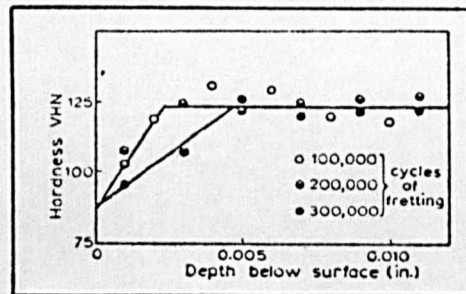


Figure 2.4. Microhardness traverses across fretted regions on sections through the surface of a fully-aged Al-4%Cu alloy. (after Bethune & Waterhouse (29))

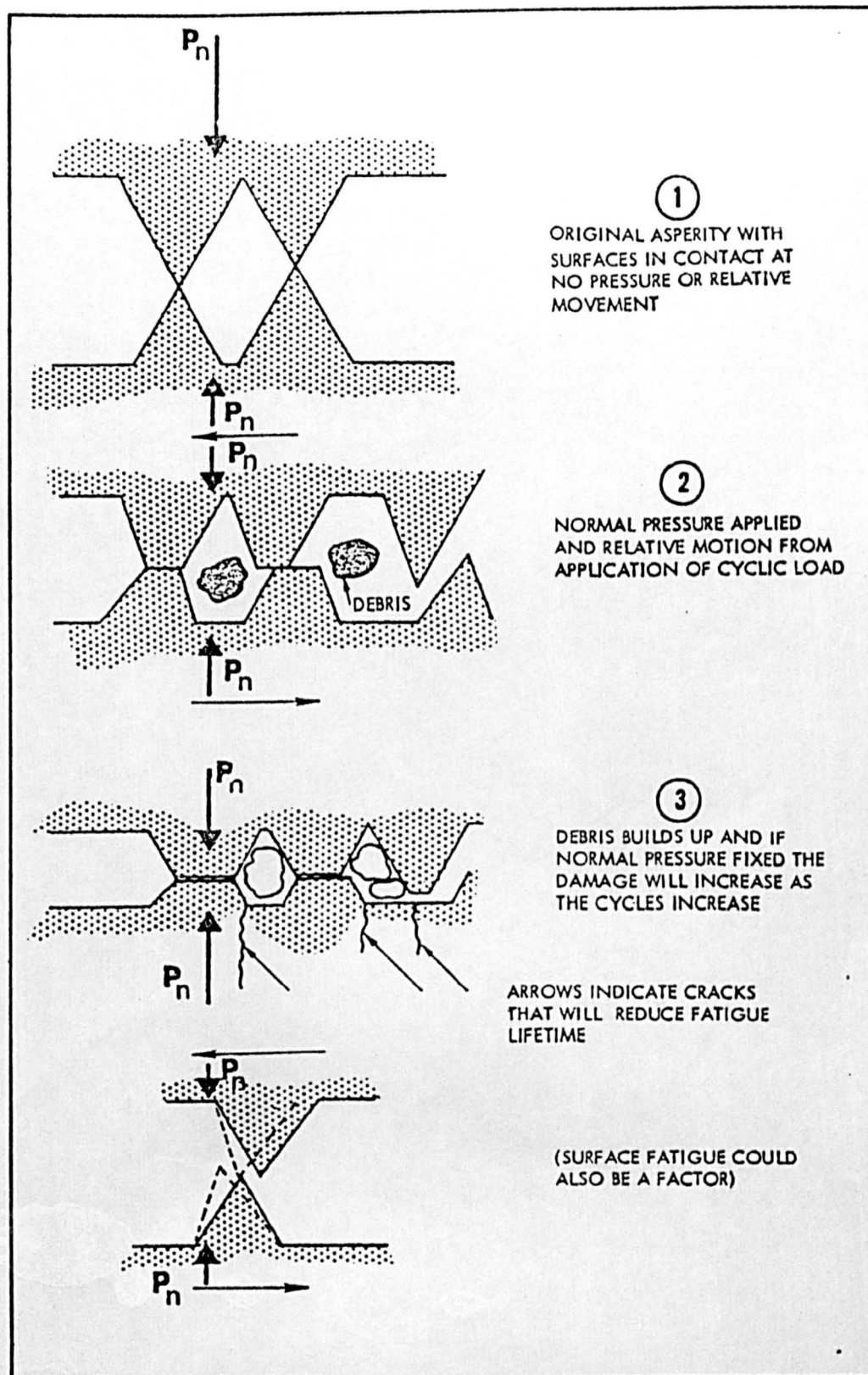


Figure 2.5. Schematic representation
of a Model for Fretting Fatigue.
(after Hoepfner & Goss (36))

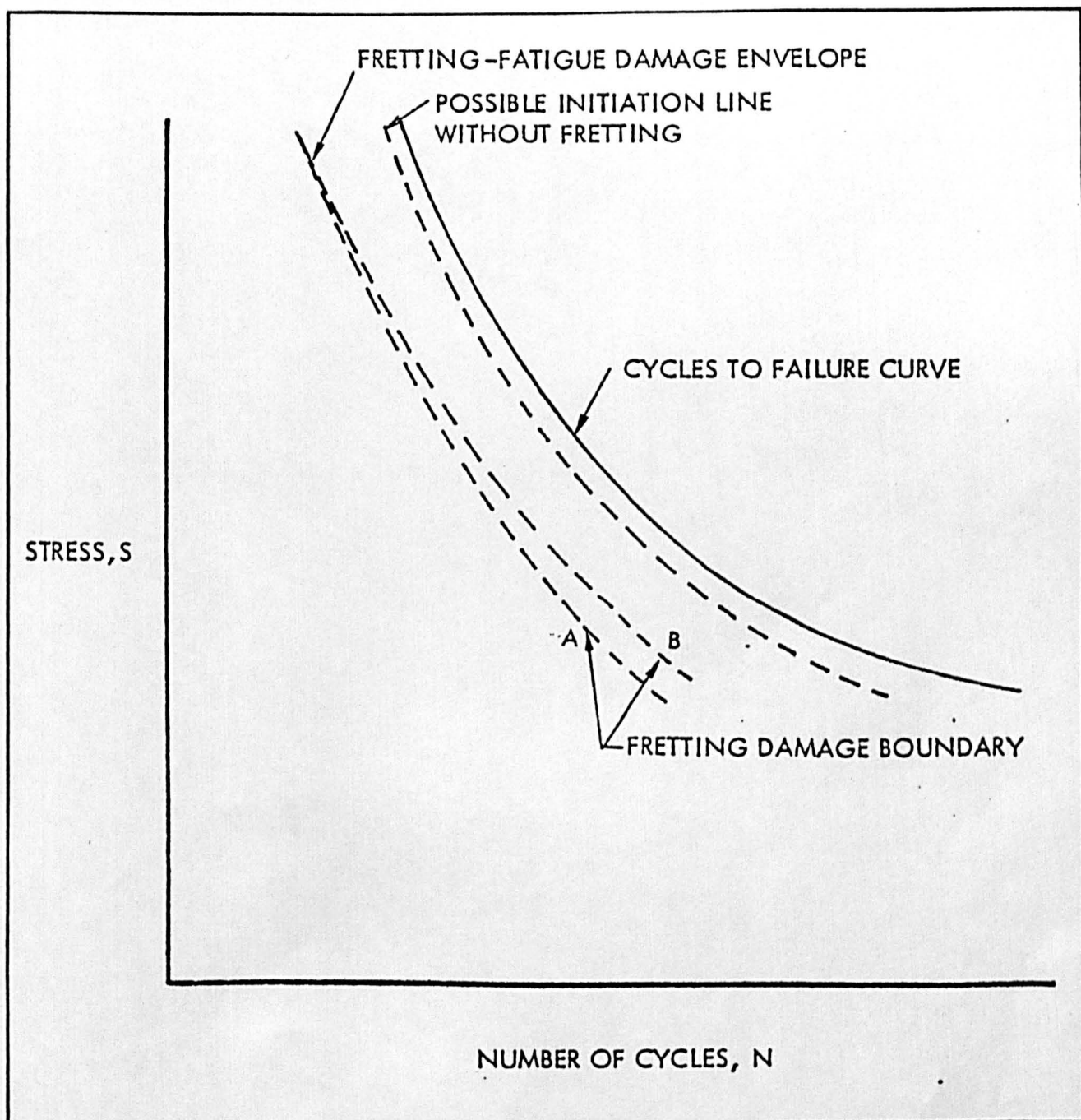


Figure 2.6. The Fretting Fatigue Damage Envelope concept as it relates to an S-N curve. (after Hoeppner & Goss (36))

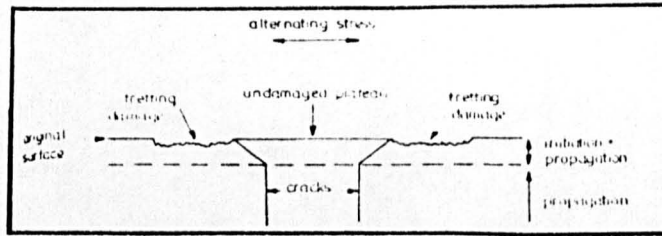


Figure 2.7. Diagram of crack formation by fretting action. (after Wharton et al (37))

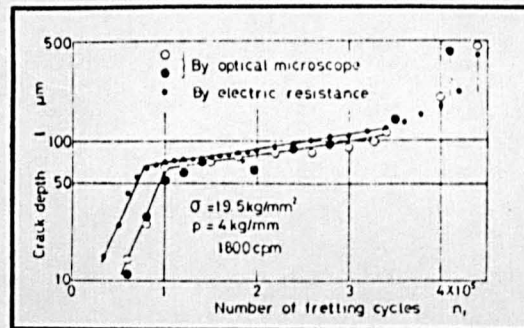


Figure 2.8. Fatigue crack propagation curves obtained by optical microscopy and electrical resistance measurements. Where σ is the fatigue stress and p is the contact pressure. (after Endo & Goto (41))

Crack length a (mm)	Growth rate da/dN (μm^{-1} cycle)	
	Plain-fatigue	Fretting-fatigue
0-0.2	not detectable	0.9
0.4-0.6	0.1	1.2
0.8-1.0	0.2	0.8
1.4-1.6	0.5	0.5
1.8-2.0	0.8	0.9
2.2-2.4	1.2	1.0

Figure 2.9. Table showing crack growth rate in plain and fretting fatigue of age hardened Al-4%Cu-1%Mg for an applied stress of 150 MPa. (after Leadbeater et al (43))

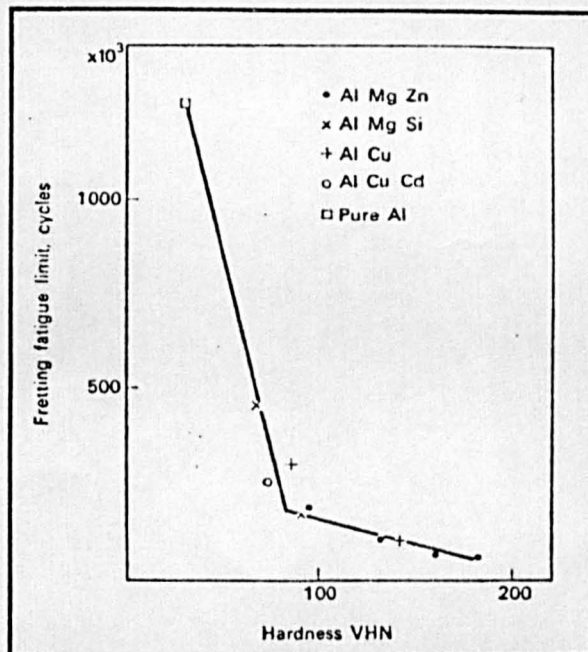


Figure 2.10. Relation between fretting fatigue limit of mild steel and hardness of aluminium fretting bridges. (after Waterhouse (24,p.152))

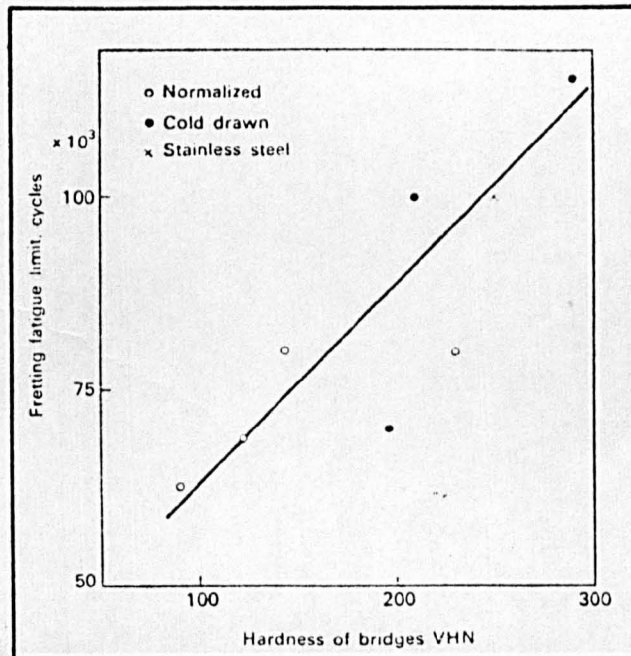


Figure 2.11. Effect of hardness of steel bridges on the fretting fatigue limit of mild steel. (after Waterhouse (24,p.153))

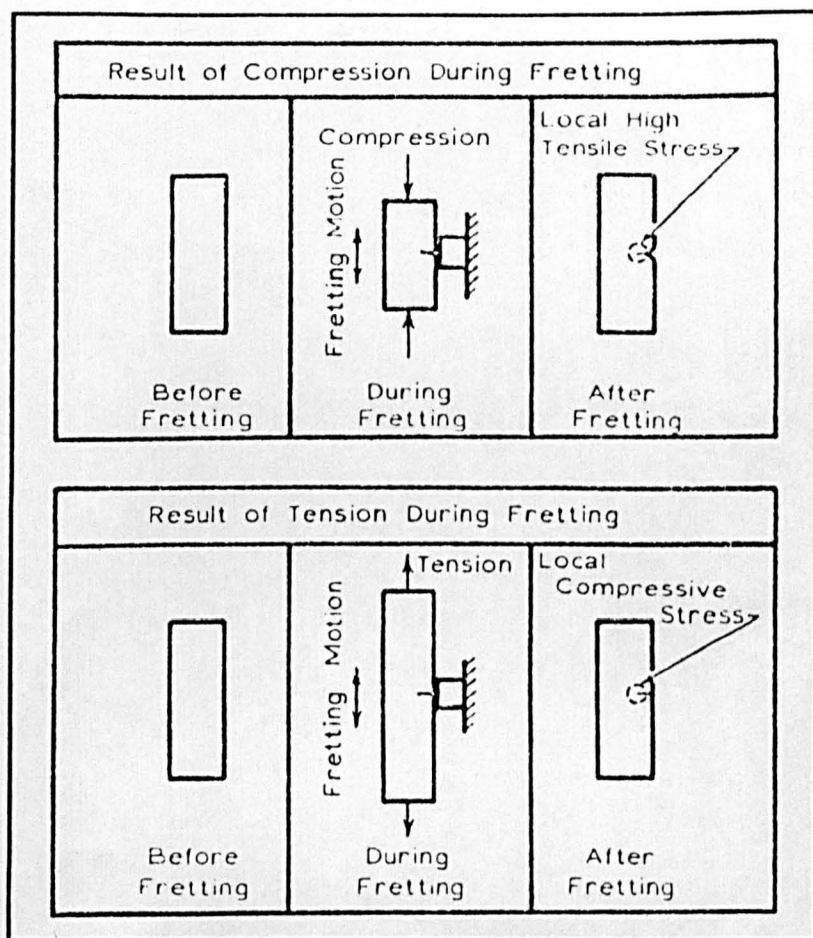


Figure 2.12. Sketches illustrating a possible explanation of why specimens fretted under static compressive stresses exhibit a lower fatigue strength than specimens fretted under static tensile stresses.(after Collins & Marco (61))

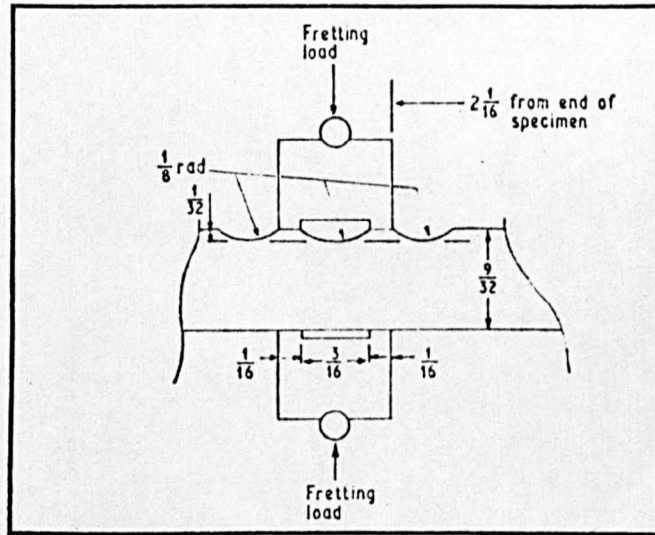


Figure 2.13. Section through a fretting fatigue specimen with grooves for stress relief at the edges of the contact areas. (after Bowers et al (64))

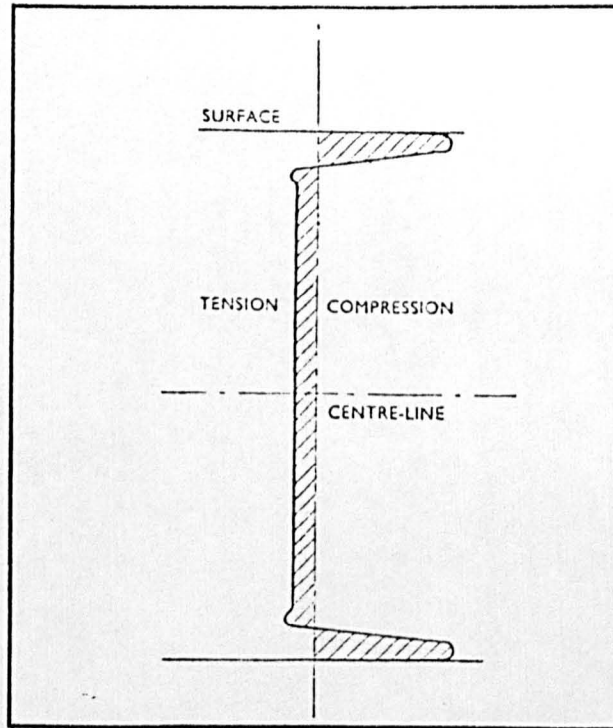


Figure 3.1. Stress distribution in a shot peened bar. (after Coombs et al (77))

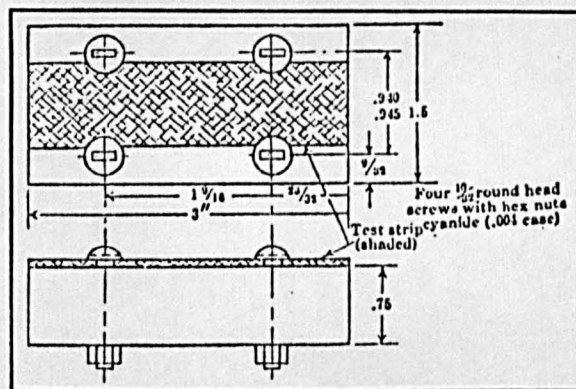


Figure 3.2. Holding fixture for shot peening test strip; units in inches. (after Almen (72))

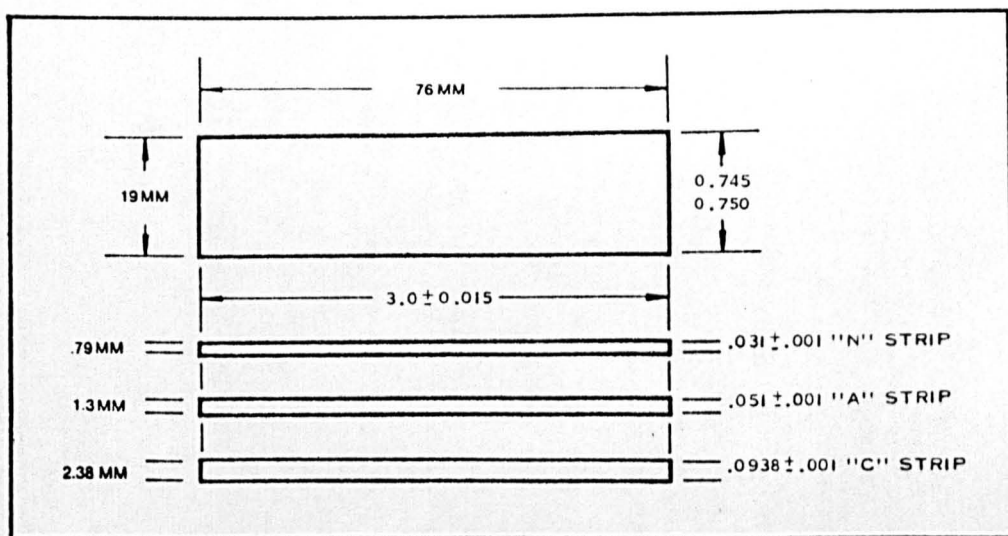


Figure 3.3. Almen test strip specifications.
(after (73))

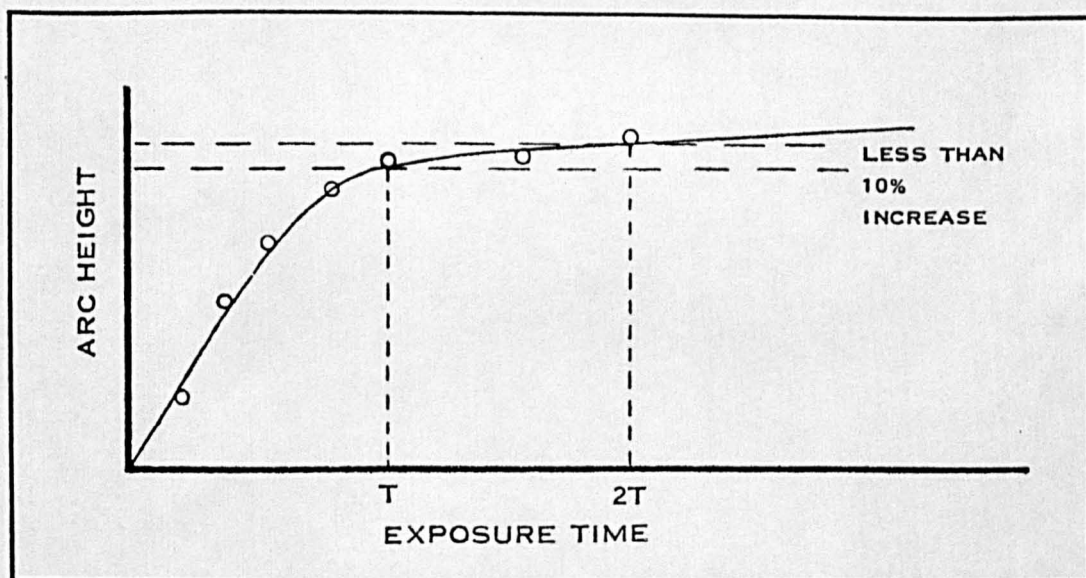


Figure 3.4. Saturation curve to ensure
adequate coverage in shot peening.
(after (73))

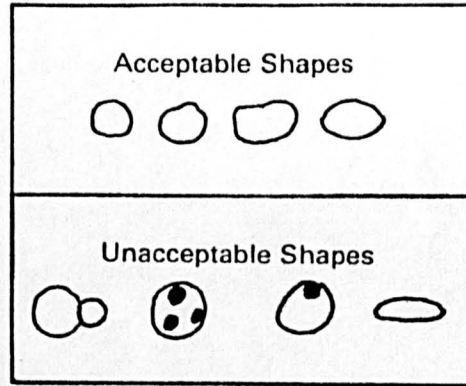


Figure 3.5. Shapes of shot media. (after (73))

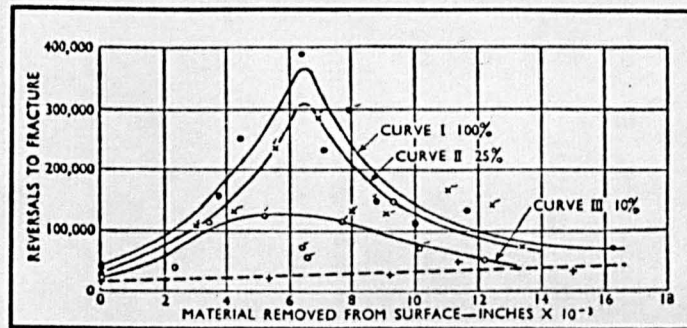


Figure 3.6. Depth of maximum effect of shot peening with variations in total energy of 25% and 10% on a heat treated alloy steel. (after Coombs et al (77))

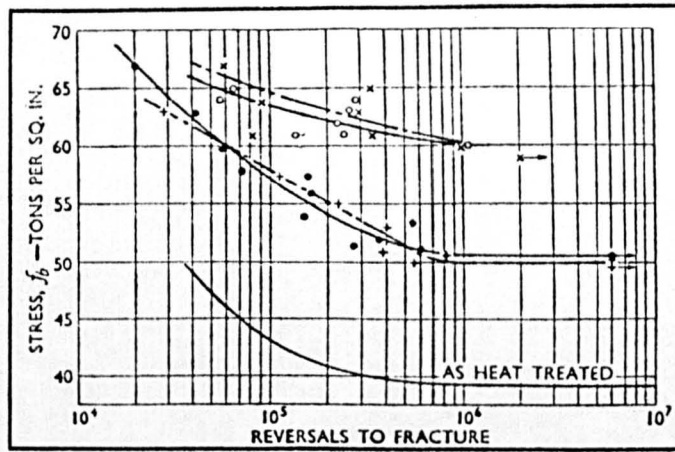


Figure 3.7. Influence of polishing after shot peening on fatigue life curves on a heat treated alloy steel, where;

● = as-peened (low intensity) specimens,
 + = as-peened (high intensity) specimens,
 ○ = peened (low intensity) and polished specimens,
 × = peened (high intensity) and polished specimens.
 (after Coombs et al (77))

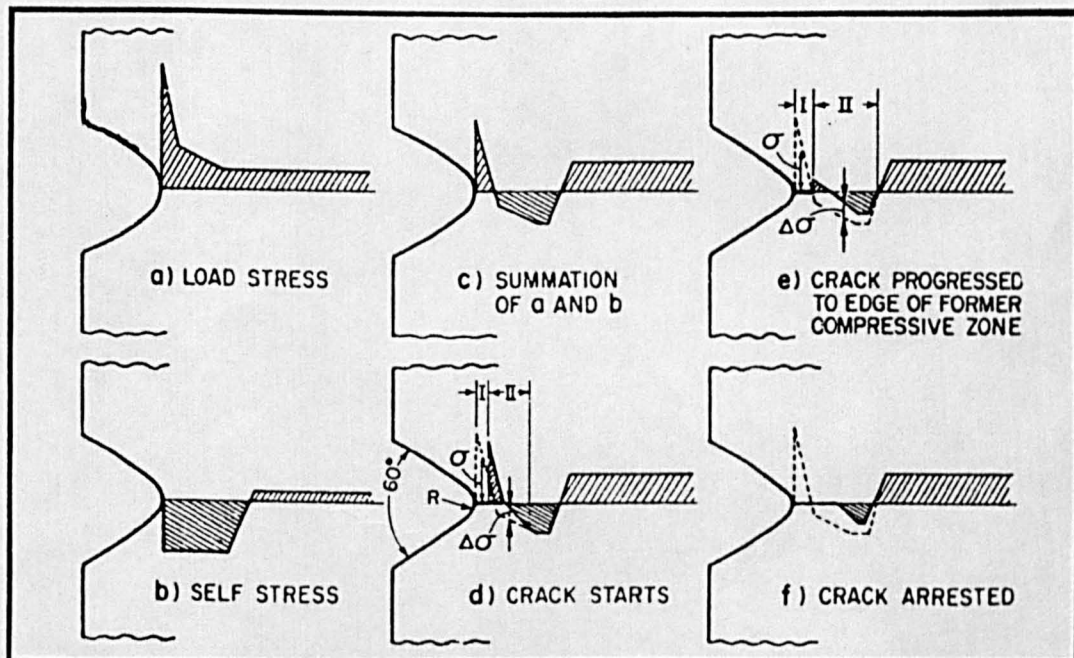


Figure 3.8. Crack arrest by compressive residual stress. (after Fuchs (88))

FIG. 4.1.

Outline of Experiments

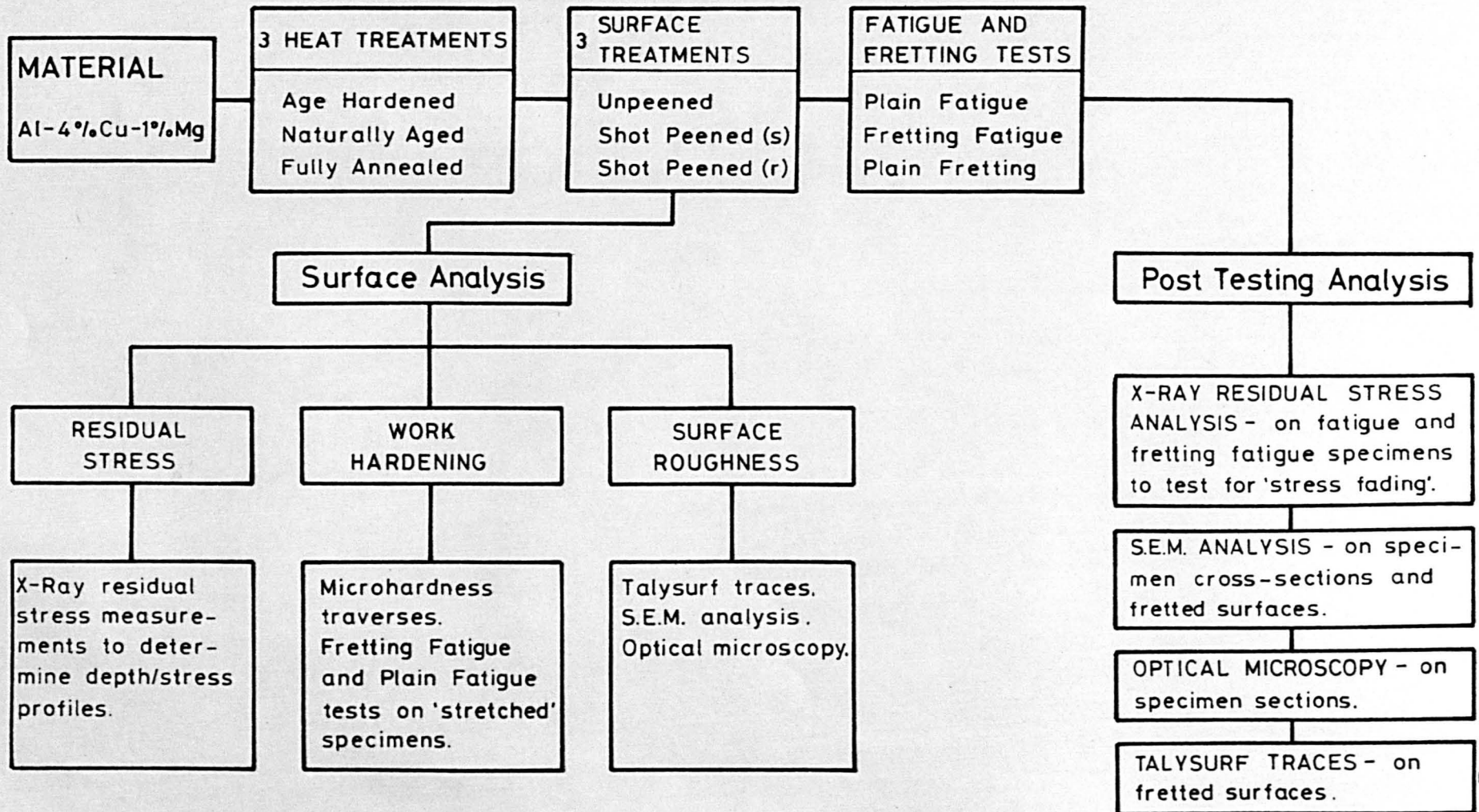


TABLE 4.1.

CHEMICAL COMPOSITION OF Al-4%Cu-1%Mg. (%)

Al	Cu	Mg	Si	Fe	Mn	Ni	Zn	OTHERS
rem	4.4	0.8	0.7	1.0	0.8	0.2	0.2	Pb, Sn, Ti <0.05

TABLE 4.2.

HEAT TREATMENTS OF Al-4%Cu-1%Mg.

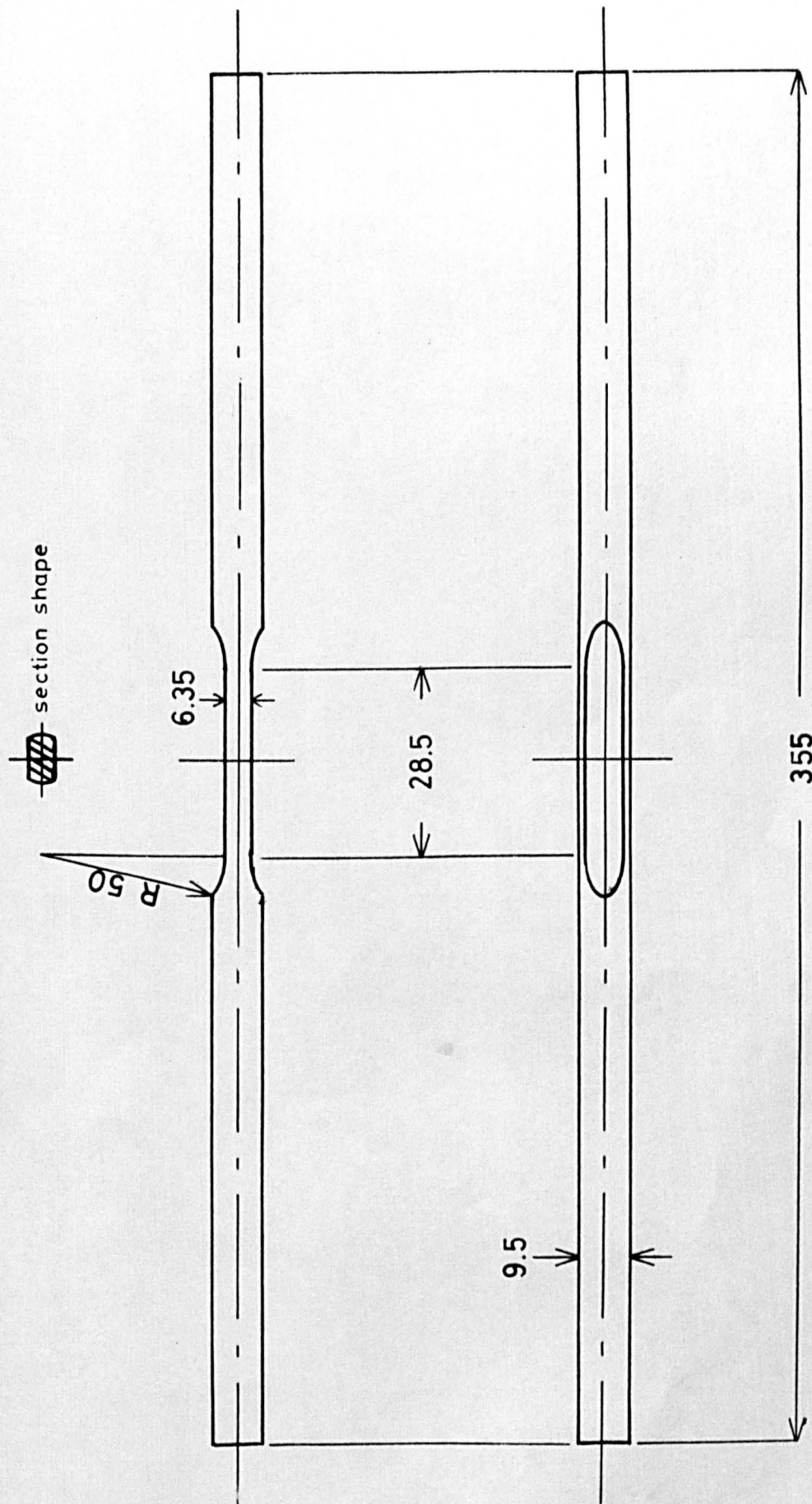
AGE HARDENED	Solution treated for 45 minutes at $505 \pm 1^\circ\text{C}$ Water quenched Age hardened for 5 hours at $185 \pm 1^\circ\text{C}$
NATURALLY AGED	Solution treated for 45 minutes at $505 \pm 1^\circ\text{C}$ Water quenched Naturally aged at room temperature (20°) for 2 days minimum
FULLY ANNEALED	Solution treated for 45 minutes at $505 \pm 1^\circ\text{C}$ Water quenched Heated for 2 hours at $400 \pm 1^\circ\text{C}$ Furnace cooled from 400°C to 250°C and held at that temperature for 2 hours, then air cooled.

TABLE 4.3.

MECHANICAL PROPERTIES OF Al-4%Cu-1%Mg.

Heat Treatment	Yield Stress (MPa)	U.T.S. (MPa)	1% Proof Stress (MPa)	Elongation (%)	Hardness (VHN)
Age Hardened	343	543	365	9.4	140
Naturally Aged	242	440	316	10.4	125
Fully Annealed	78	203	140	10.5	61

FIG. 4.2.
Specimen used for Plain Fatigue and Fretting Fatigue Tests.



(units in mm.)

FIG. 4.3.

Fretting Device.

(units in mm)

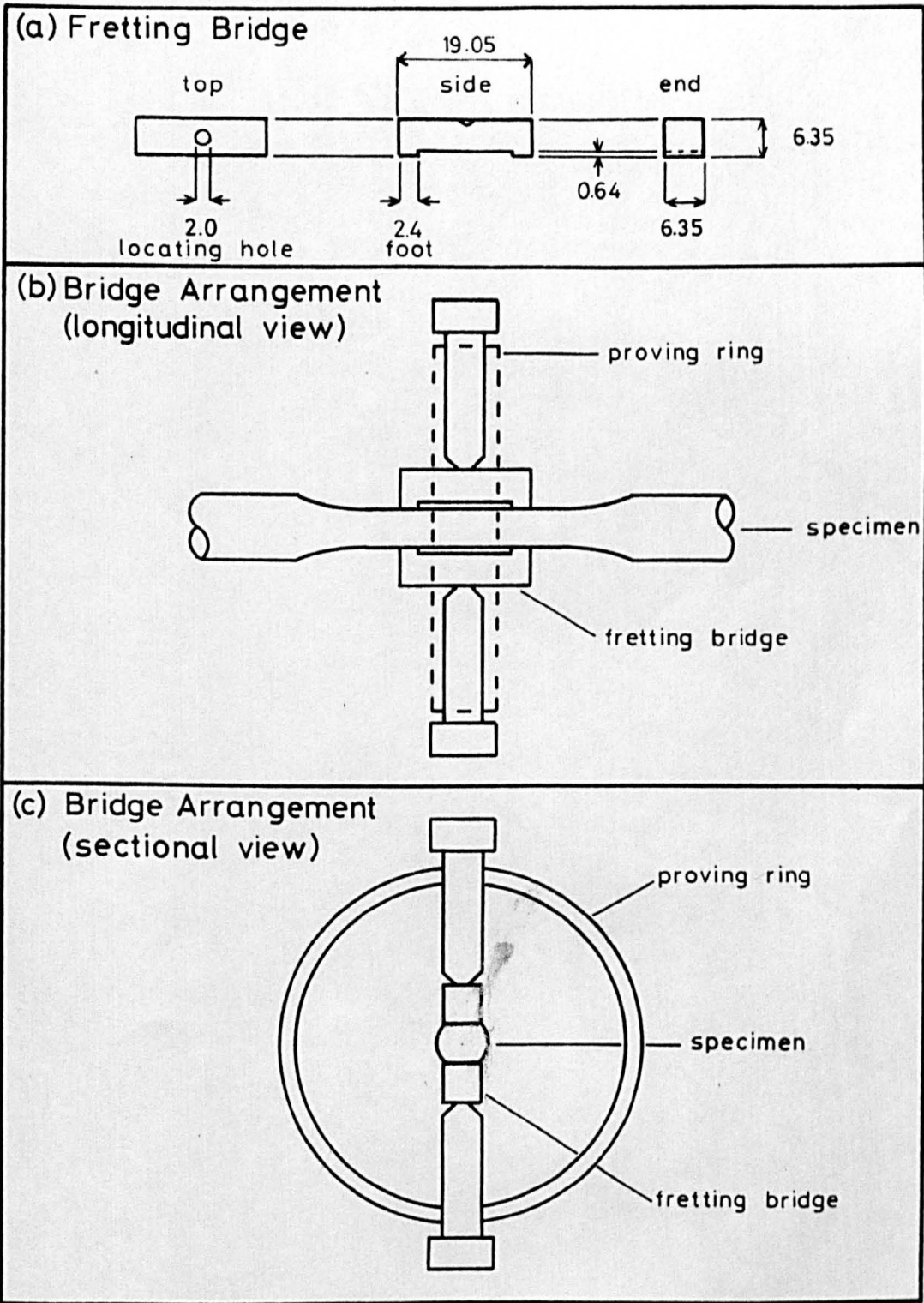


FIG. 4.4.

Schematic of the Fatigue Machine.

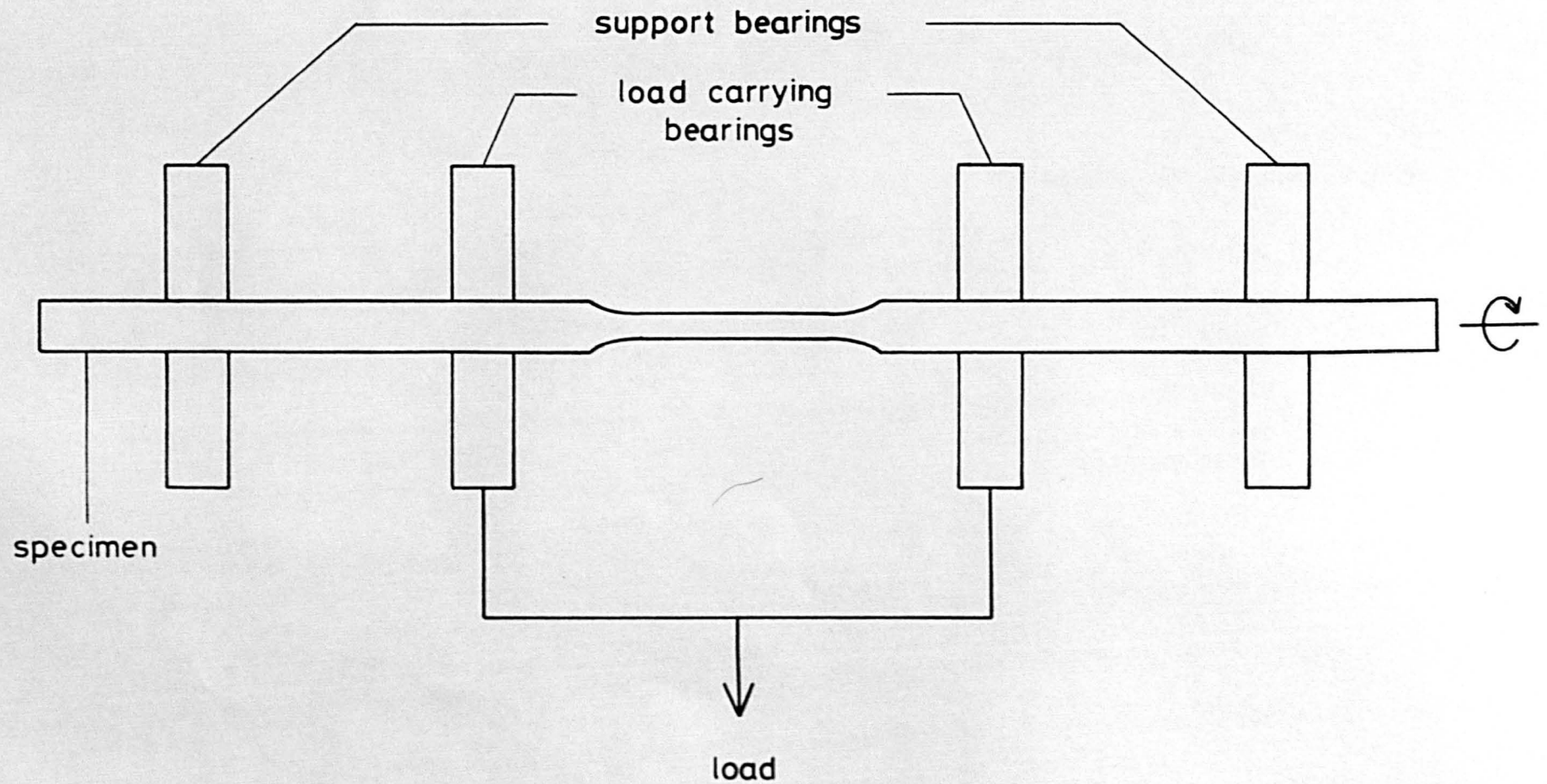
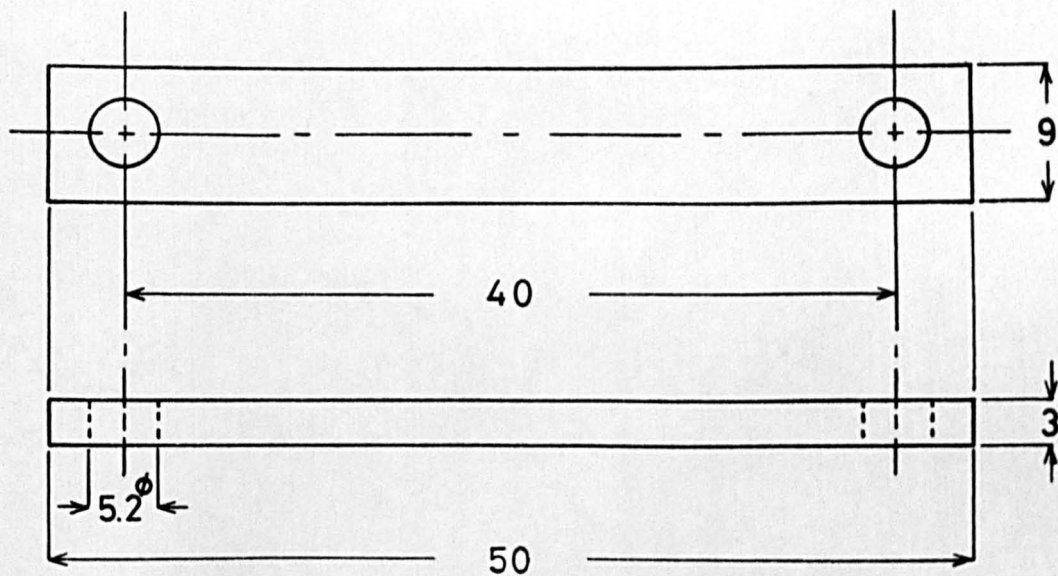


FIG. 4.5.
Plain Fretting Specimens

(units in mm)

(a) Flat.



(b) Rider.

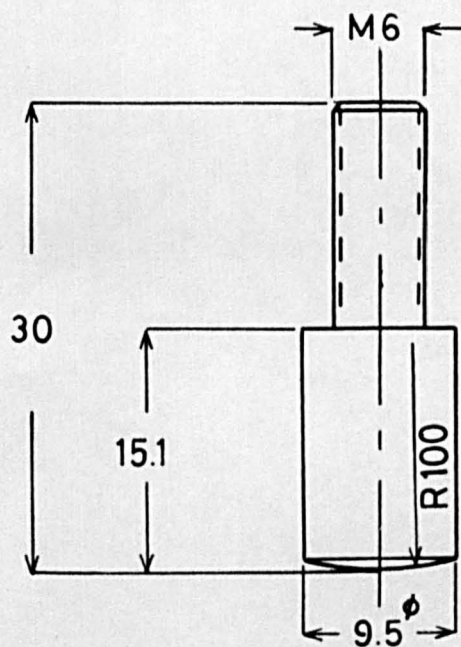


FIG. 4.6.

Schematic Diagram of the Plain Fretting Apparatus

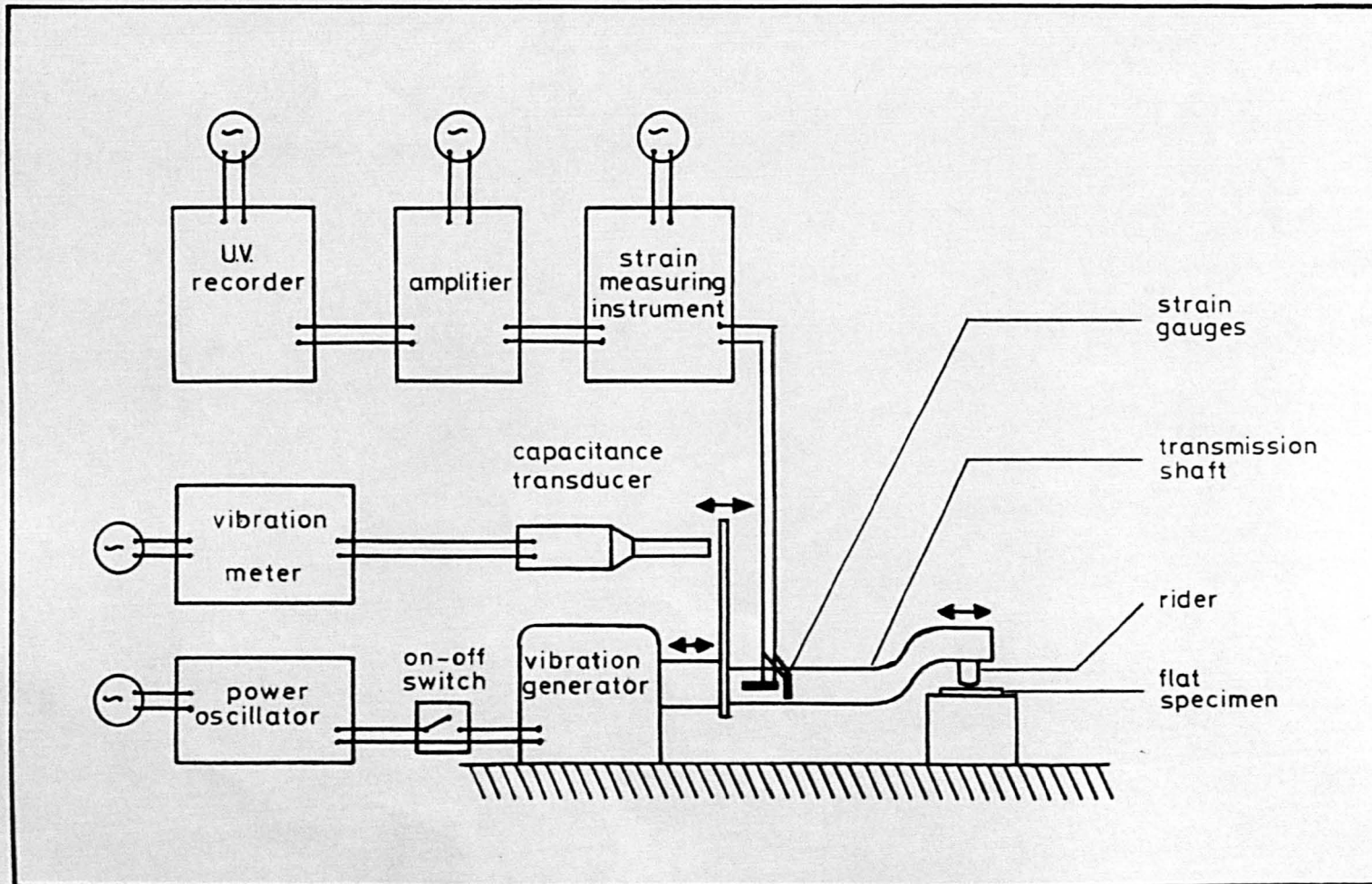
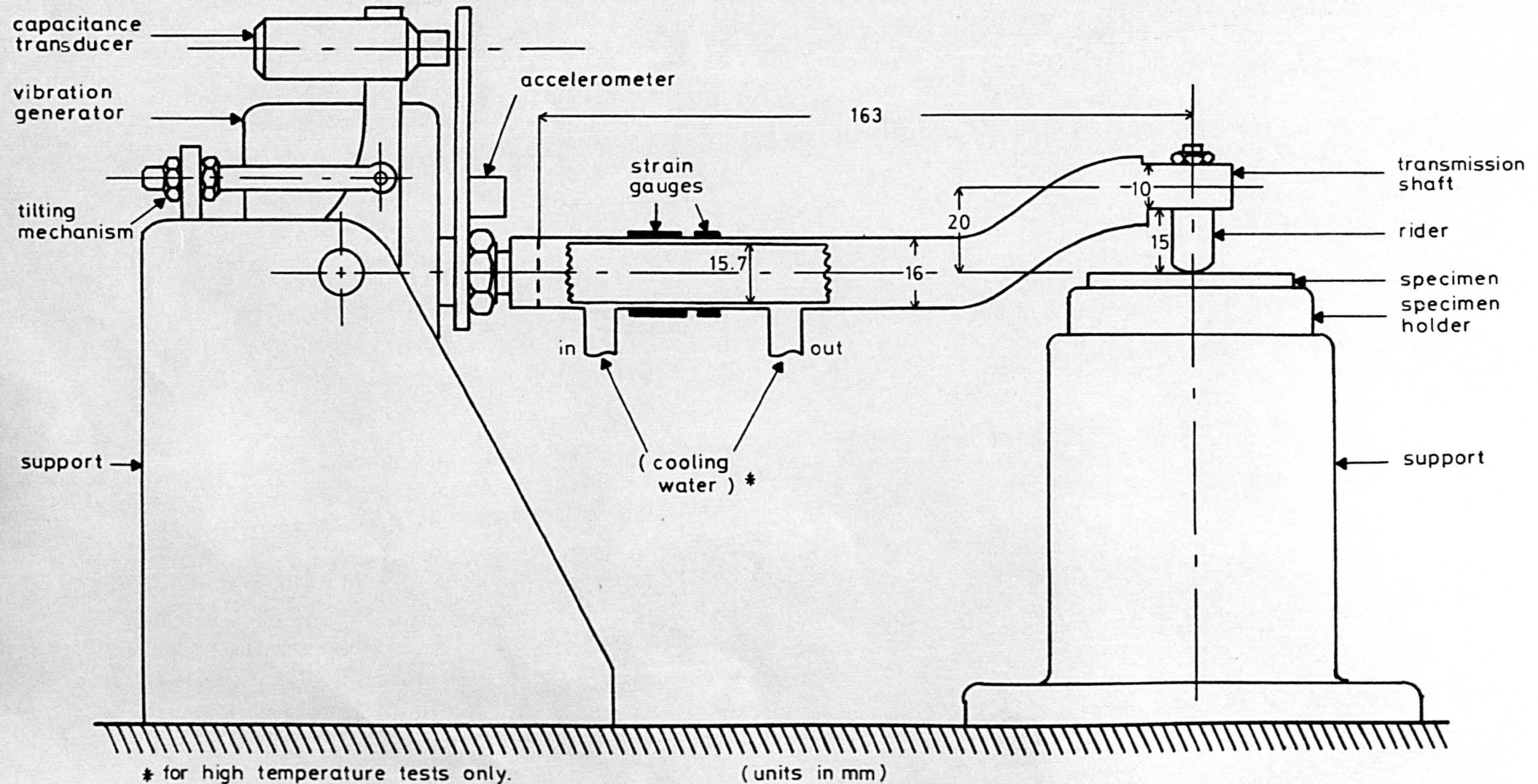


FIG. 4.7.
Schematic of the Plain Fretting Machine.



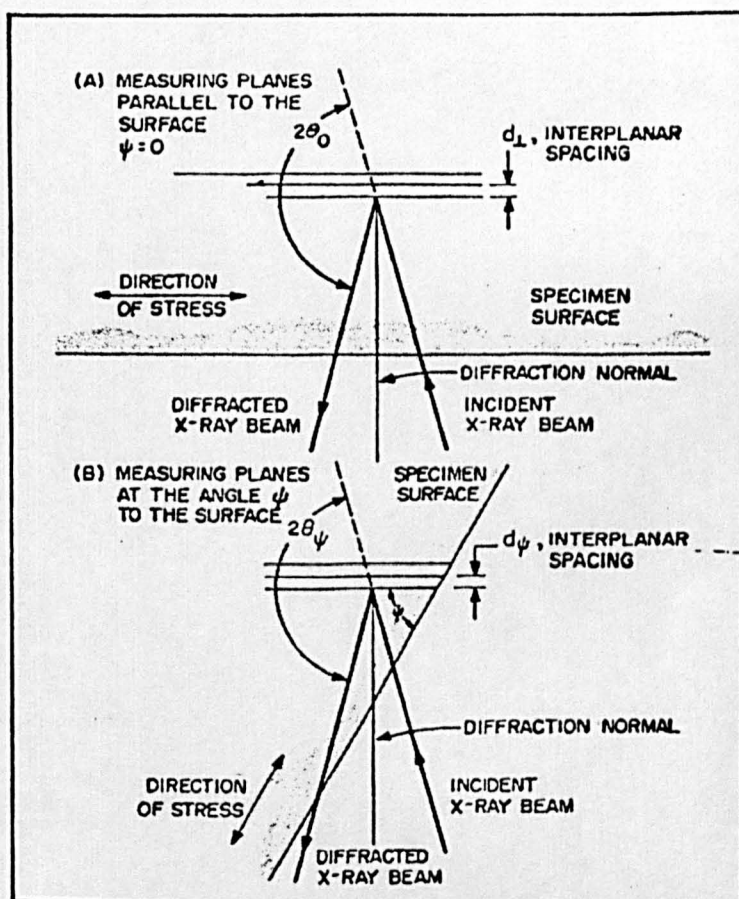


Figure 4.8. Schematic of X-ray stress measurement principle. (after Hilley et al (93))

TABLE. 4.4.

Summary of Testing in the Experimental Procedure.

<u>Specimen</u> <u>Treatment</u>	Surface Analysis						Testing			Post Testing Analysis			
	Res. Stre.	Stre. Prof.	Micr. Hard	Stret- ching	Taly- surf.	O.M. S.E.M.	Plain Fatigue	Fretting Fatigue	Plain Fretting	Resid. Stress	Opt. Micros.	S.E.M.	Taly- surf.
Age Hardened													
UNPEENED	•	•	•				•	•	•	•	•	•	•
SHOT PEENED (SMOOTH)	•	•	•	•			•	•	•	•	•	•	•
SHOT PEENED (ROUGH)					•	•	•	•	•		•	•	•
Naturally Aged													
UNPEENED	•	•	•				•	•	•	•	•	•	•
SHOT PEENED (SMOOTH)	•	•	•				•	•	•	•	•	•	•
SHOT PEENED (ROUGH)					•	•	•	•	•		•	•	•
Fully Annealed													
UNPEENED	•		•				•	•			•	•	
SHOT PEENED (SMOOTH)	•		•		•	•	•	•			•	•	

FIG. 5.1.

S-N Curves for Unpeened Age Hardened Al-4%Cu-1%Mg

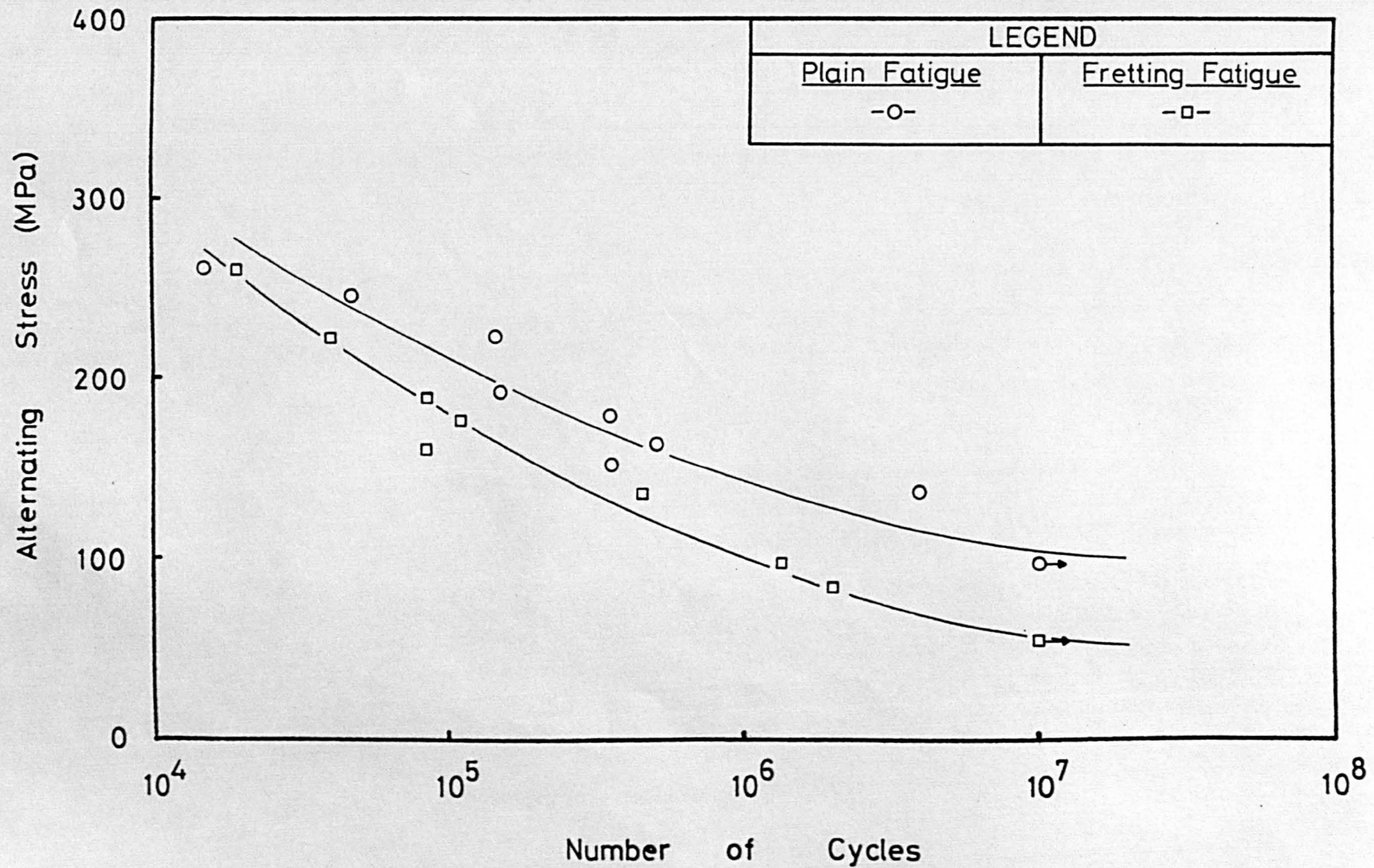


FIG. 5.2.

S-N Curves for Unpeened Naturally Aged Al-4%Cu-1%Mg

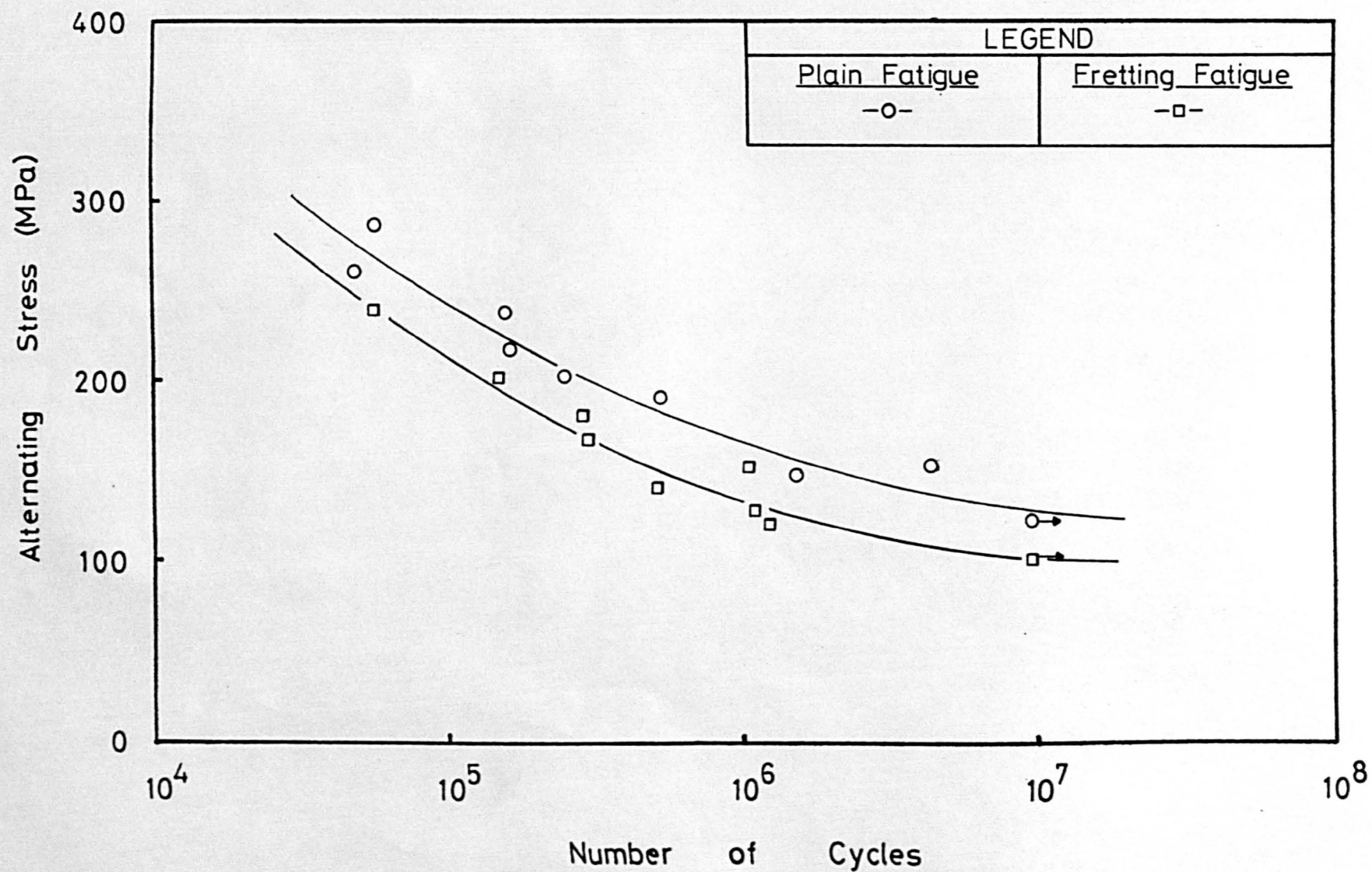


FIG. 5.3.

S-N Curves for Shot Peened (smooth) Age Hardened
Al-4%Cu-1%Mg.

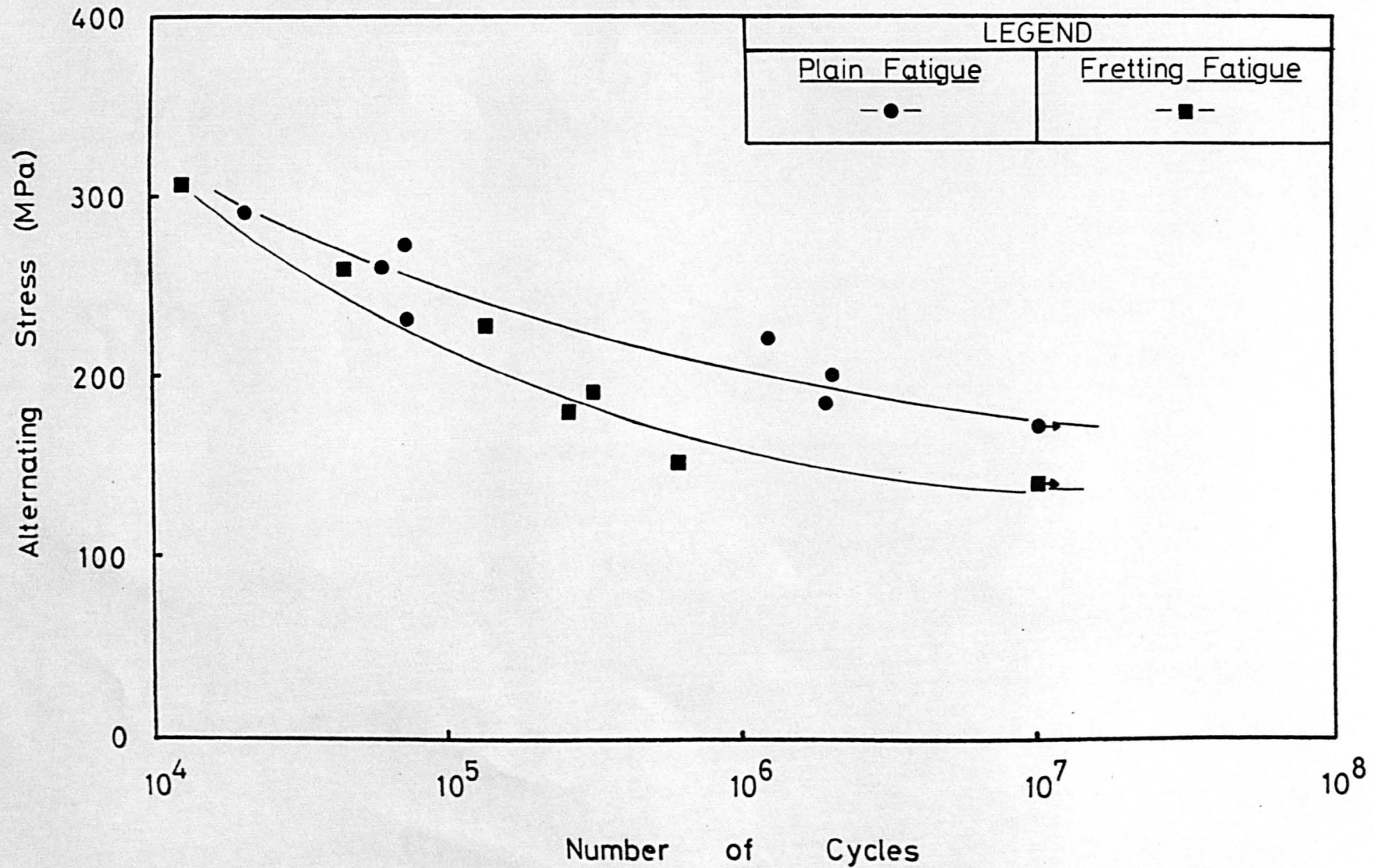


FIG. 5.4.

S-N Curves for Shot Peened (smooth) Naturally Aged
Al-4%Cu-1%Mg.

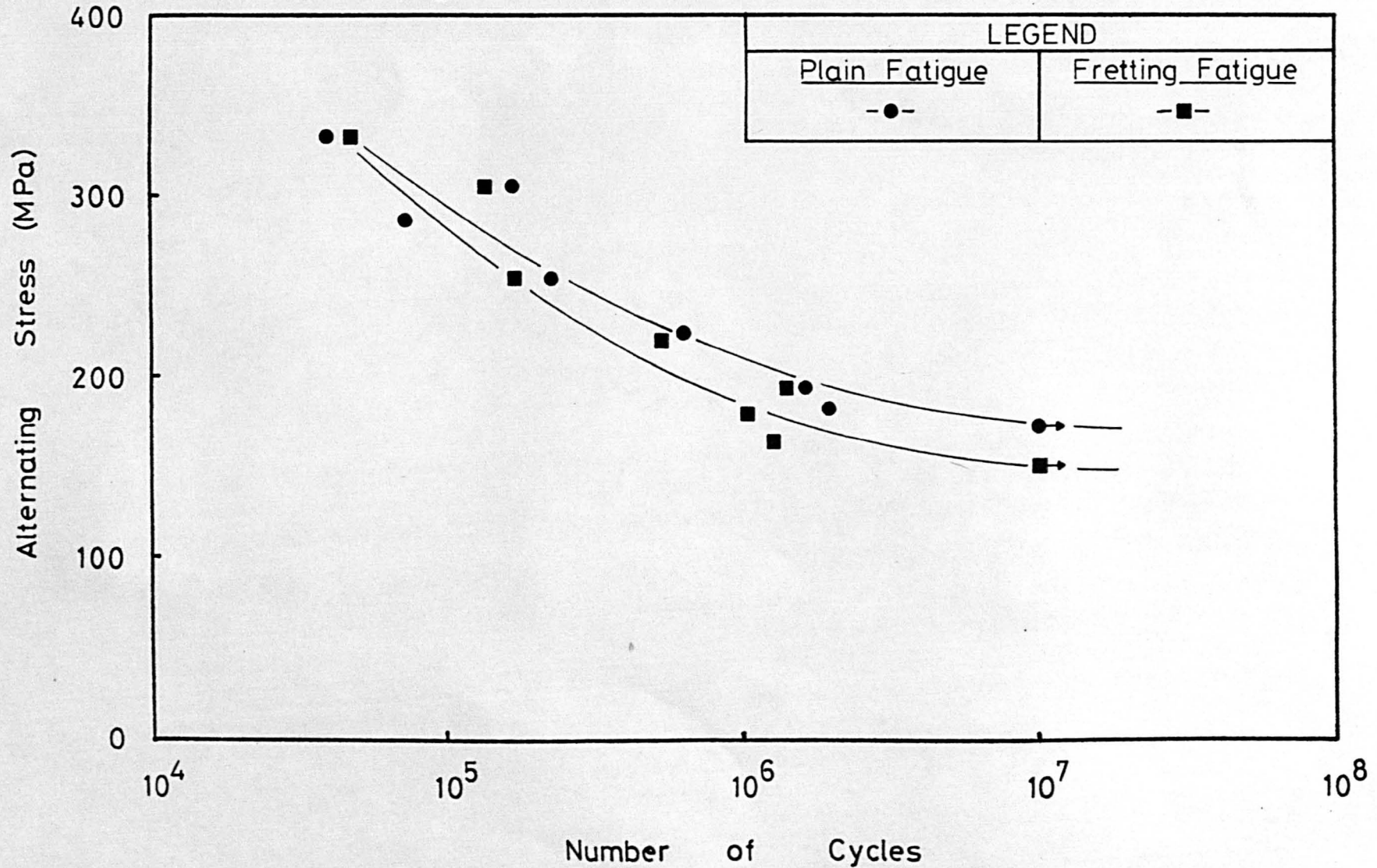


FIG. 5.5.

S-N Curves for Shot Peened (rough) Age Hardened
Al-4%Cu-1%Mg.

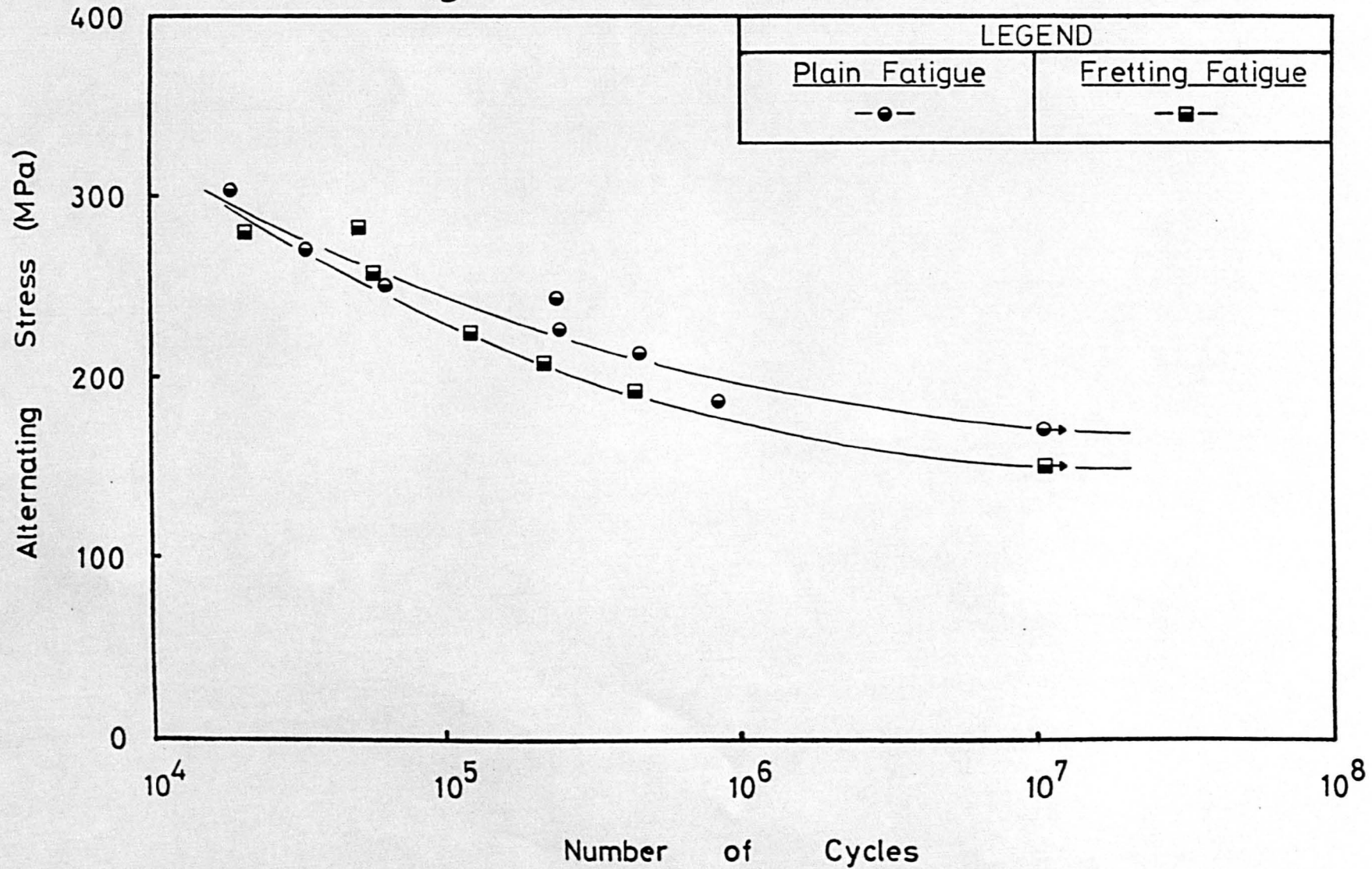


FIG. 5.6.

S-N Curves for Shot Peened (rough) Naturally Aged
Al-4%Cu-1%Mg.

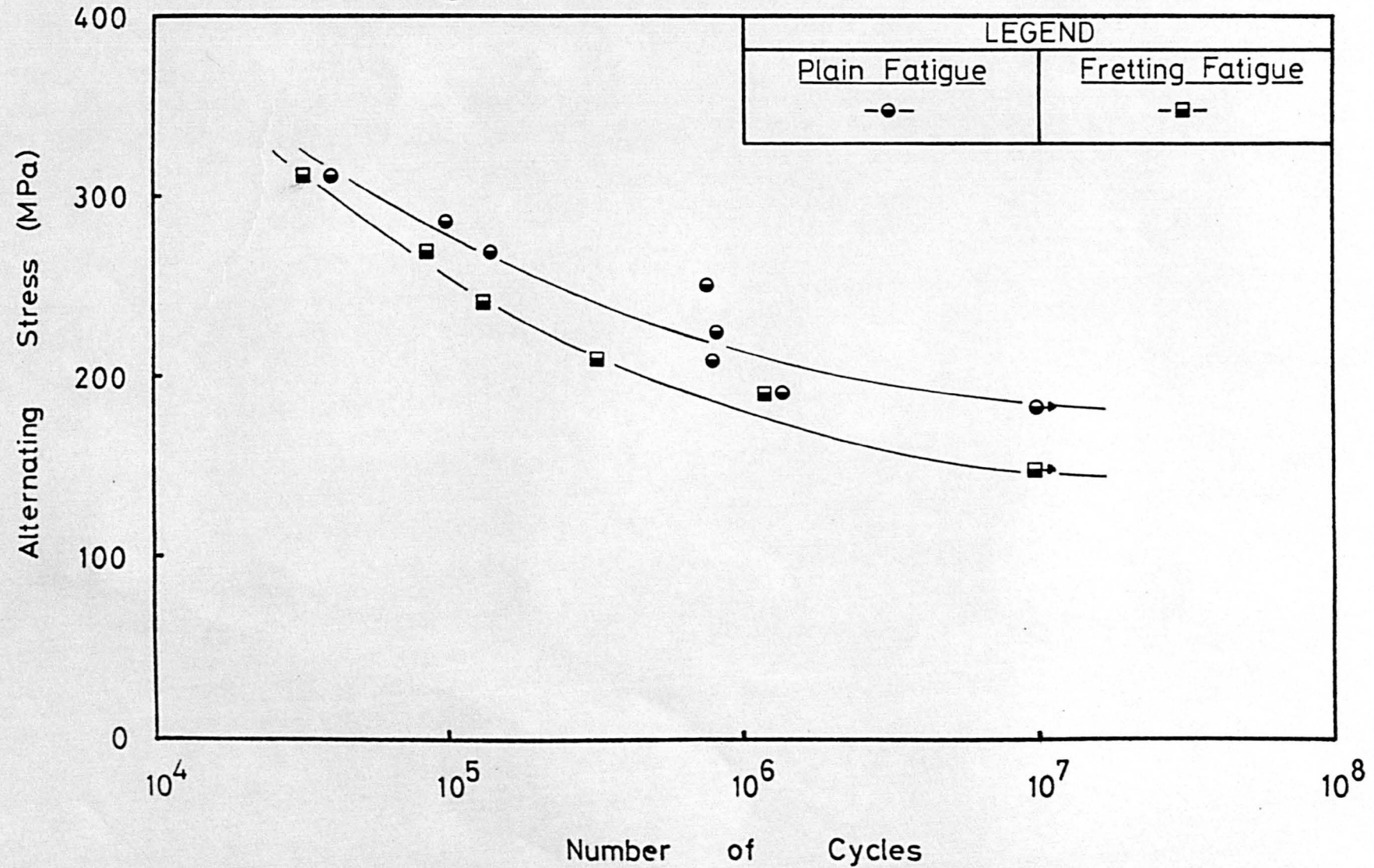


FIG. 5.7.

S-N Curves for Unpeened and Shot Peened (smooth)
Fully Annealed Al-4%Cu-1%Mg.

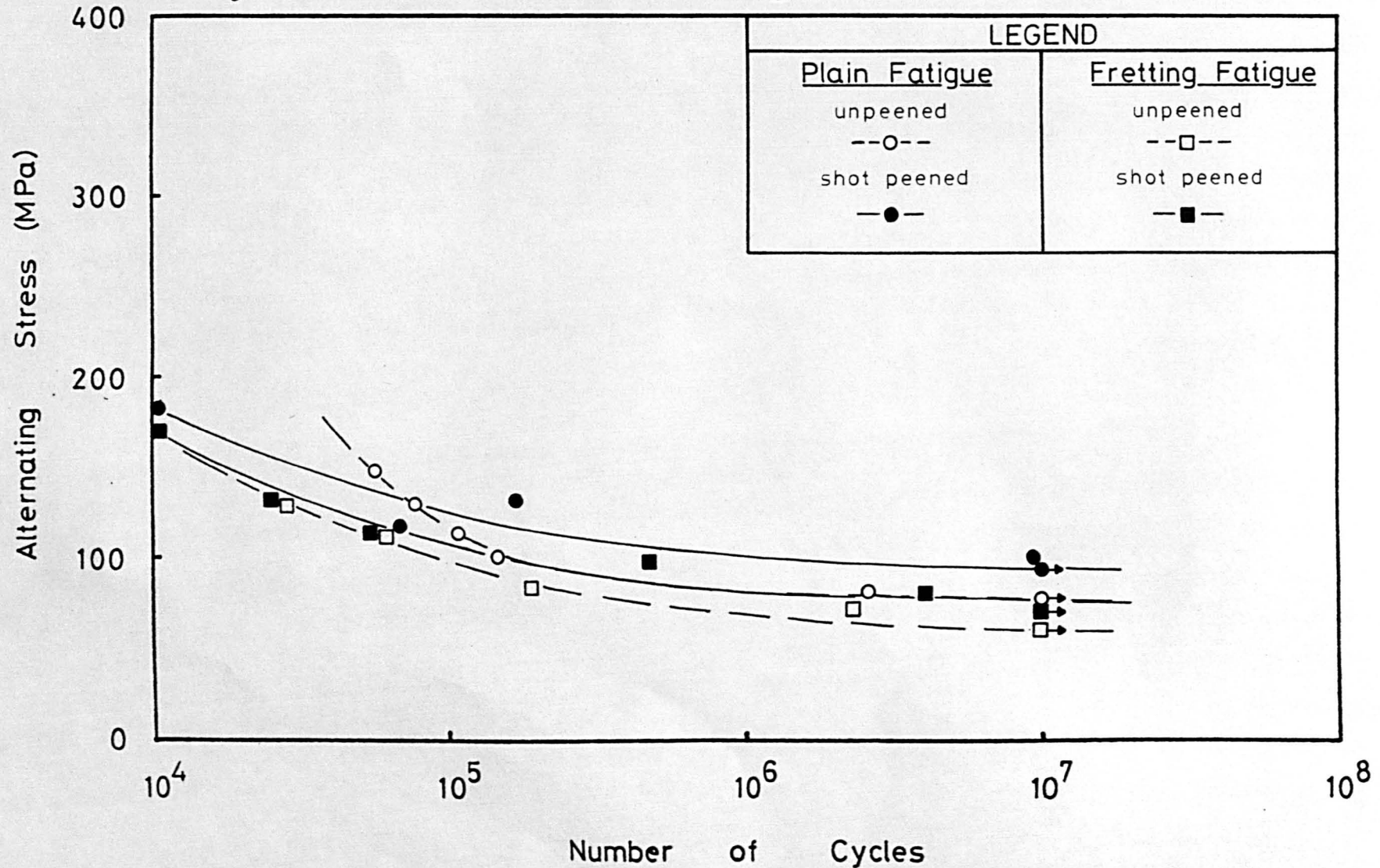


FIG. 5.8.

S-N Curve Compilation for the Surface Treatments on Age Hardened Al-4%Cu-1%Mg.

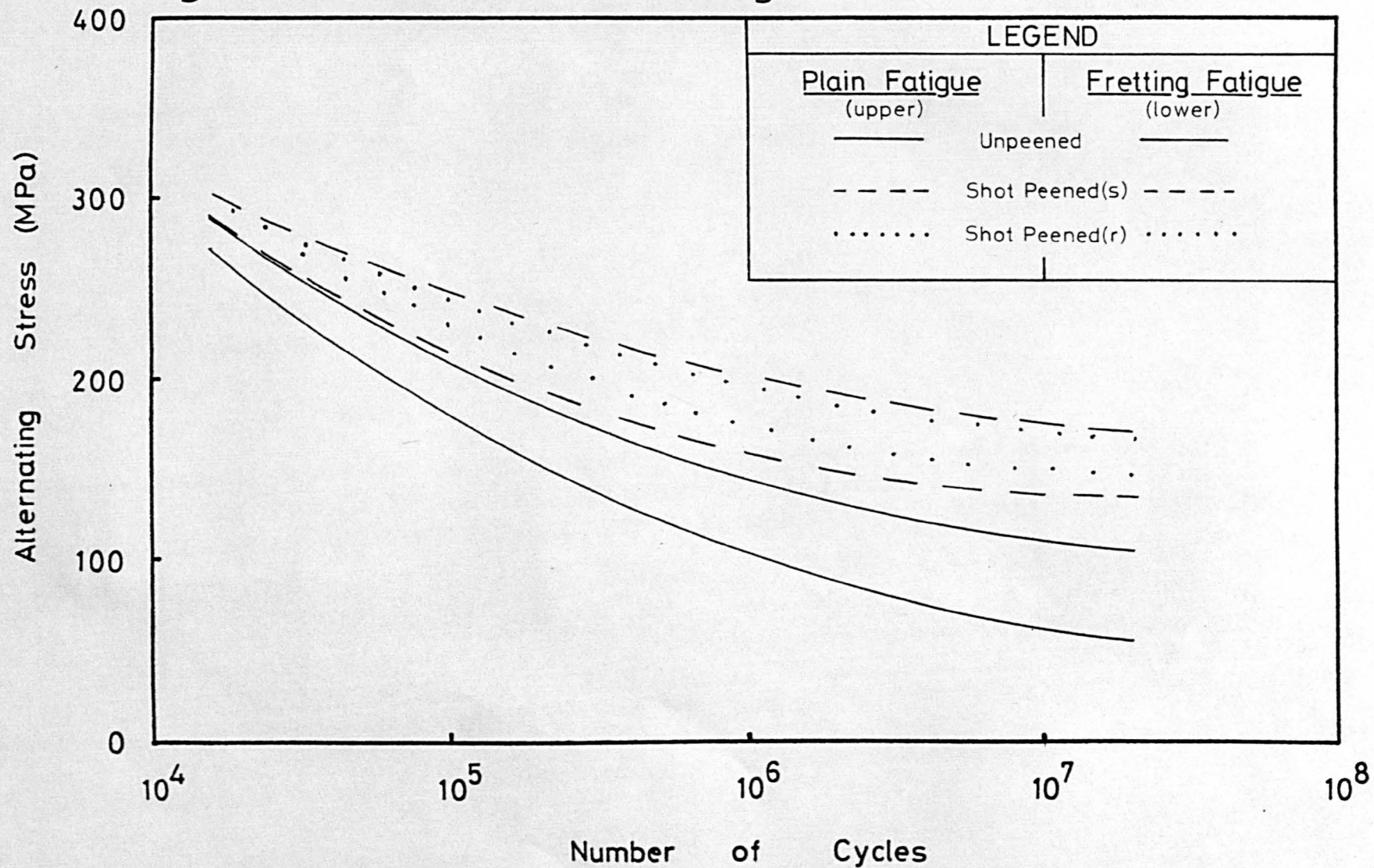


FIG. 5.9.

S-N Curve Compilation for the Surface Treatments on Naturally Aged Al-4%Cu-1%Mg.

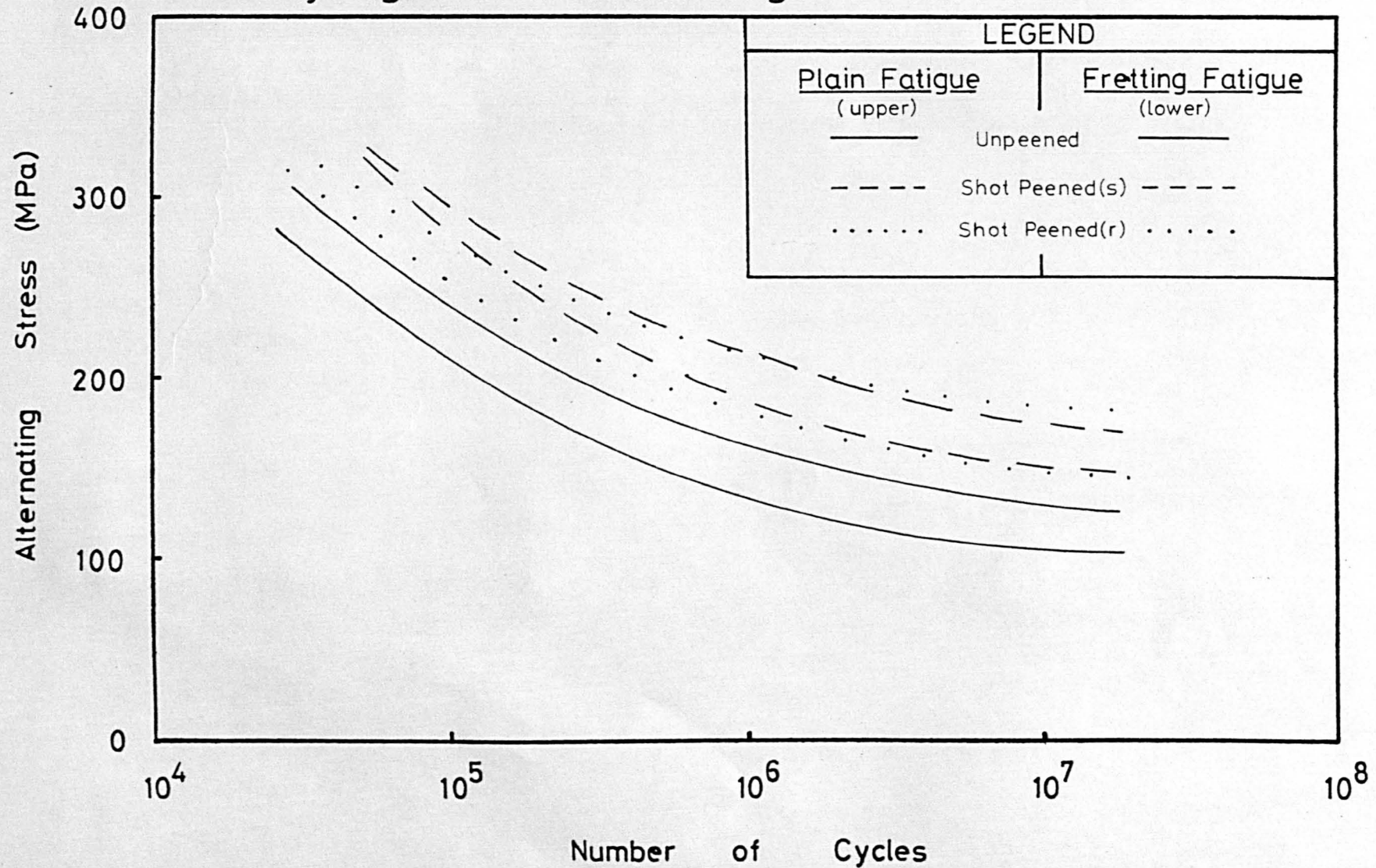


TABLE 5.1.

Summary of Plain Fatigue and Fretting Fatigue Test Results. (after 10^7 cycles).

HEAT TREATMENT	Reduction in fatigue strength due to fretting.	Increase in plain fatigue strength due to shot peening.	Increase in fretting fatigue strength due to shot peening.
Age Hardened	45%	50%	130%
Naturally Aged	10%	45%	40%
Fully Annealed	20%	25%	20%

FIG. 5.10.

Variation in Coefficient of Friction with No. of Fretting Cycles for Age Hardened Al-4%Cu-1%Mg.

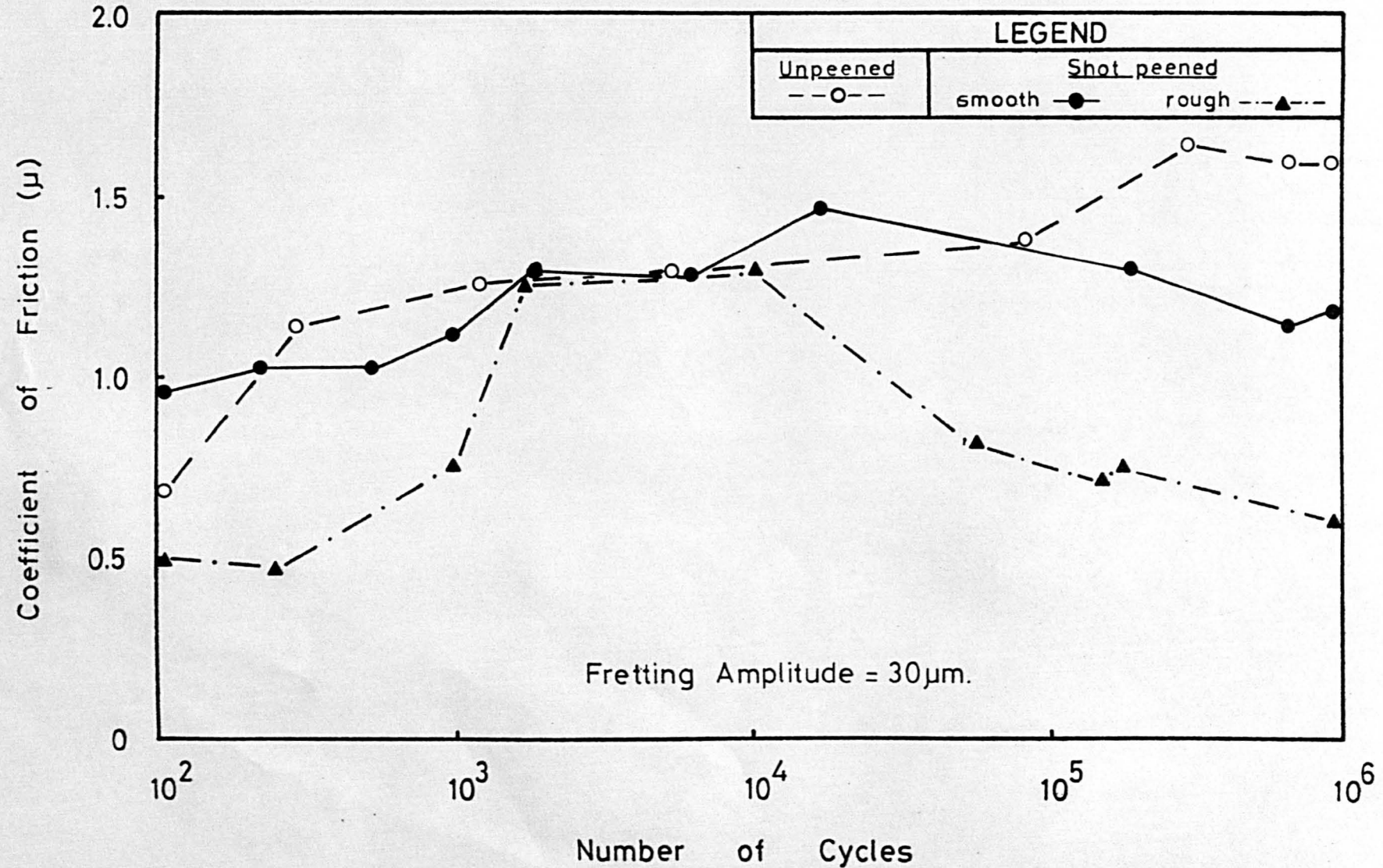


FIG. 5.11.

Variation in Coefficient of Friction with No. of Fretting Cycles for Naturally Aged Al-4%Cu-1%Mg.

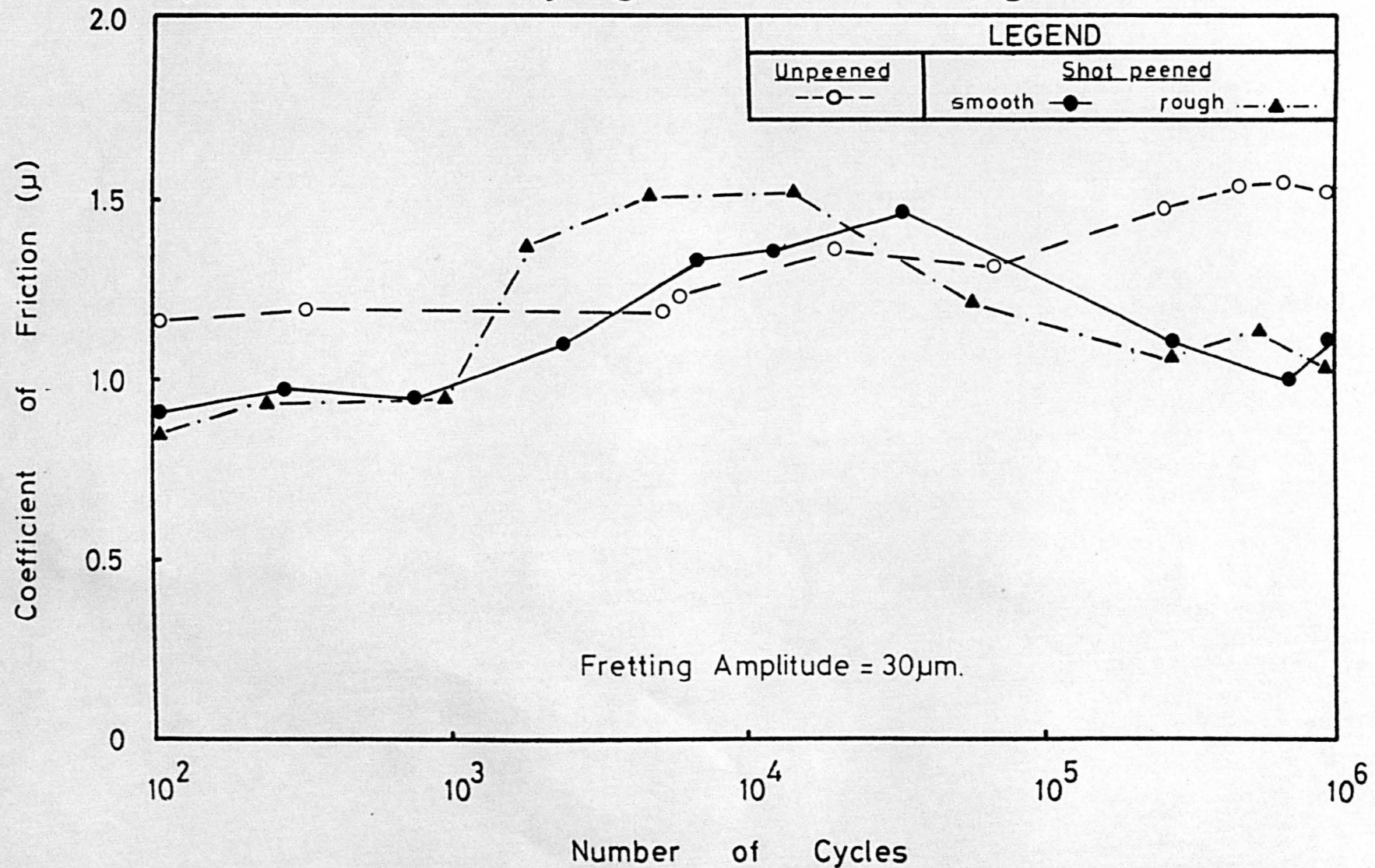


FIG. 5.12.

Residual Stress/Depth Profiles for Age Hardened and Naturally Aged Al-4%Cu-1%Mg Alloy.

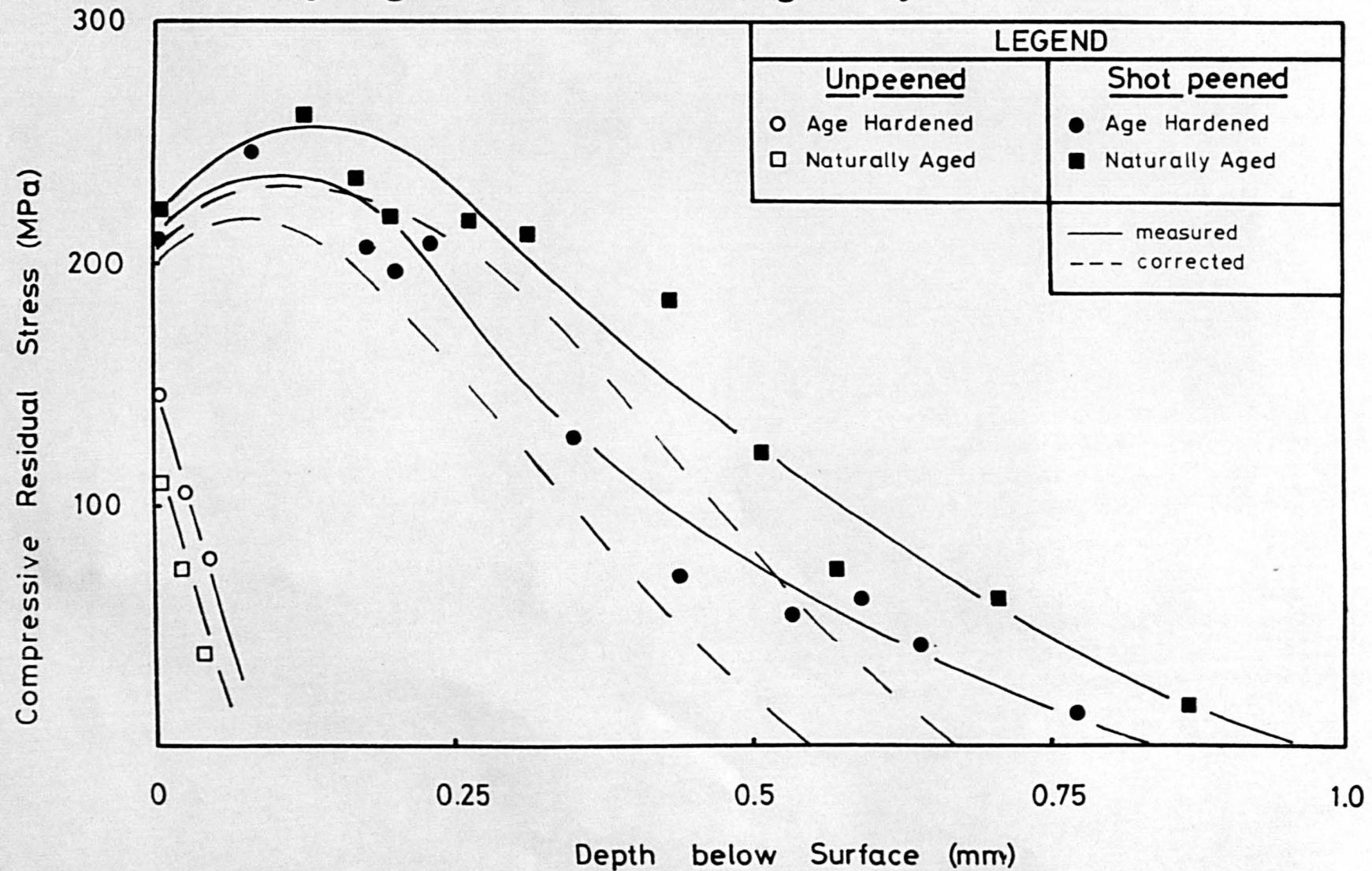


FIG. 5.13.
Microhardness Traverses For Al-4%Cu-1%Mg Alloy.

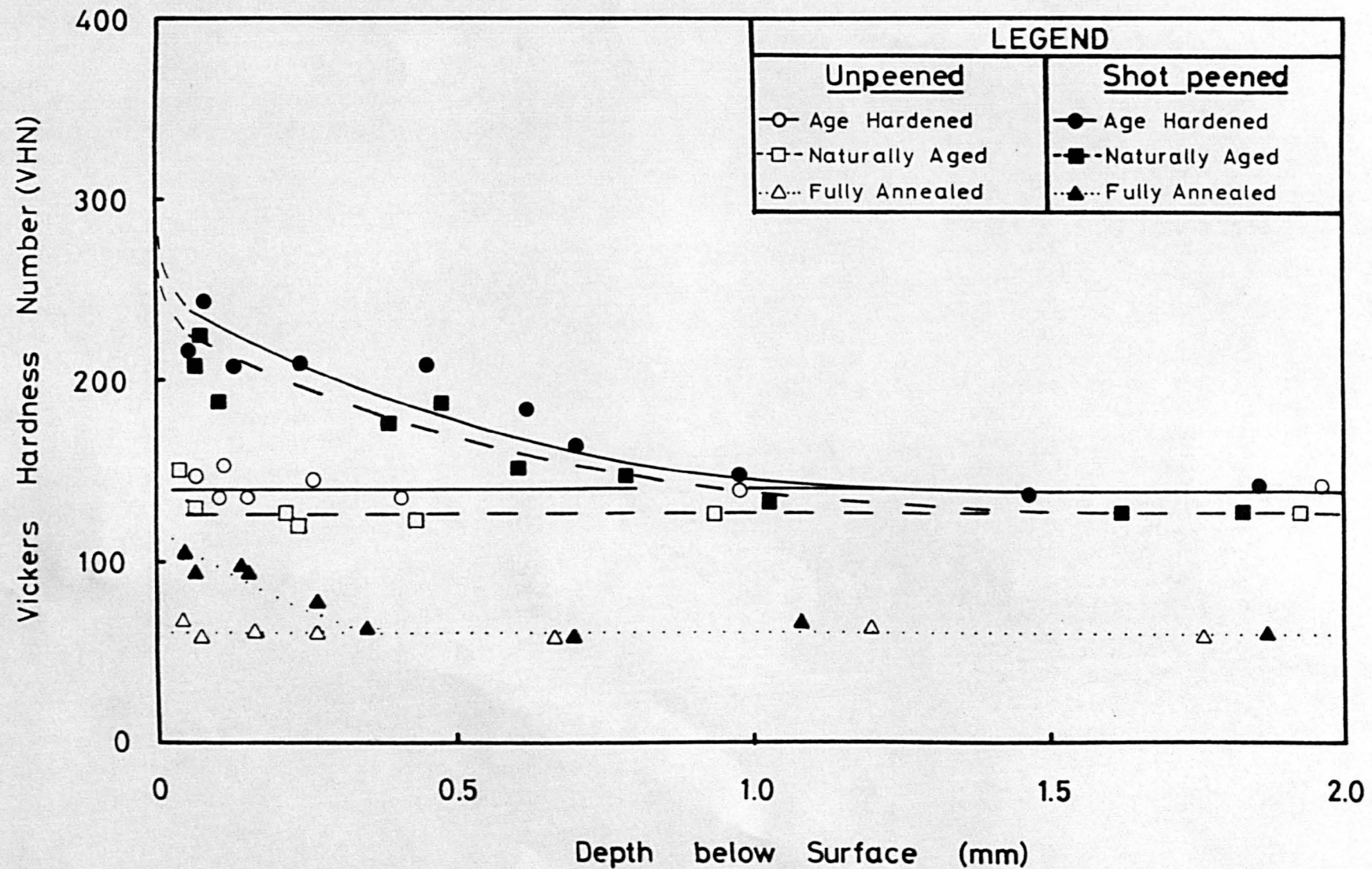
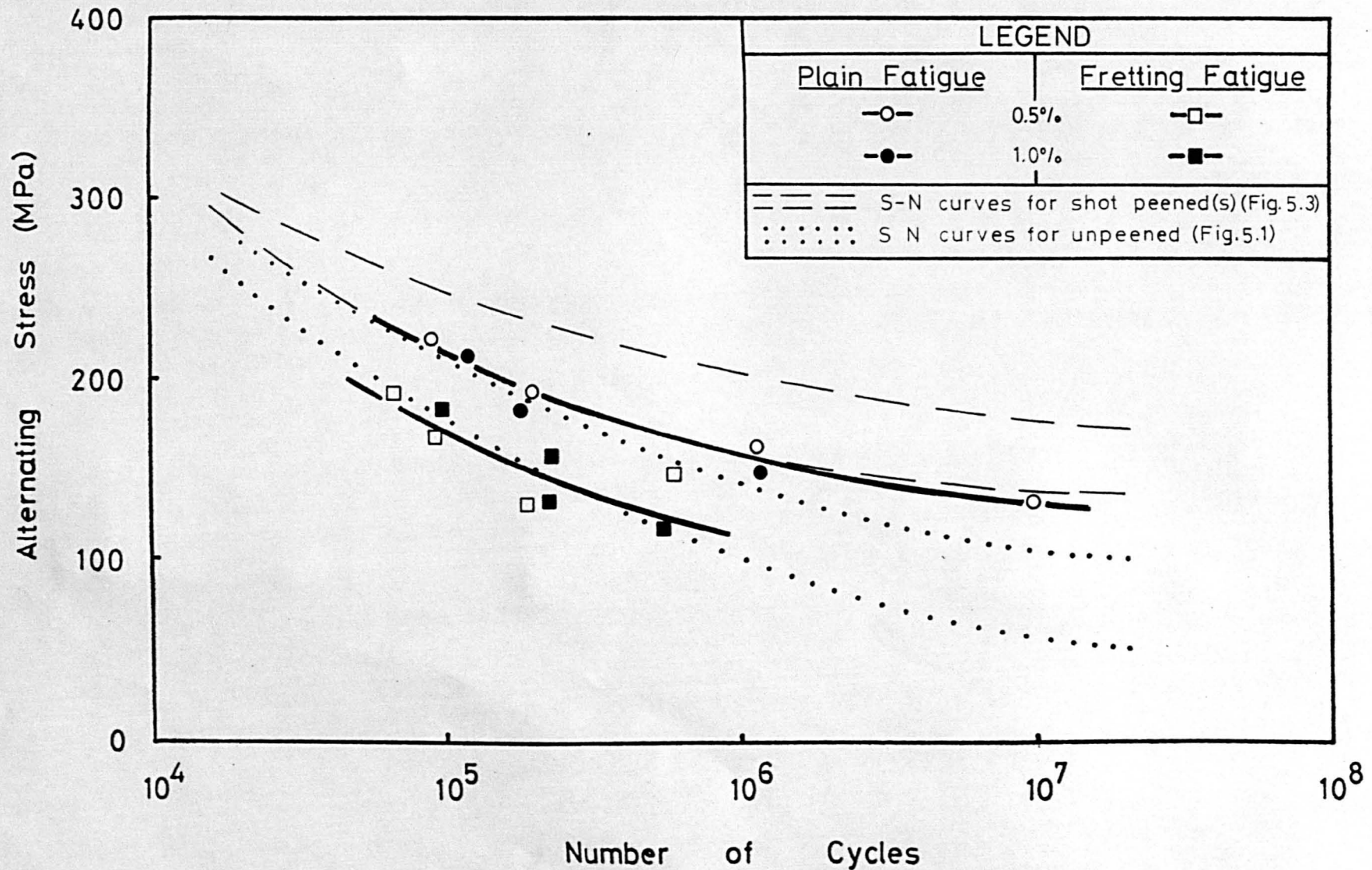
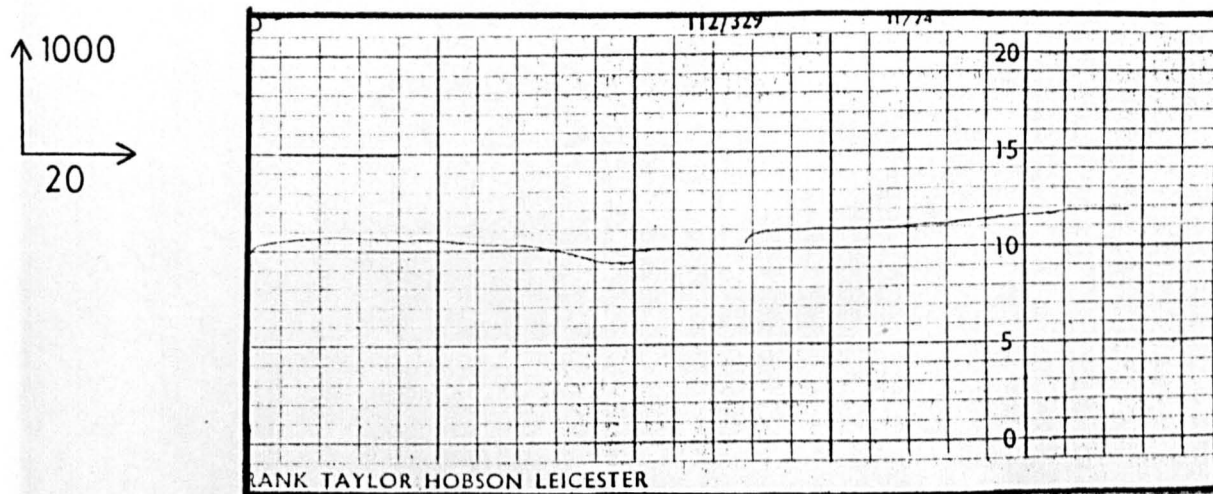


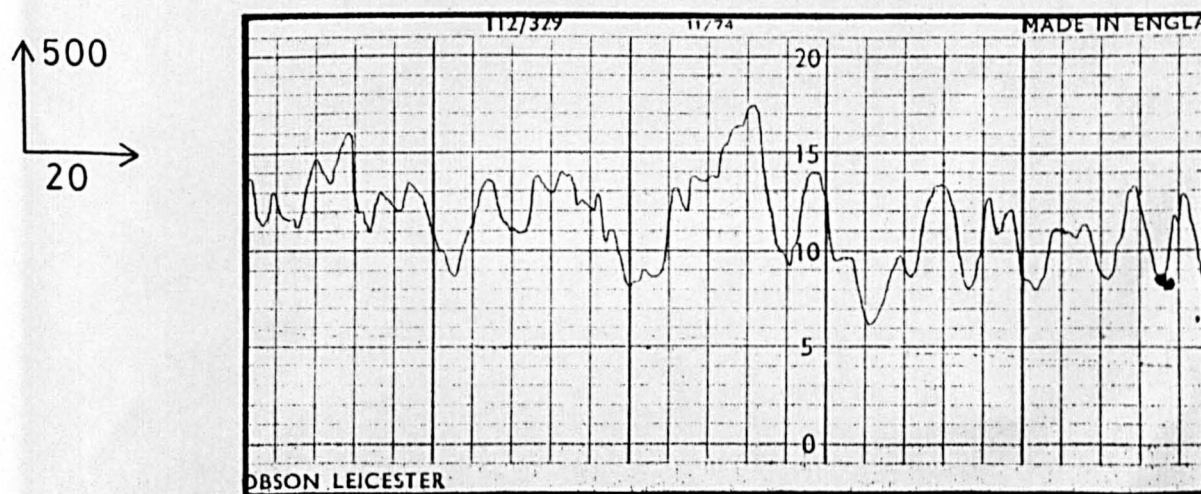
FIG. 5.14.

S-N Curves for 0.5% and 1.0% 'Stretched' Shot Peened (smooth) Age Hardened Al-4%Cu-1%Mg.





(a) for the polished surface.



(b) for the shot peened (rough) surface.

Figure 5.15. Talysurf traces.

FIG. 5.16.

Effect of Fatigue Cycling on the Residual Compressive Stress in Age Hardened Al-4%Cu-1%Mg.

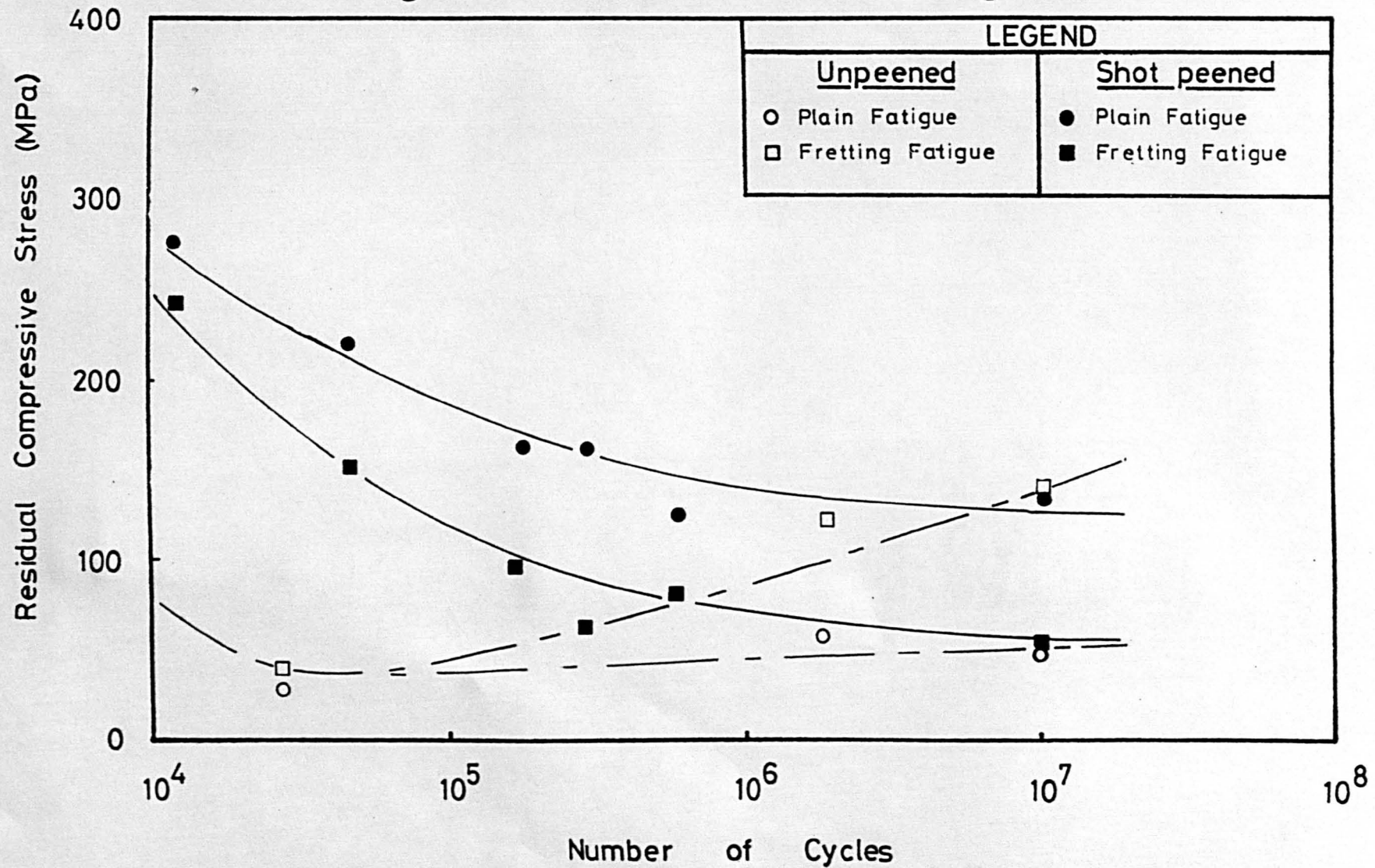
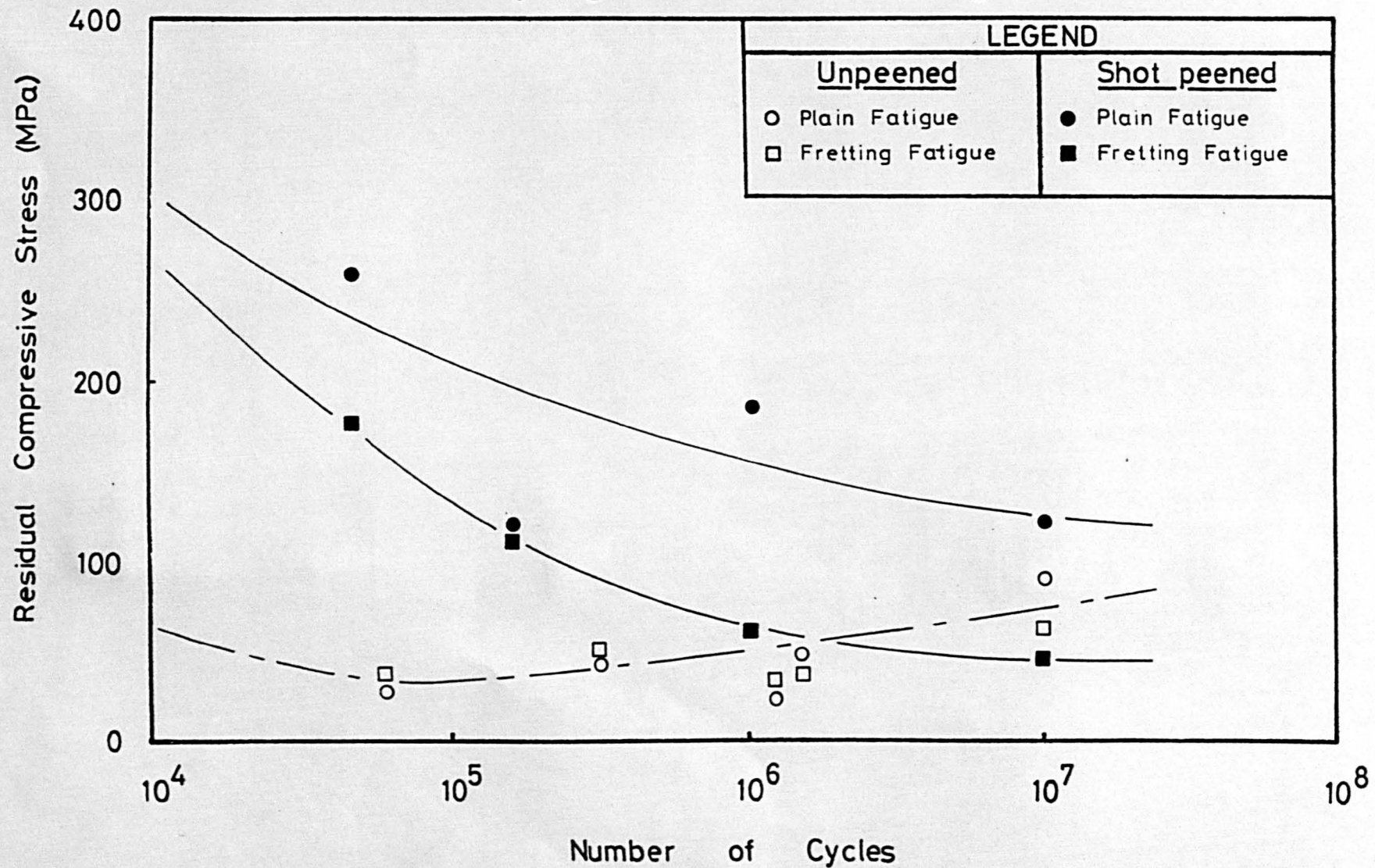
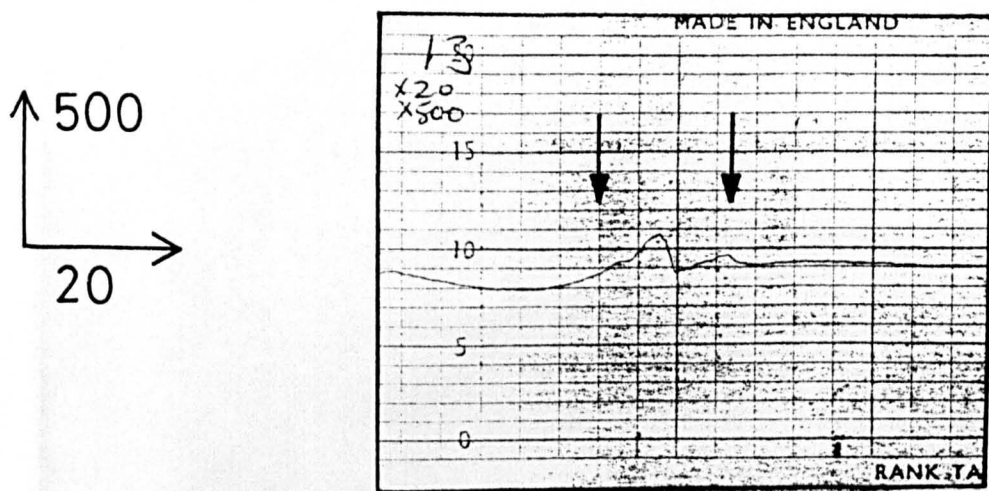


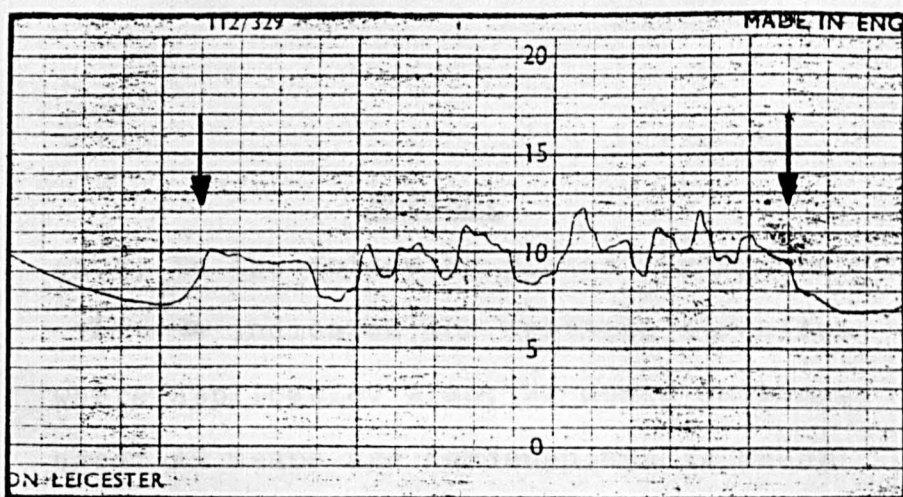
FIG. 5.17.

Effect of Fatigue Cycling on the Residual Compressive Stress in Naturally Aged Al-4%Cu-1%Mg.

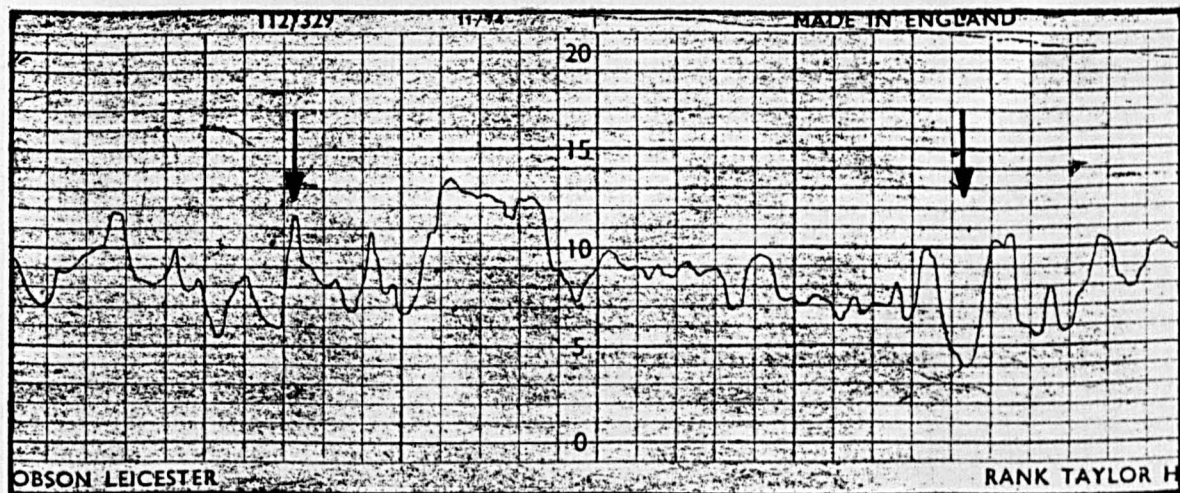




(a) for the unpeened surface.



(b) for the shot peened (smooth) surface.



(c) for the shot peened (rough) surface.

Figure 5.18. Talysurf traces on fretting scars.

PLATES.

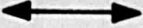
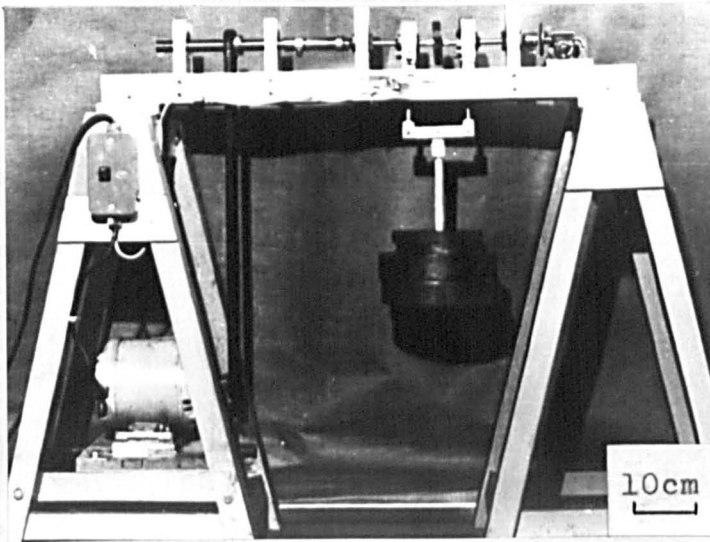
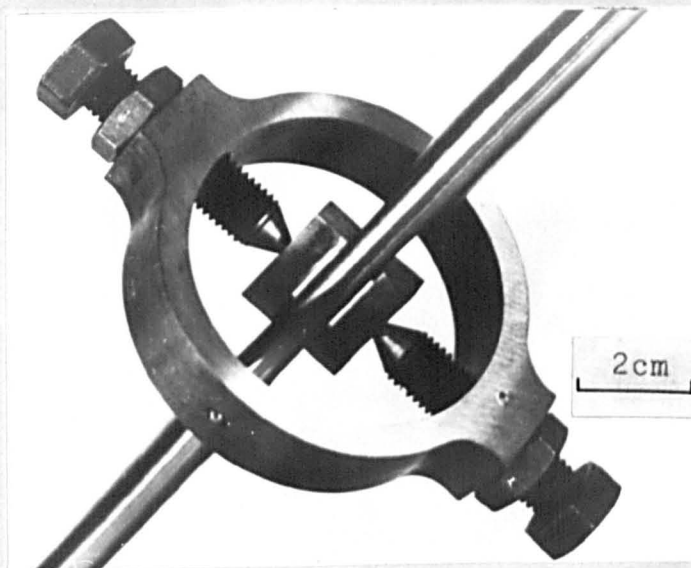
(N.B. In the following plates the symbol
 indicates the fretting direction
where applicable. Also; NA means naturally
aged; AH means age hardened; and FA means
fully annealed.)

PLATE 1.

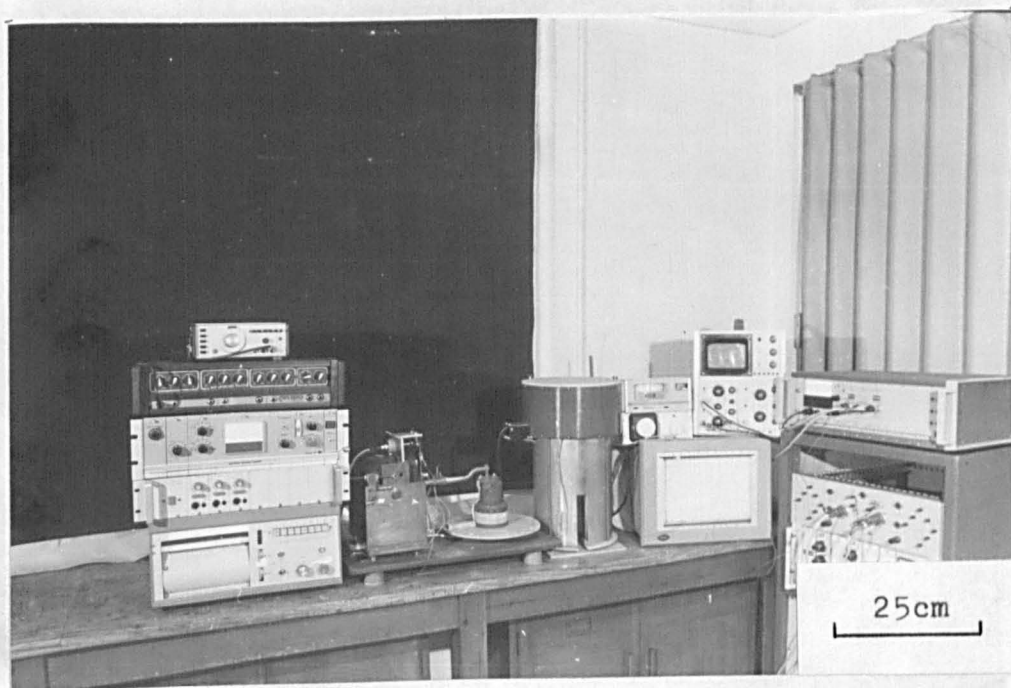


(a) The rotating-bending fatigue machine.

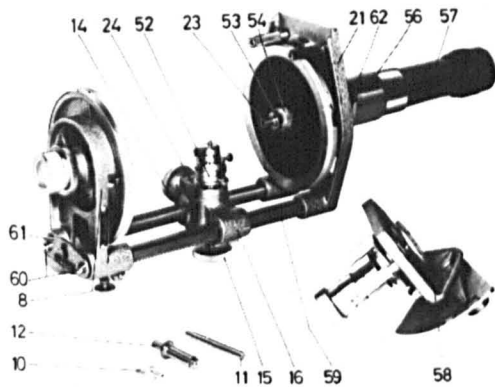
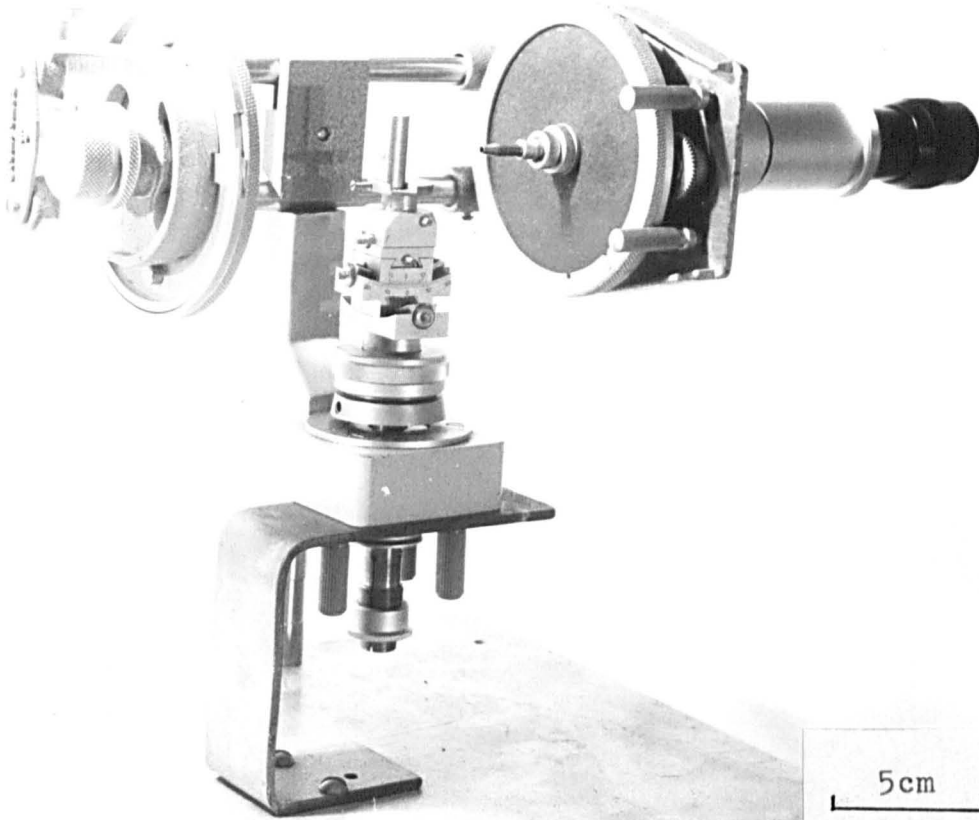


(b) The fretting device.

PLATE 2.



The plain fretting apparatus.

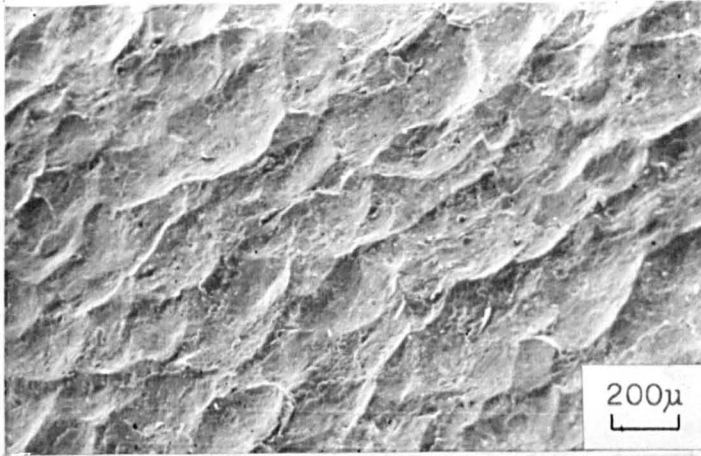


- | | | | |
|----|--|----|---|
| 8 | Cassette holder for transmission patterns | 54 | Knurled screw for closing the film cassette for reflection patterns |
| 10 | Specimen aperture | 56 | Stand for the adjusting microscope |
| 11 | Focusing aperture | 57 | Adjusting microscope |
| 12 | Inlet aperture | 58 | Specimen holder for precision measurements of lattice constants |
| 14 | Knurled screw for fixing the carriage (16) | 59 | Scale for setting the distance between film and specimen in reflection patterns |
| 15 | Knurled screw for height adjustment of the crystal | 60 | Mounting screws of the front plate |
| 16 | Specimen holder carriage | 61 | Front plate |
| 21 | Base plate | 62 | Locking lever for the stand (56) |
| 23 | Aperture holder | | |
| 24 | Groove for guiding the specimen holder | | |
| 52 | Small goniometer head | | |
| 53 | Knurled screw for fixing the film cassette for reflection patterns on the aperture holder (23) | | |

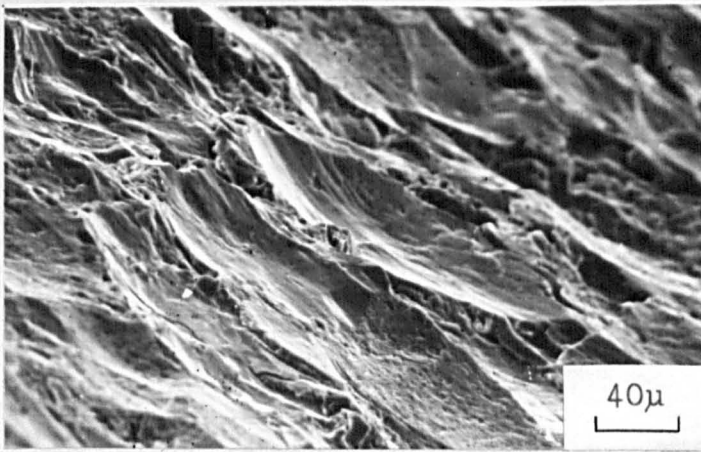
The back-reflection x-ray camera system.

PLATE 4.

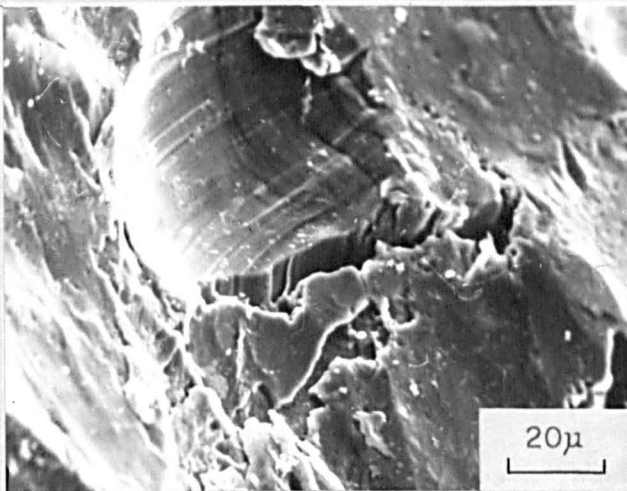
Scanning electron micrographs of the shot
peened (rough) surface.



(a) low magnification showing the dimples



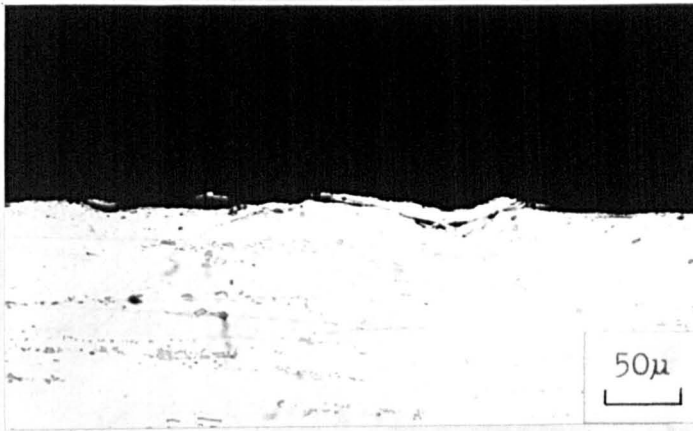
(b) higher magnification



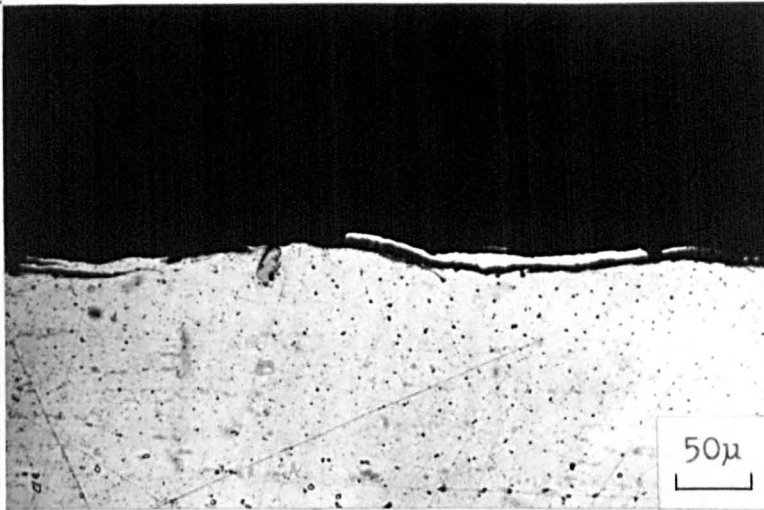
(c) higher magnification showing material
folding.

PLATE 5.

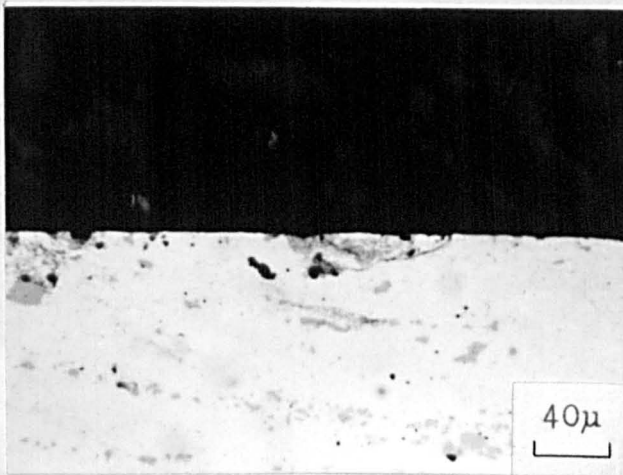
Optical micrographs of specimen sections
showing the damage produced by shot peening.



(a) material folding on an as-peened surface



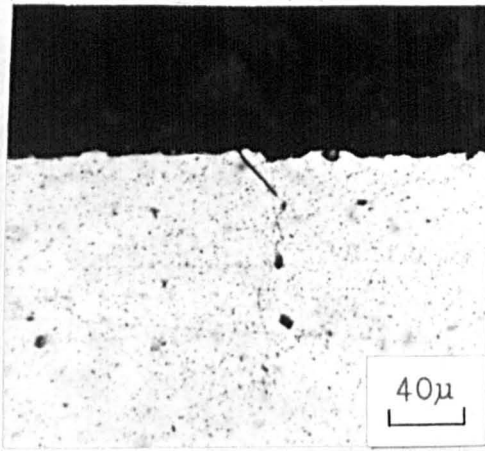
(b) as above



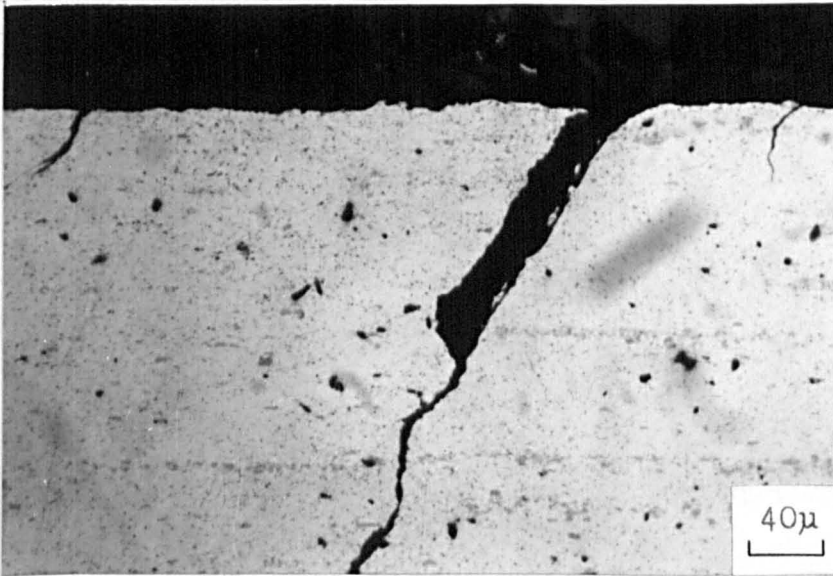
(c) subsurface damage on a smoothed specimen.

PLATE 6.

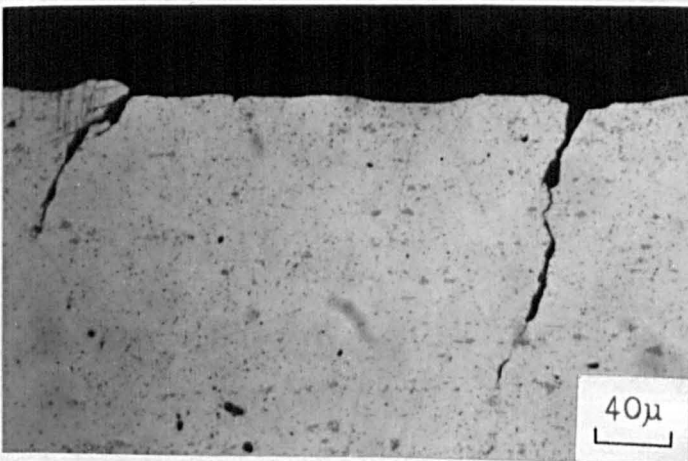
Optical micrographs of fretting fatigue cracks in the NA unpeened material.



(a) after 1.5×10^5 cycles at 205 MPa



(b) after 2.8×10^5 cycles at 183 MPa



(c) after 10^7 cycles at 100 MPa.

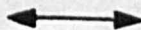
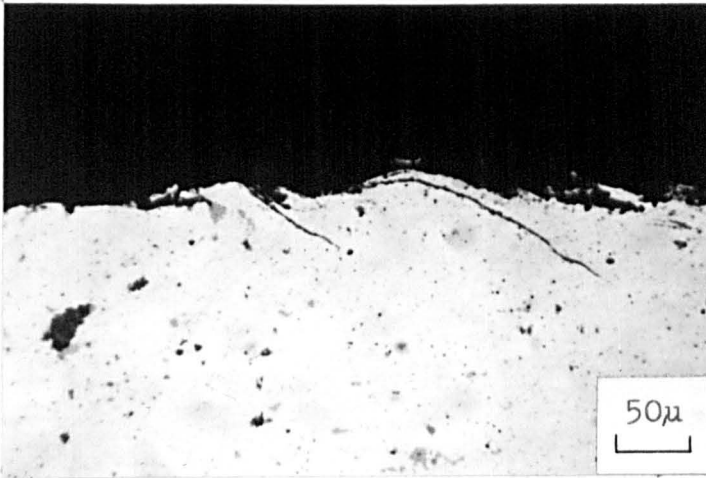
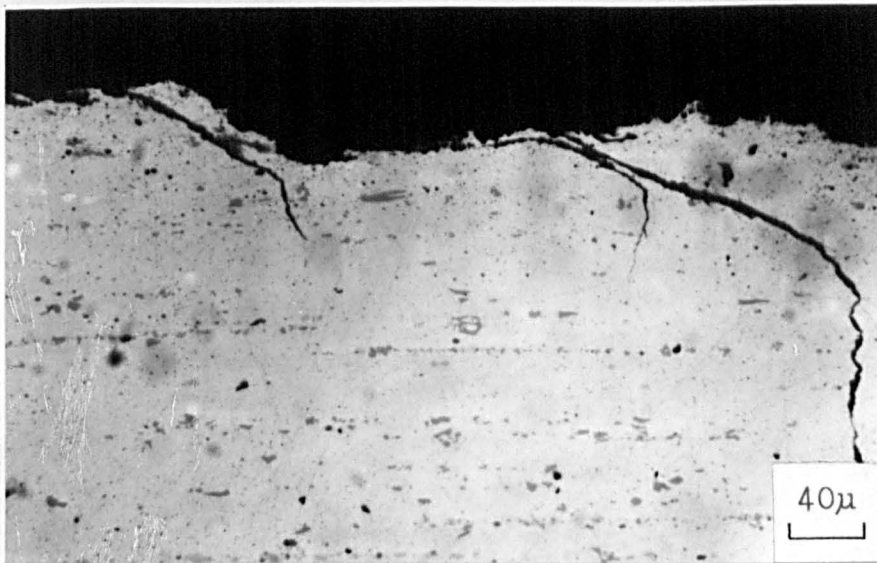


PLATE 7.

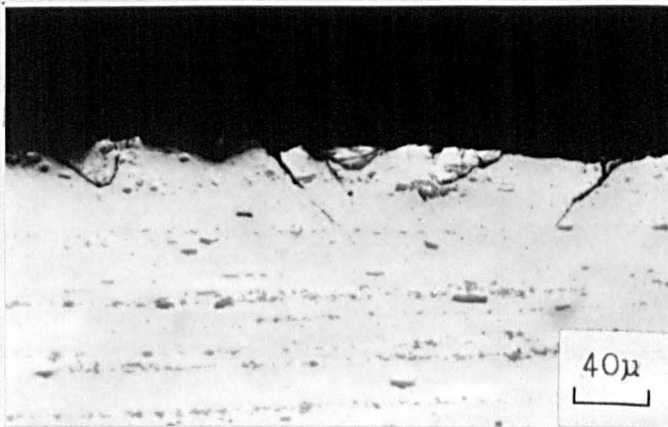
Optical micrographs of fretting fatigue cracks in shot peened (smooth) specimens.



(a) NA specimen after 1.3×10^5 cycles at 300 MPa



(b) as above, but from a different fretting site



(c) AH specimen after 10^7 cycles at 145 MPa.

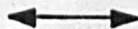
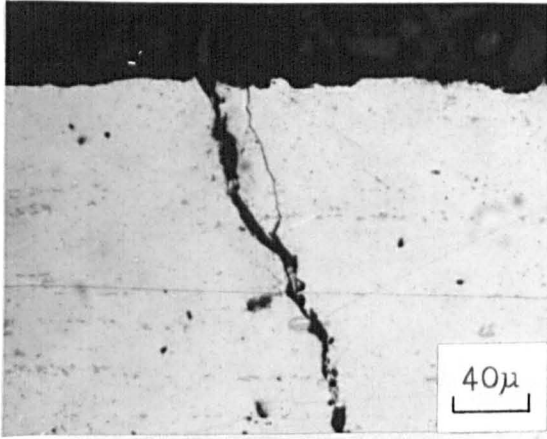
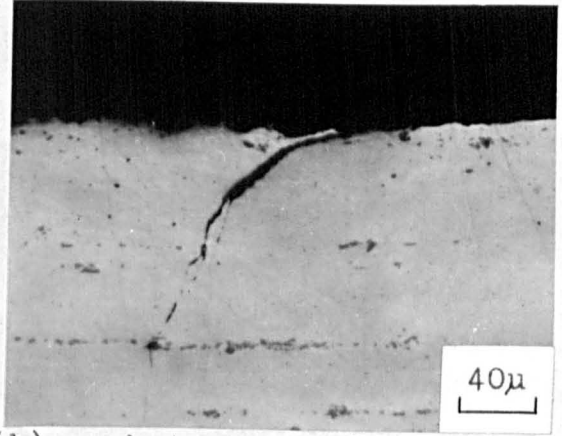


PLATE 8.

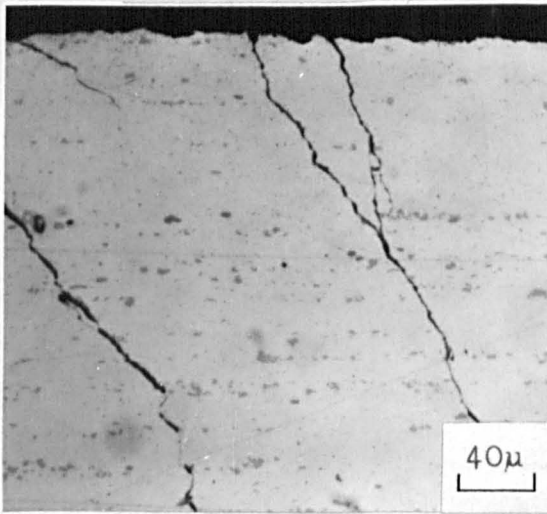
Optical micrographs of fretting fatigue cracks in the AH material.



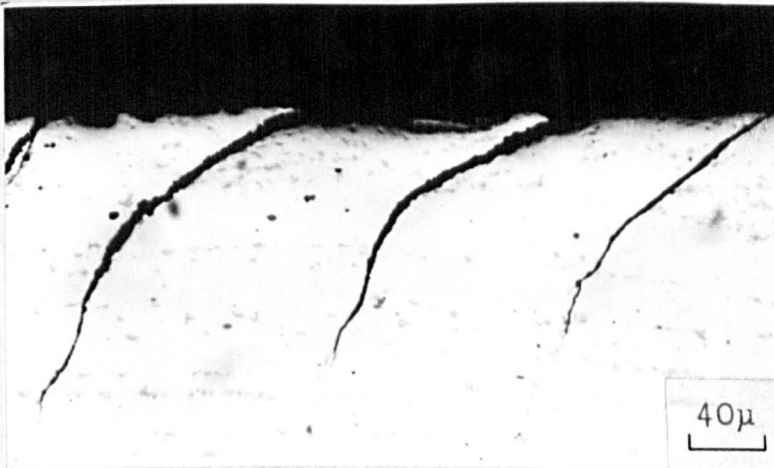
(a) an unpeened specimen
after 1.2×10^5 cycles at
180 MPa



(b) a shot peened (smooth)
specimen after 3.2×10^5
cycles at 190 MPa



(c) multiple cracking in an unpeened specimen
after 9.8×10^4 cycles at 160 MPa

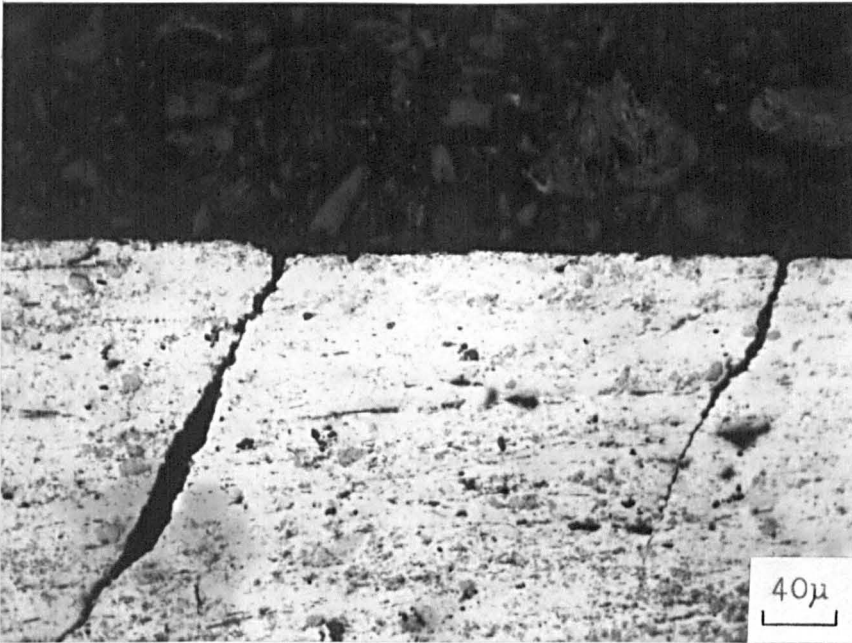


(d) multiple cracking in a shot peened (smooth)
specimen after 2.6×10^5 cycles at 180 MPa.

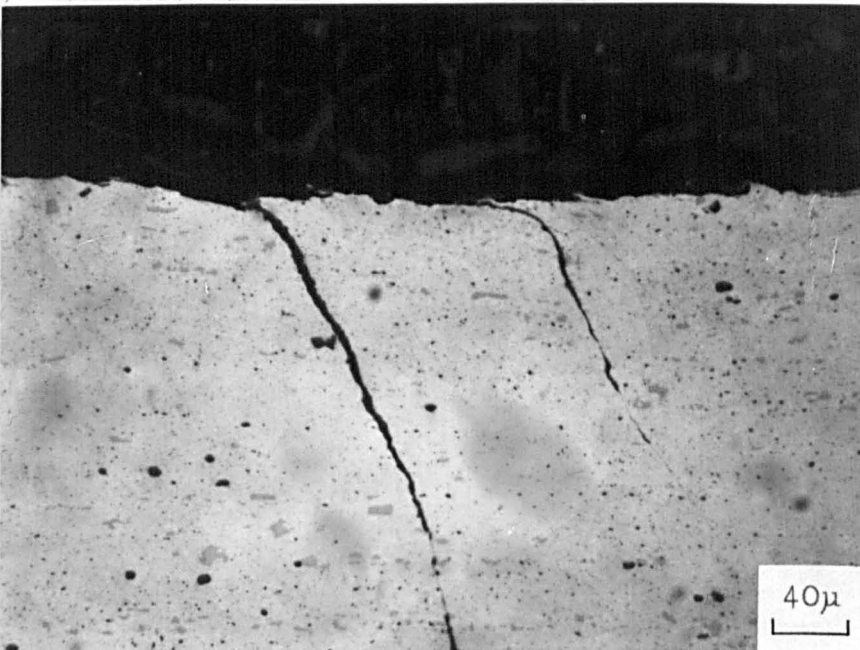


PLATE 9.

Optical micrographs of fretting fatigue cracks in the FA material.



(a) an unpeened specimen after 1.9×10^5 cycles at 90 MPa



(b) a shot peened specimen after 4.5×10^5 cycles at 100 MPa.

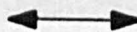
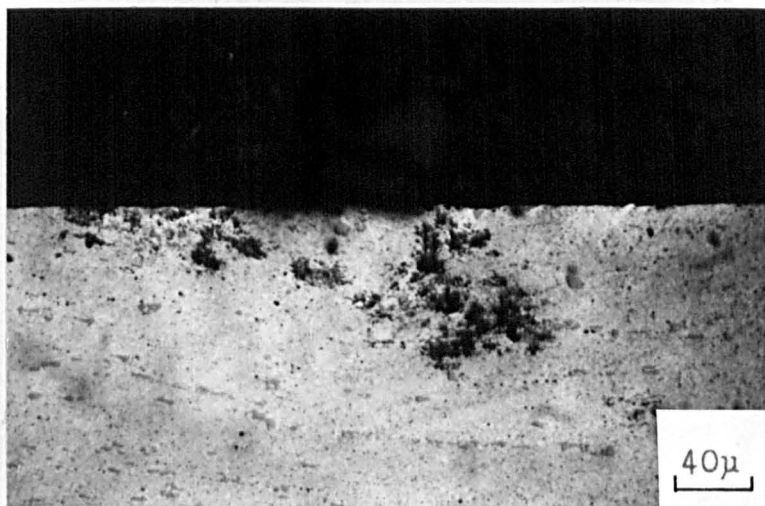
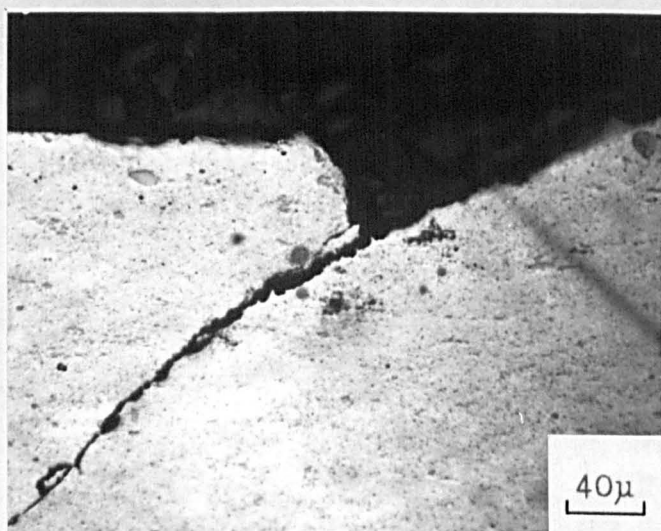


PLATE 10.

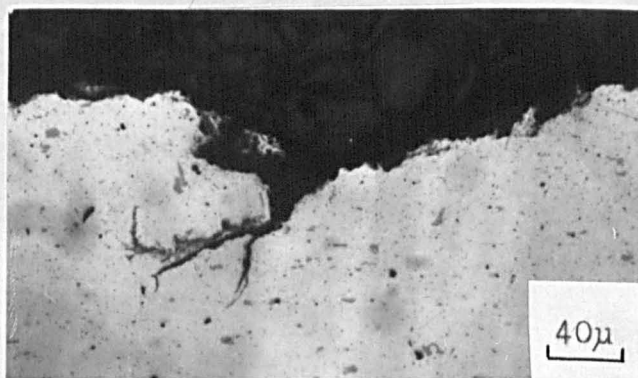
Optical micrographs of damage observed on sections through FA specimens.



(a) subsurface damage due to shot peening



(b) fretting fatigue damage on a shot peened specimen after 2.5×10^4 cycles at 130 MPa



(c) fretting fatigue damage on a shot peened specimen after 5.0×10^4 cycles at 115 MPa.

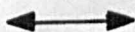
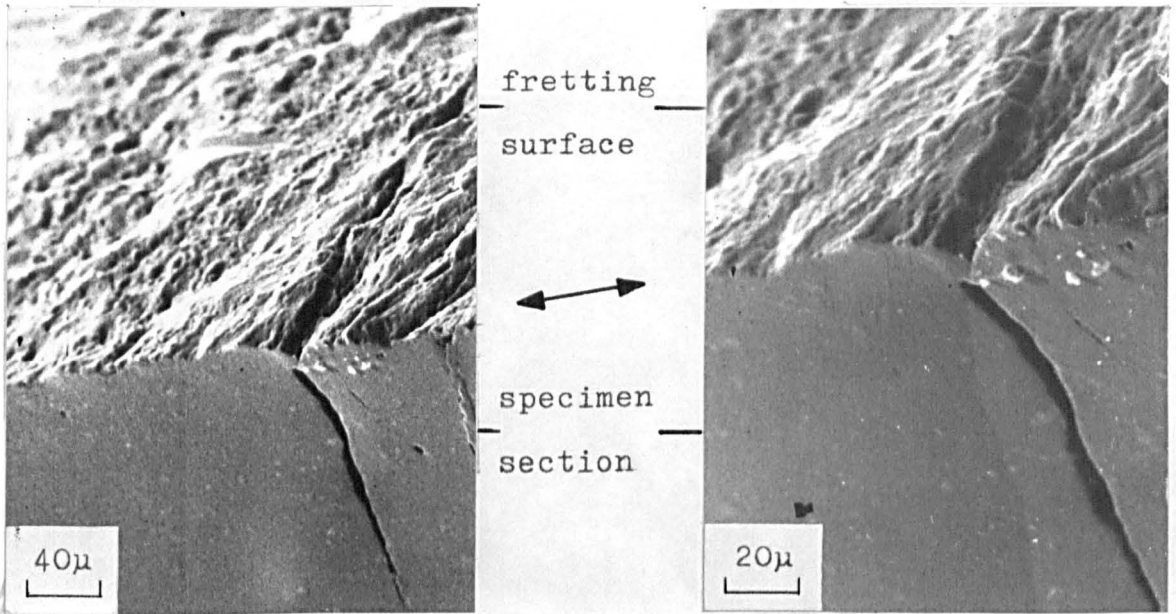


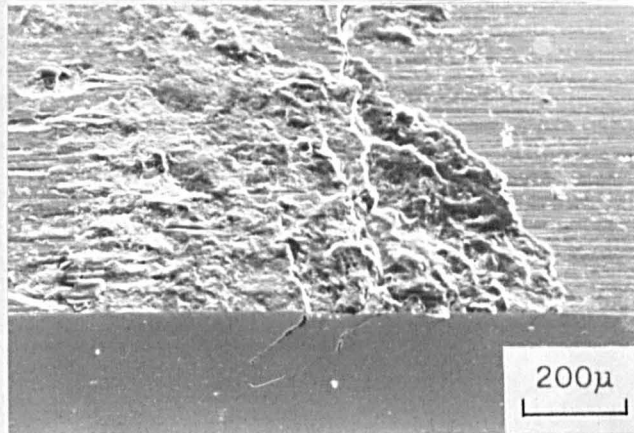
PLATE 11.

Scanning electron micrographs showing fretting fatigue cracks in an unpeened NA specimen; after 1.1×10^6 cycles at 130 MPa.

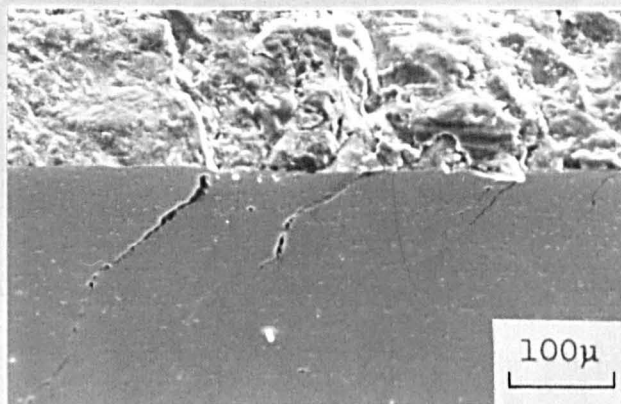


(a) from the central
region of the fretting site

(b) higher magnification
of (a)



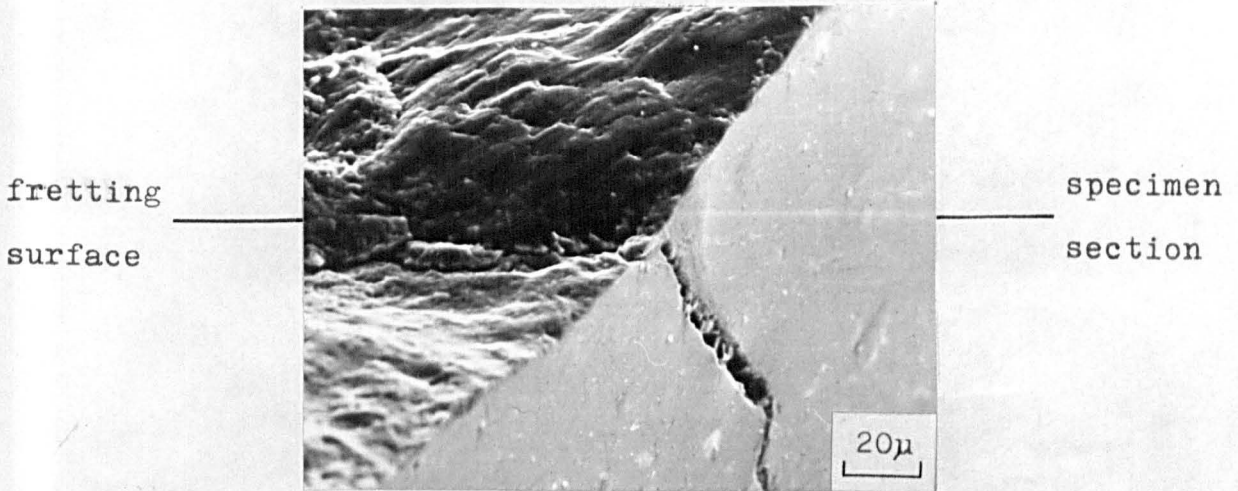
(c) from close to the fretted/non-fretted
boundary



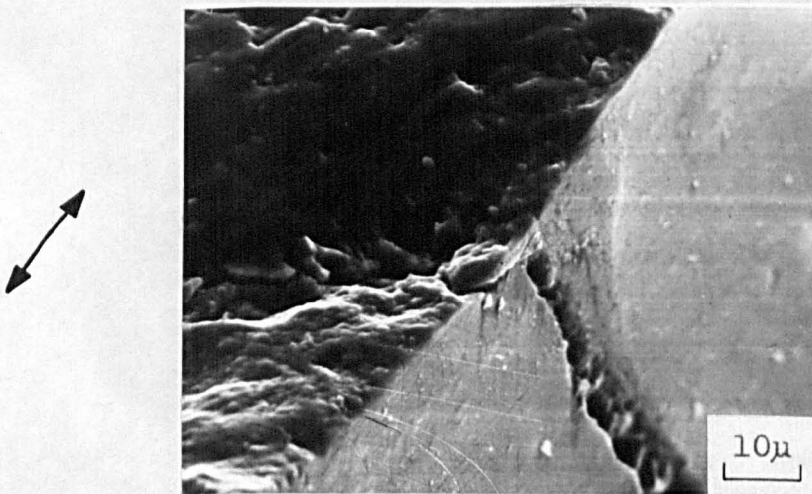
(d) higher magnification of (c).

PLATE 12.

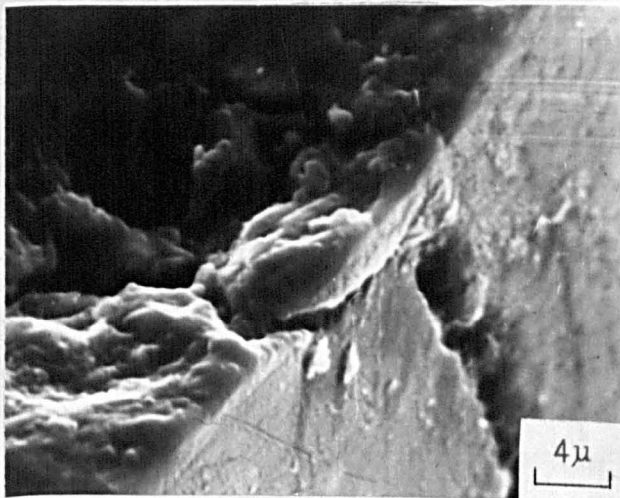
Scanning electron micrographs of a shot peened (smooth) NA specimen showing a fretting fatigue crack at the surface and through the section; after 5.2×10^5 cycles at 220 MPa.



(a) low magnification



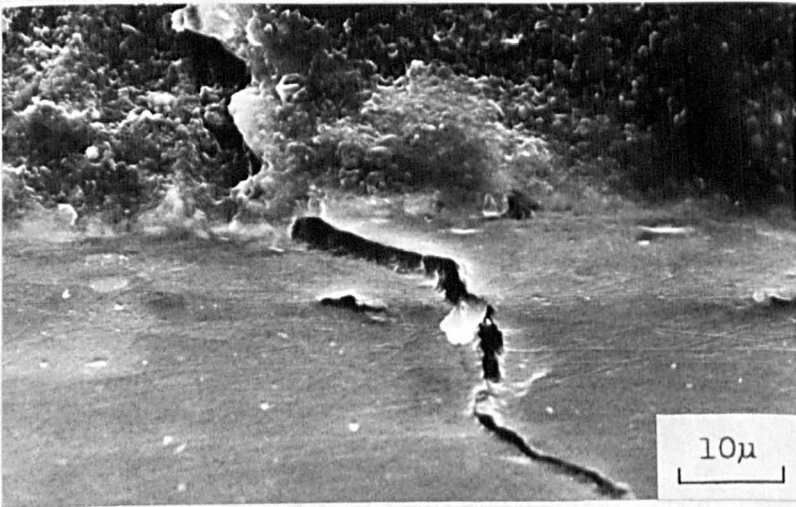
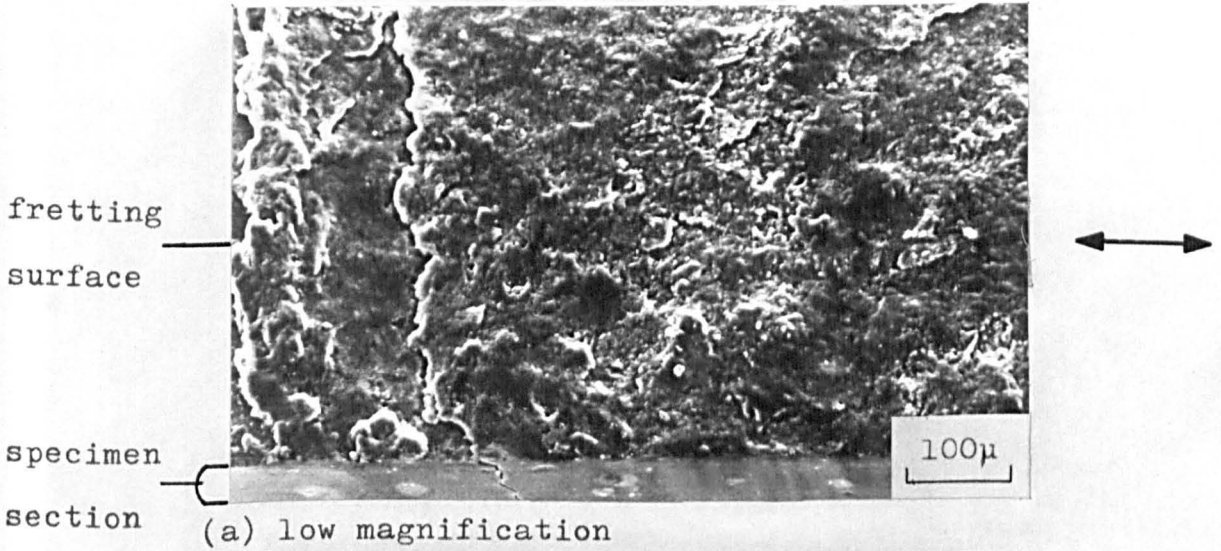
(b) higher magnification of above



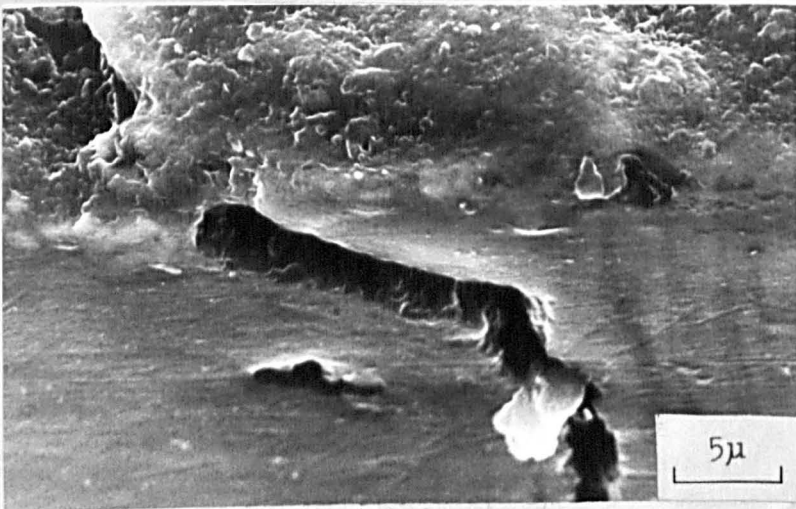
(c) higher magnification of above.

PLATE 13.

Scanning electron micrographs of a shot peened (smooth) AH specimen showing a fretting fatigue crack at the surface and through the section; after 1.3×10^5 cycles at 220 MPa.



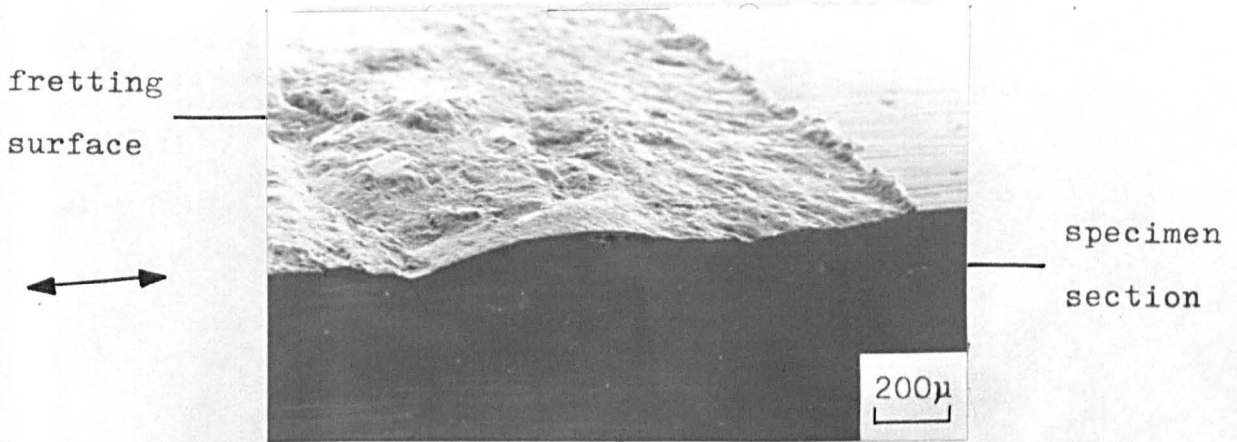
(b) higher magnification of above



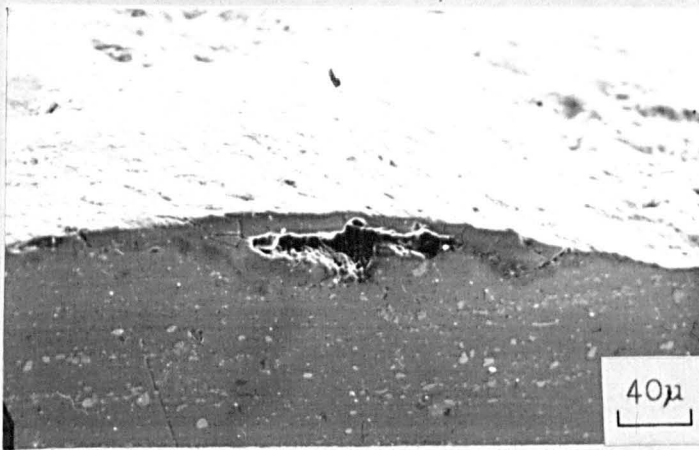
(c) higher magnification of above.

PLATE 14.

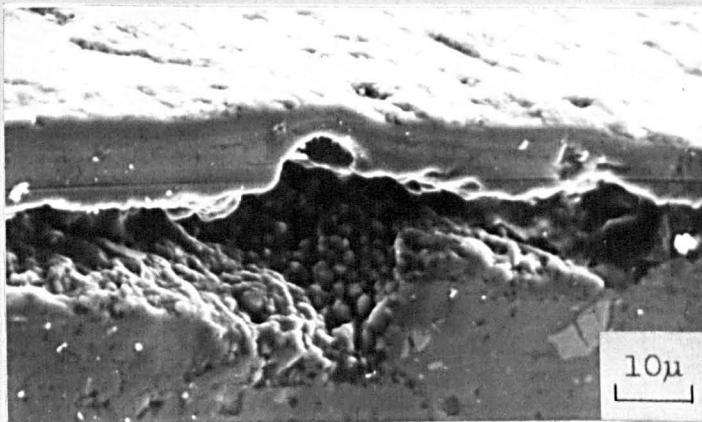
Scanning electron micrographs of the subsurface fretting fatigue damage observed in a shot peened (smooth) NA specimen; after 1.7×10^5 cycles at 260 MPa.



(a) low magnification



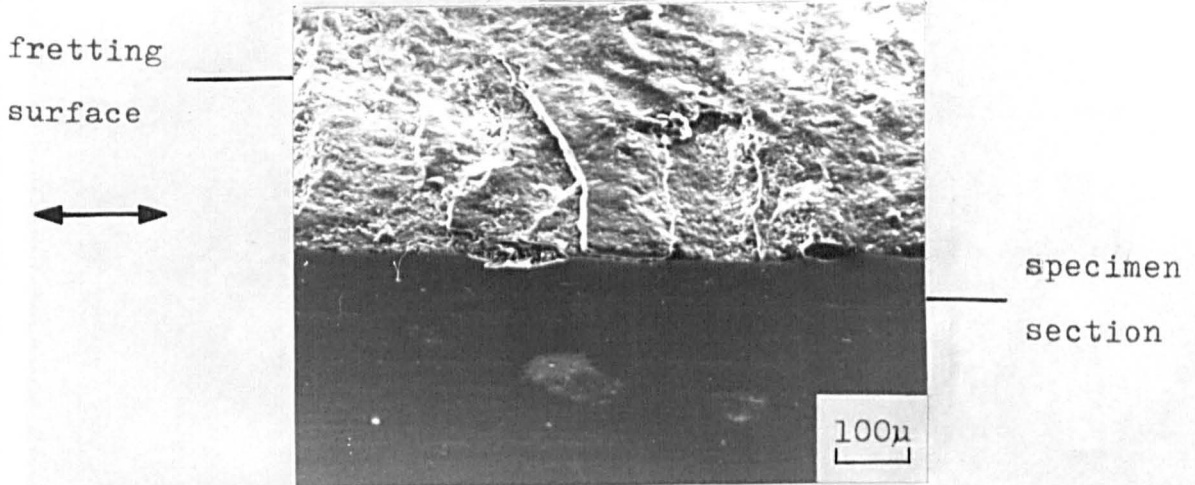
(b) higher magnification of above clearly showing a subsurface cavity



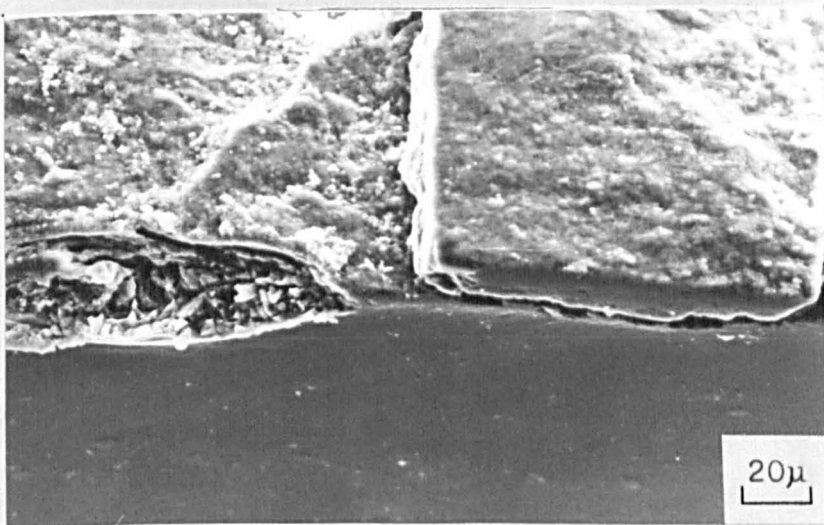
(c) higher magnification of above showing spherical particles within the cavity.

PLATE 15.

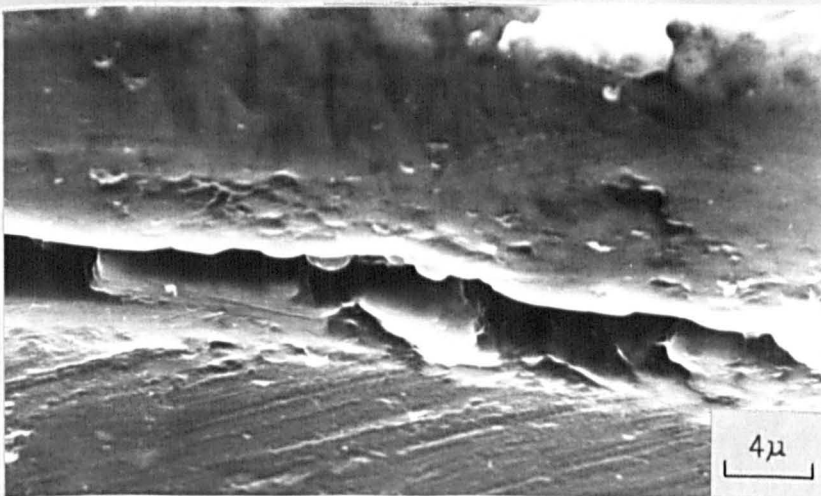
Scanning electron micrographs showing the delamination caused by fretting fatigue on a shot peened (smooth) NA specimen; after 1.5×10^6 cycles at 195 MPa.



(a) low magnification



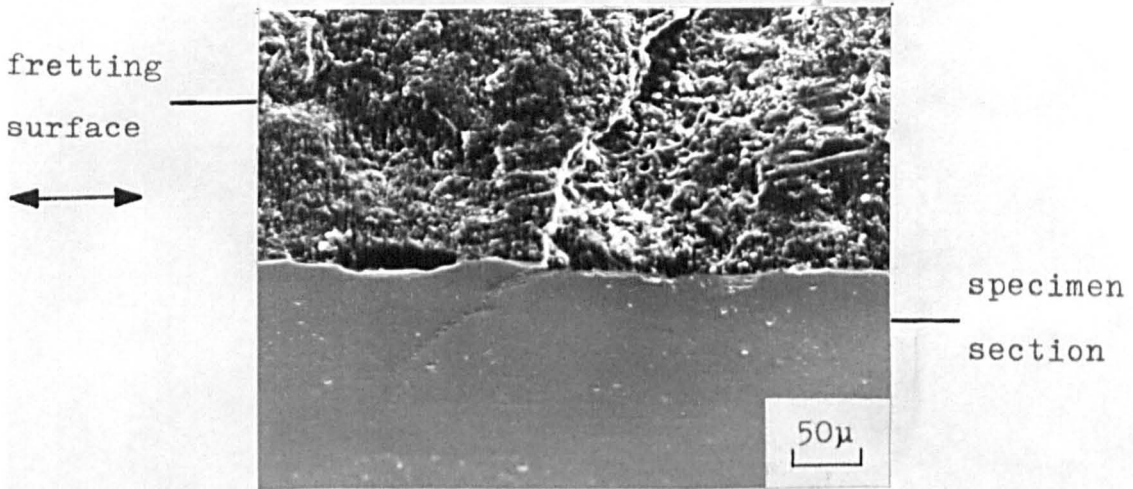
(b) higher magnification of above



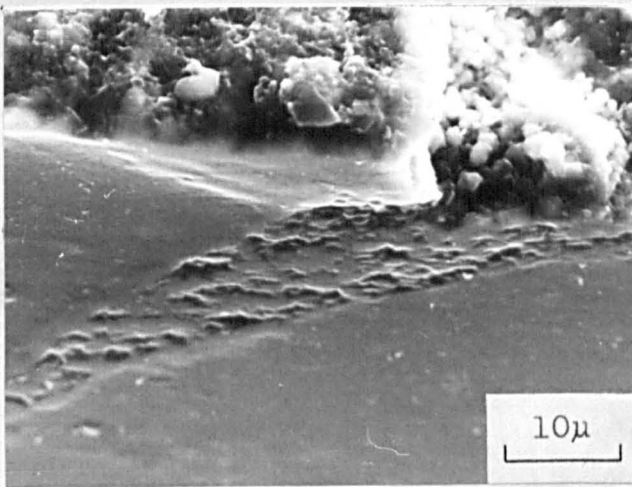
(c) higher magnification of above.

PLATE 16.

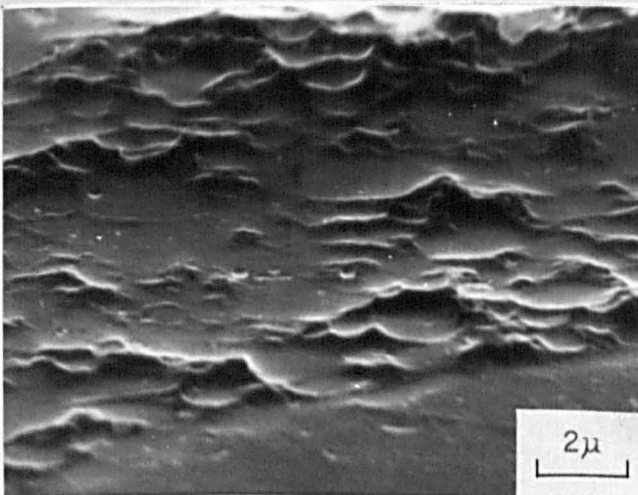
Scanning electron micrographs showing fretting fatigue damage on a shot peened (rough) NA specimen; after 8.4×10^4 cycles at 270 MPa.



(a) low magnification showing a crack



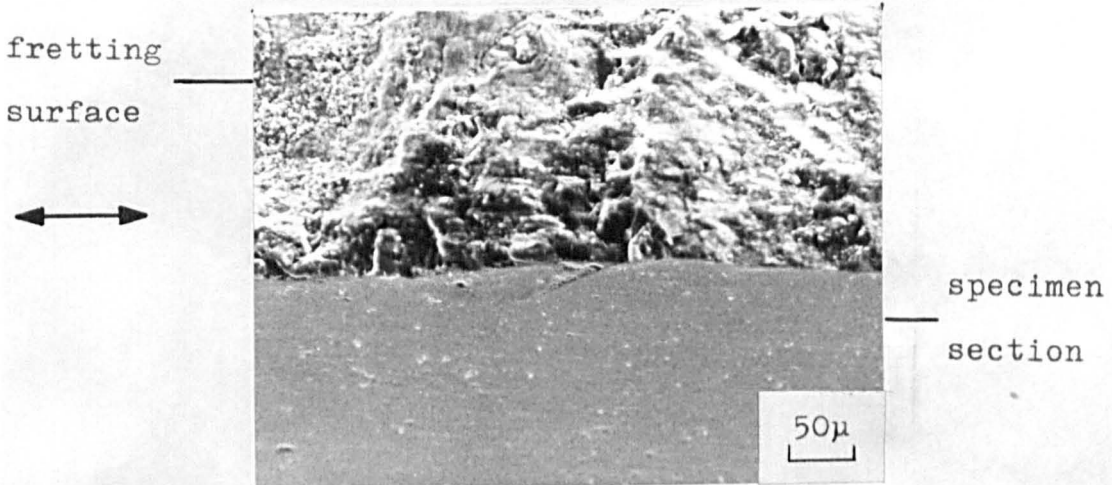
(b) higher magnification of above showing the crack packed with debris



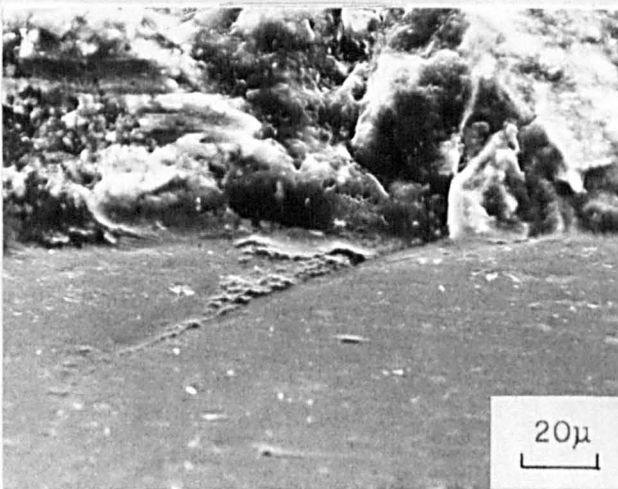
(c) higher magnification of above.

PLATE 17.

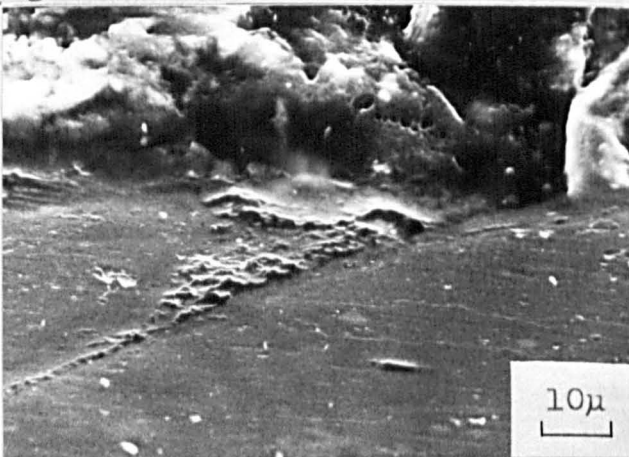
Scanning electron micrographs showing fretting fatigue damage on a shot peened (smooth) NA specimen; after 10^6 cycles at 180 MPa.



(a) low magnification



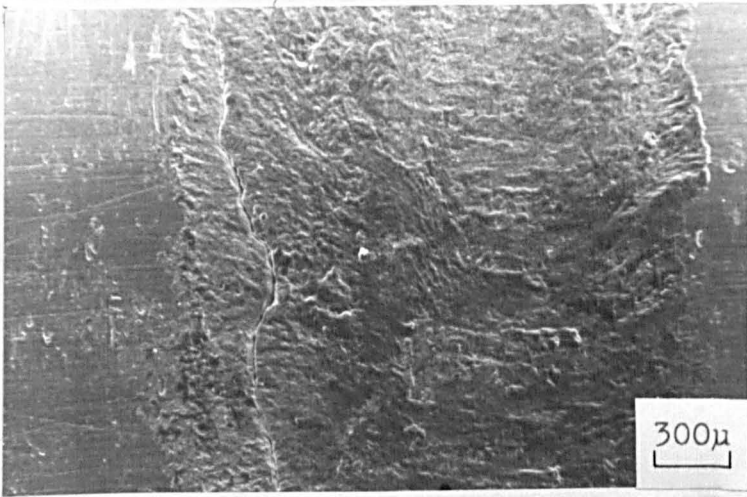
(b) higher magnification of above showing a damaged crack face



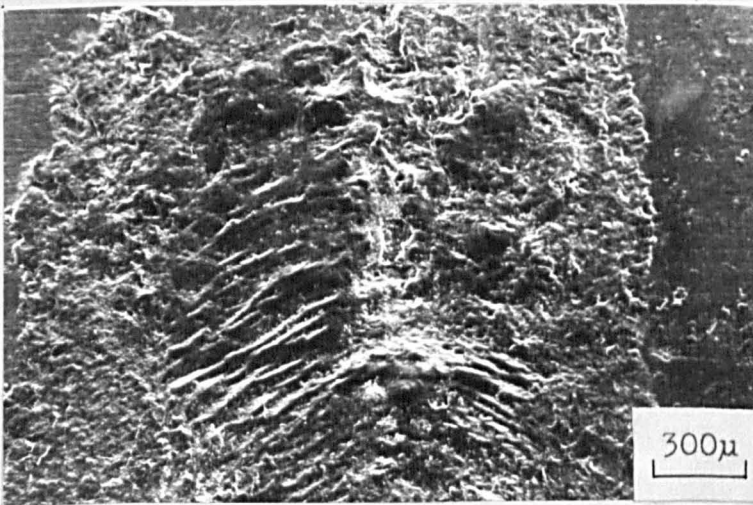
(c) higher magnification of above.

PLATE 18.

Scanning electron micrographs showing
fretting fatigue scars.



(a) from an unpeened NA specimen after 1.4×10^5 cycles at 170 MPa; note the crack near to the fretted/non-fretted boundary

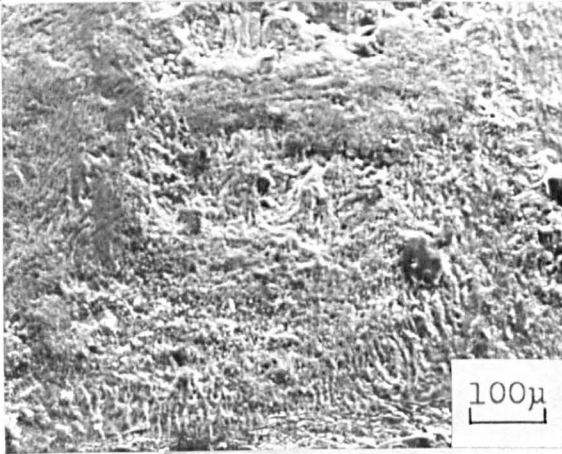


(b) from a shot peened (smooth) AH specimen after 1.3×10^5 cycles at 220 MPa; note the unusual 'fish bone' configuration and areas of delamination.

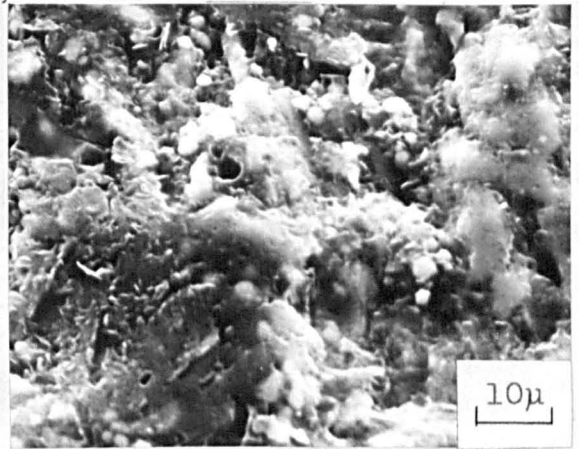


PLATE 19.

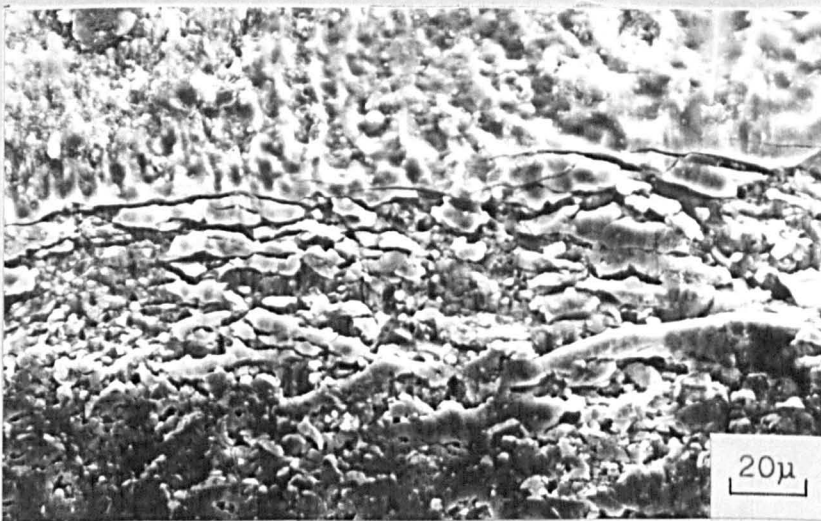
Scanning electron micrographs of the fretting debris on an unpeened NA fretting fatigue specimen after 1.5×10^5 cycles at 205 MPa.



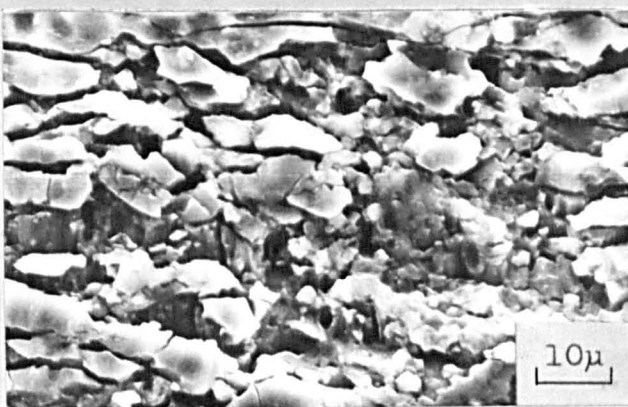
(a) low magnification view of surface distress



(b) higher magnification of (a)



(c) oxide film break-up parallel to the fretting direction



(d) higher magnification of (c).

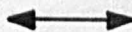
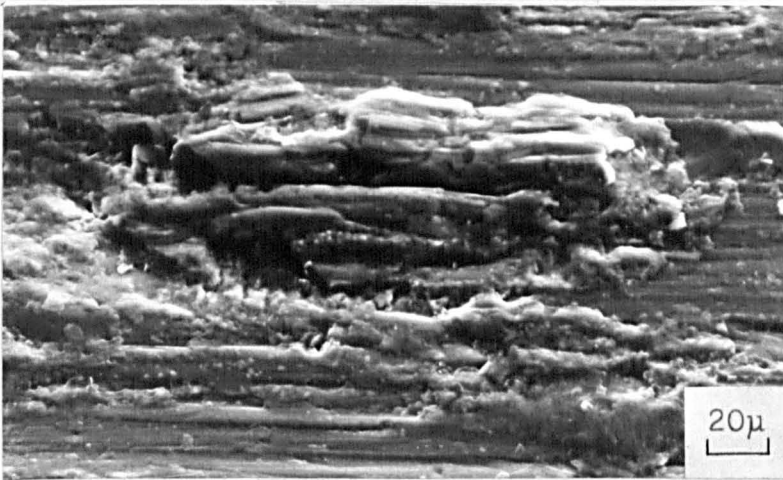
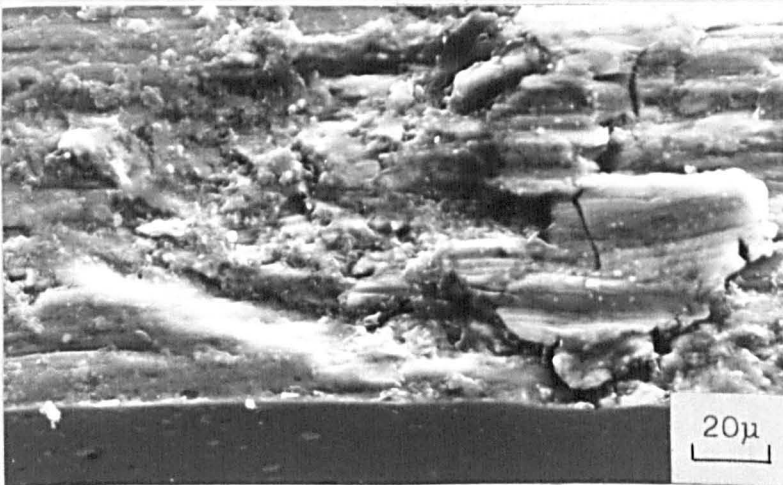


PLATE 20.

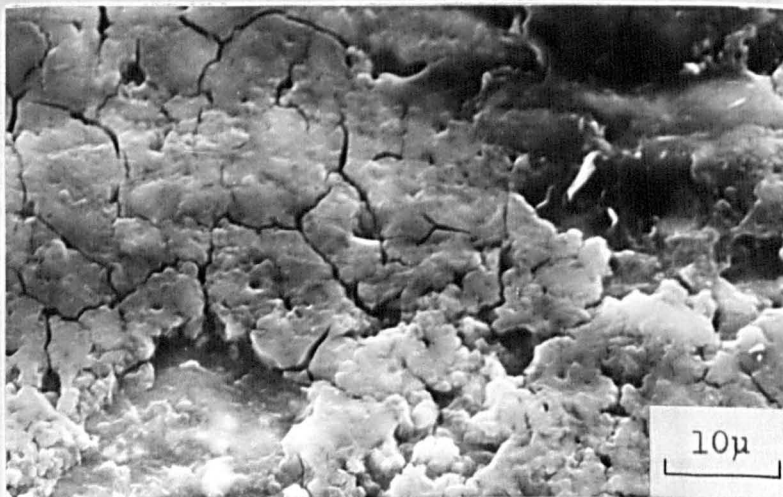
Scanning electron micrographs of the fretting fatigue damage observed on an unpeened NA specimen; after 1.1×10^6 cycles at 130 MPa.



(a) smearing of material along the surface



(b) smearing of material and debris break-up



(c) break-up of the oxide film.

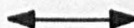
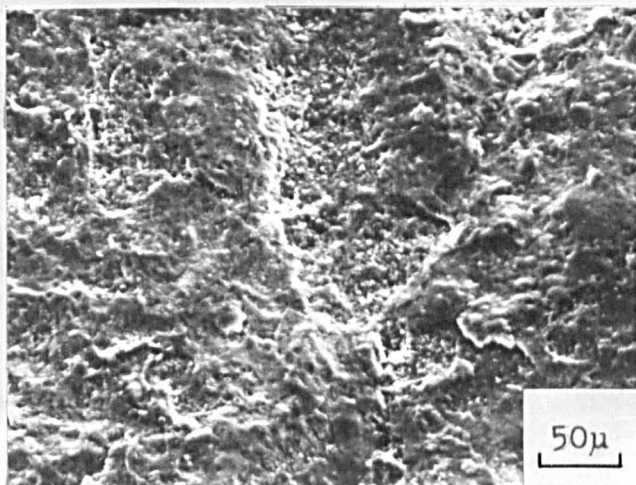
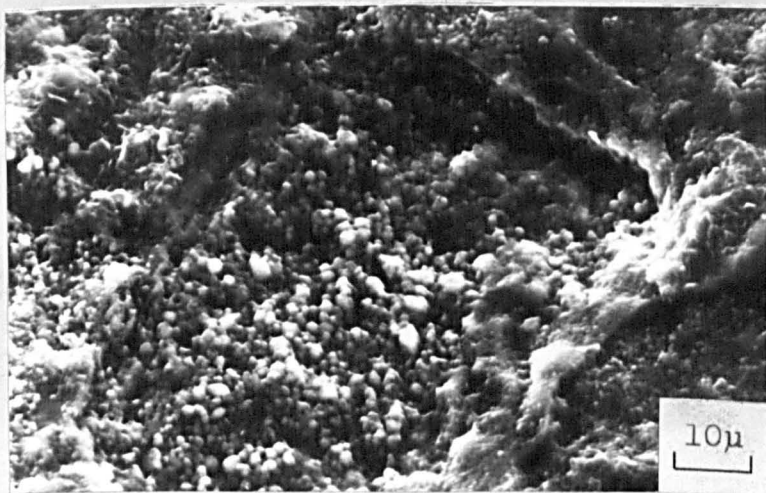


PLATE 21.

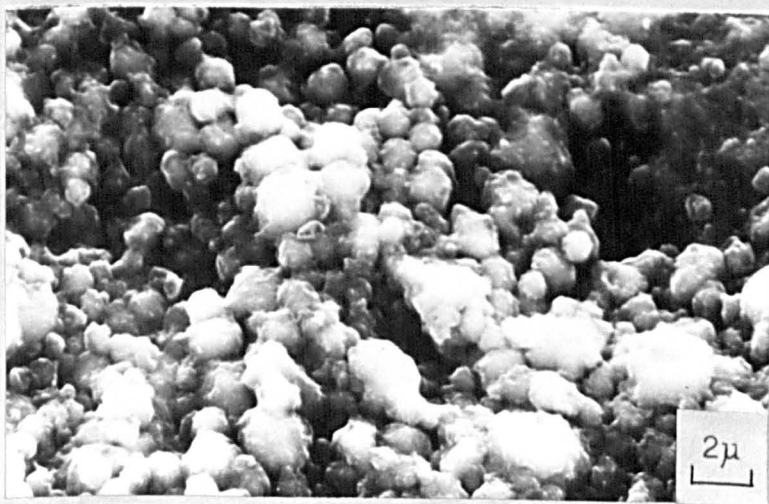
Scanning electron micrographs of the fretting scar damage on a shot peened (rough) NA fretting fatigue specimen; after 1.5×10^6 cycles at 195 MPa.



(a) delamination and exposed cavities



(b) spherical particles within a cavity

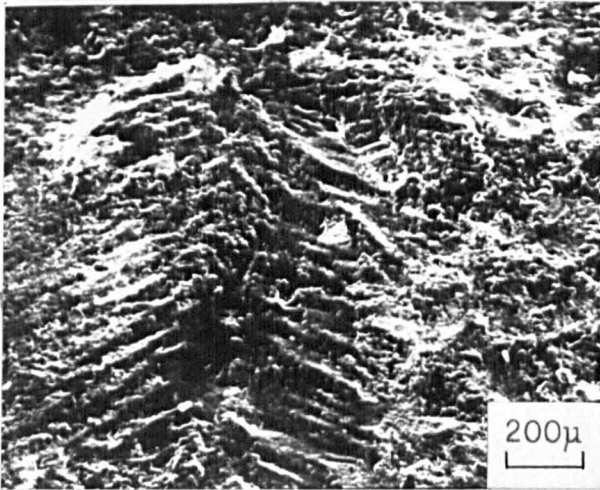


(c) higher magnification of above.

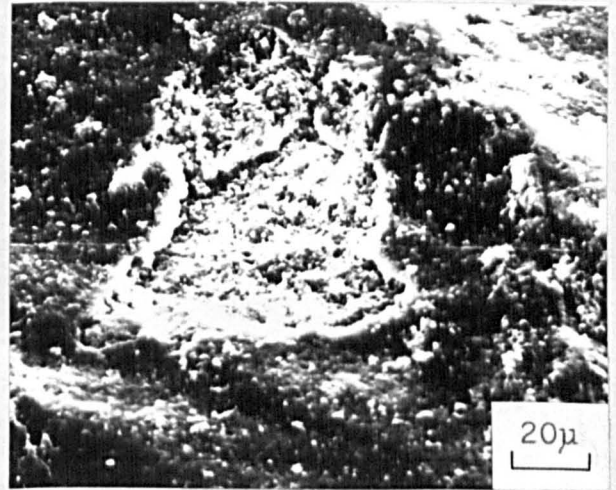


PLATE 22.

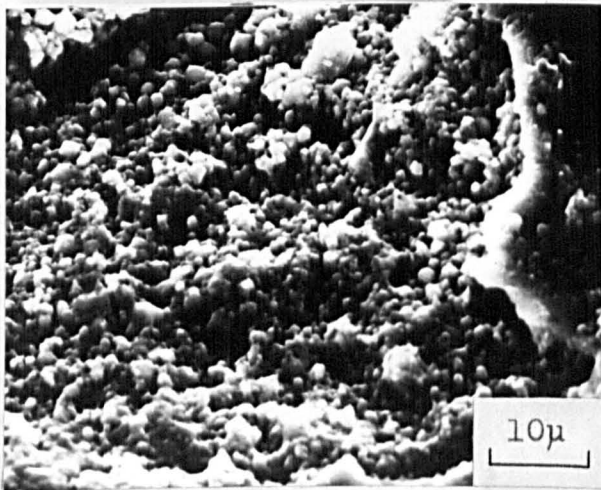
Scanning electron micrographs of the fretting scar damage on a shot peened (rough) NA fretting fatigue specimen; after 1.5×10^6 cycles at 195 MPa.



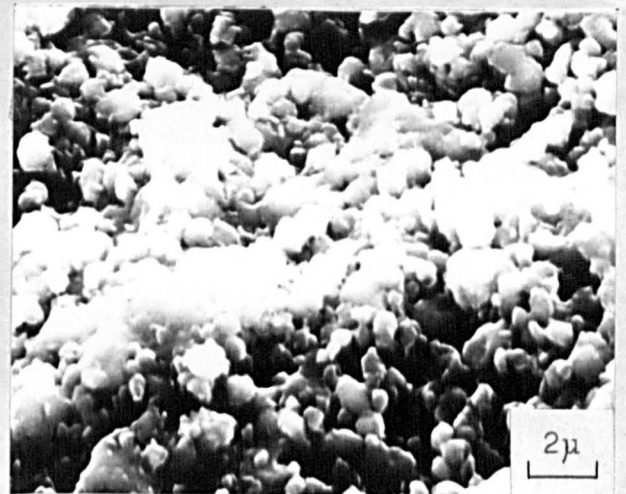
(a) low magnification showing the 'fish bone' configuration



(b) higher magnification of (a) showing an exposed cavity



(c) higher magnification of (b) showing spherical particles in the cavity



(d) higher magnification of (c).

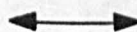
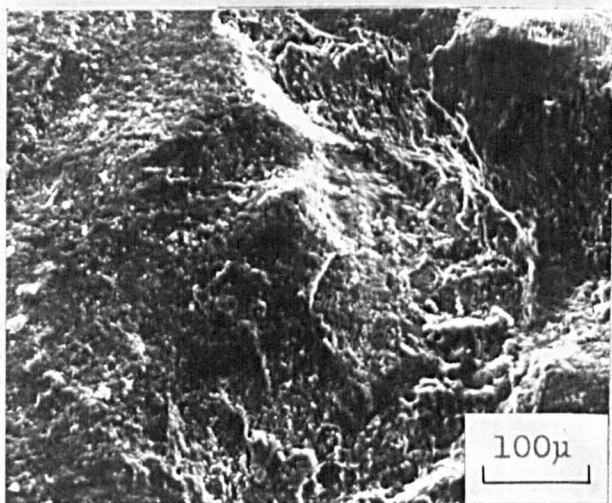
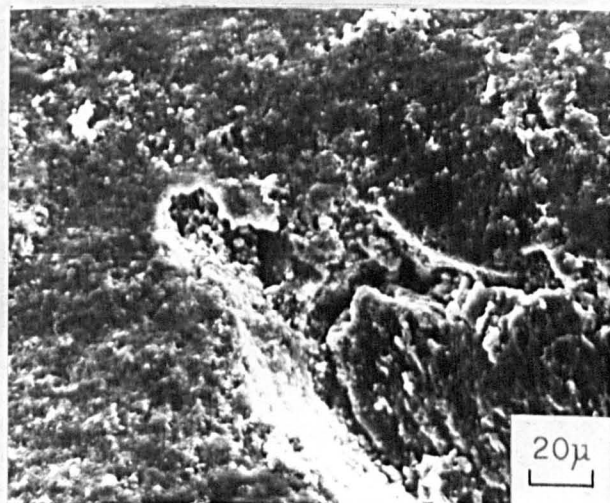


PLATE 23.

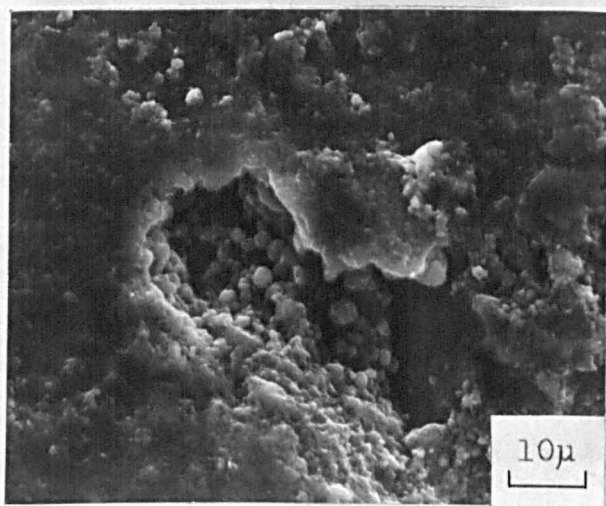
Scanning electron micrographs of the fretting scar damage on a shot peened (smooth) AH fretting fatigue specimen; after 1.3×10^5 cycles at 220 MPa.



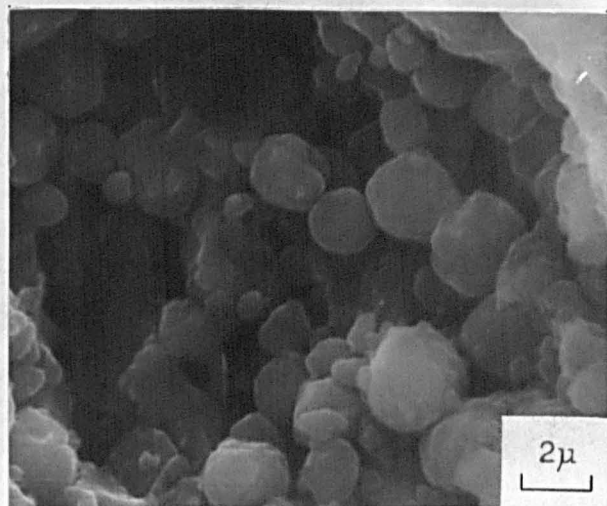
(a) low magnification of the scar showing exposed cavities



(b) higher magnification of one of the cavities shown in (a)



(c) higher magnification of (b) showing spherical particles within the cavity

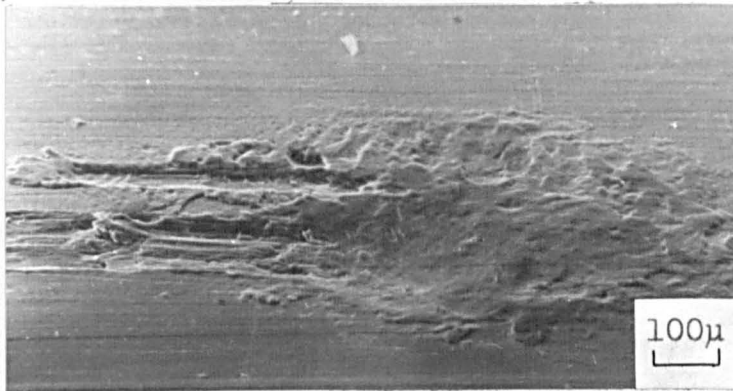


(d) higher magnification of (c).

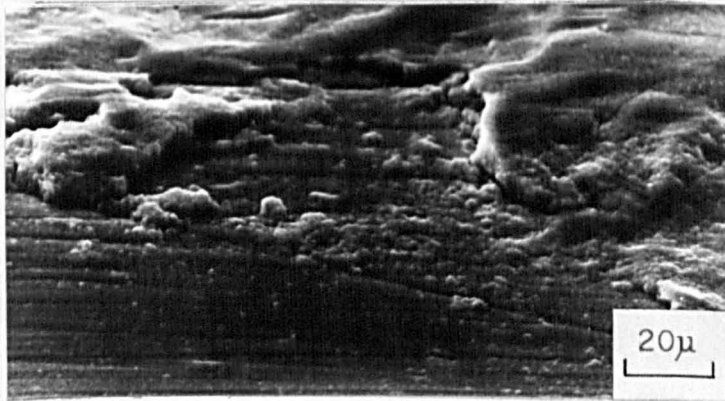


PLATE 24.

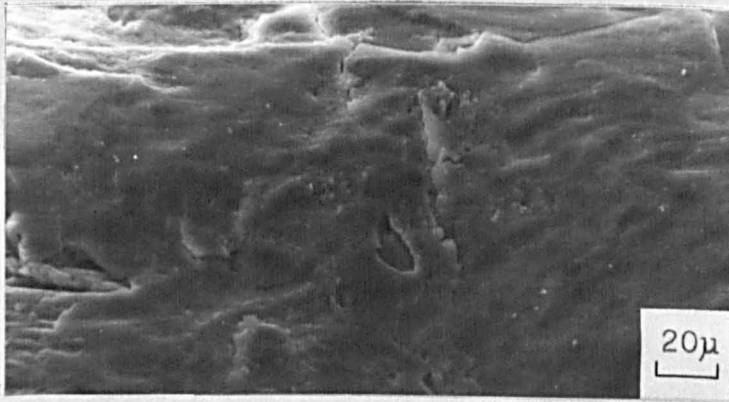
Scanning electron micrographs of the plain
fretting damage on an unpeened NA specimen.



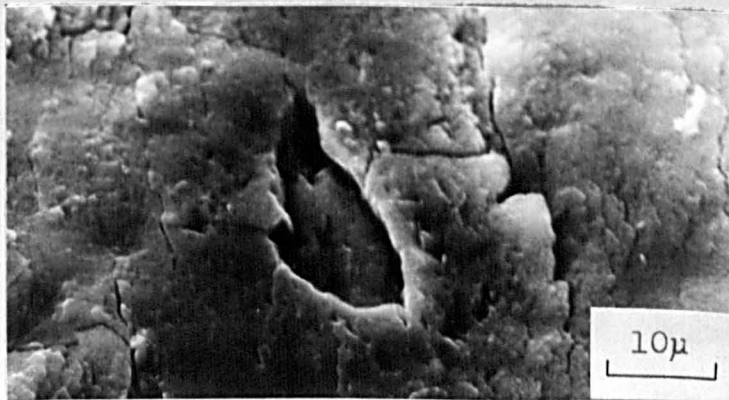
(a) wide view of the fretting scar



(b) material smeared at the edge of the scar



(c) exposed cavity in the centre of the scar

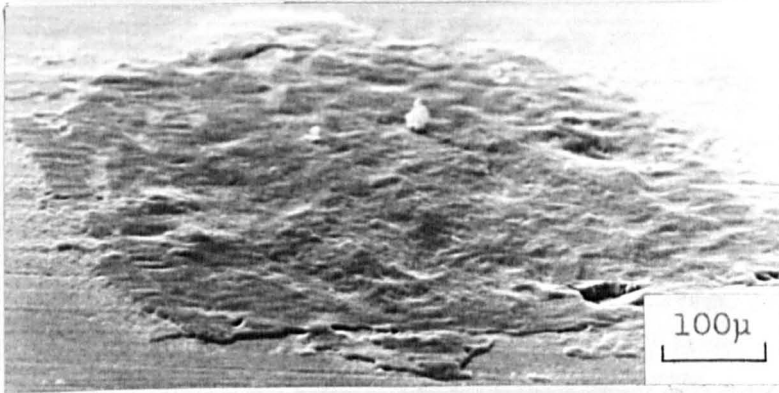


(d) exposed cavity; note the absence of
spherical particles.

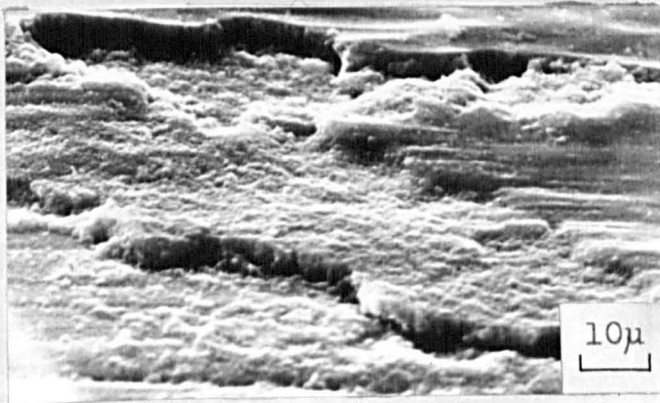


PLATE 25.

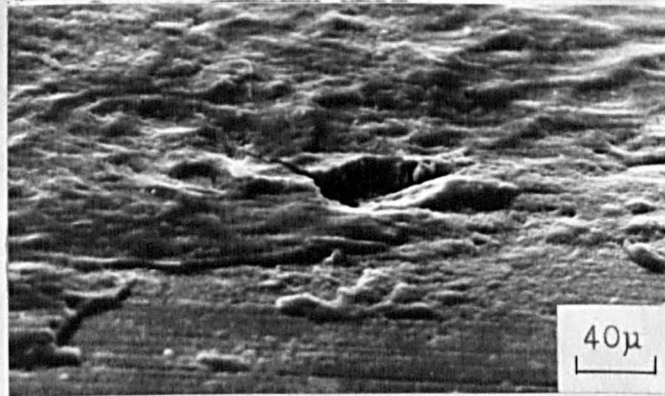
Scanning electron micrographs of the plain
fretting damage on an unpeened AH specimen.



(a) wide view of the fretting scar



(b) material smeared at the edge of the scar



(c) exposed cavity at the edge of the scar



(d) exposed cavity; note again the absence
of spherical particles.

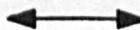
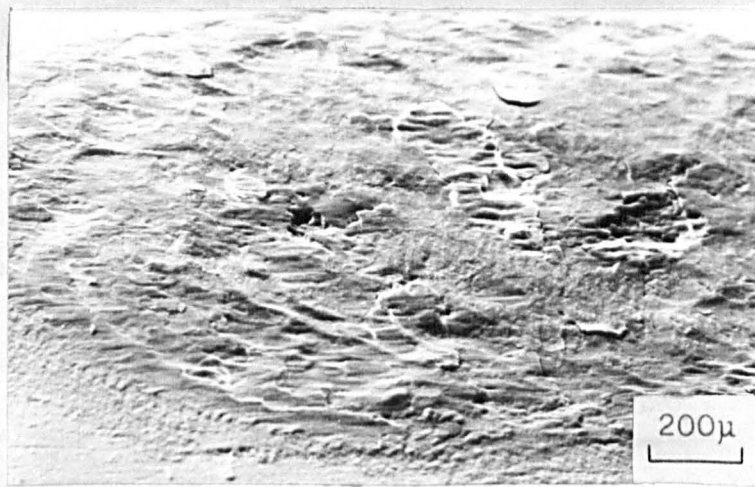
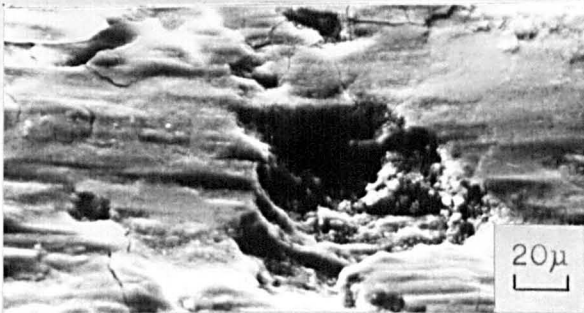


PLATE 26.

Scanning electron micrographs of the plain
fretting damage on a shot peened (smooth)
NA specimen.



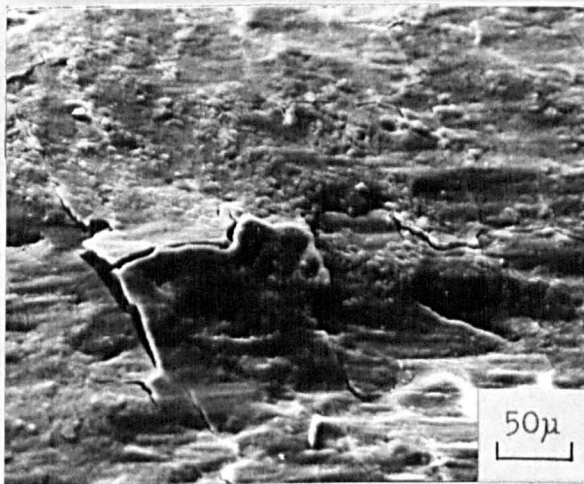
(a) wide view of the fretting scar showing
areas of delamination and exposed cavities



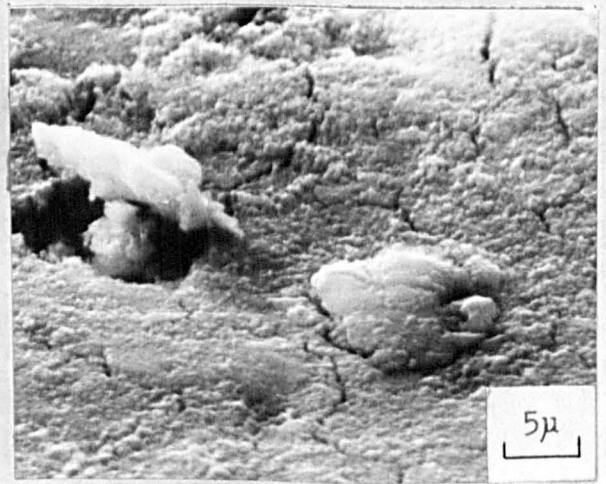
(b) higher magnification of
one of the cavities shown in
(a)



(c) higher magnification
of (b) showing spherical
particles within the cavity



(d) higher magnification of
one of the areas of delamination film.
shown in (a)



(e) break-up of the oxide

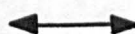
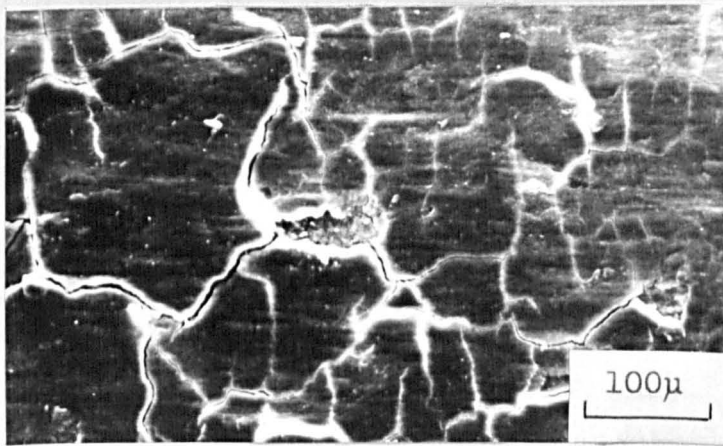
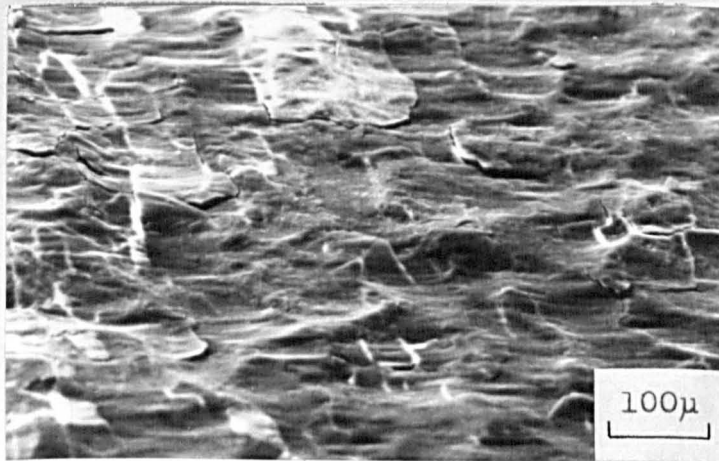


PLATE 27.

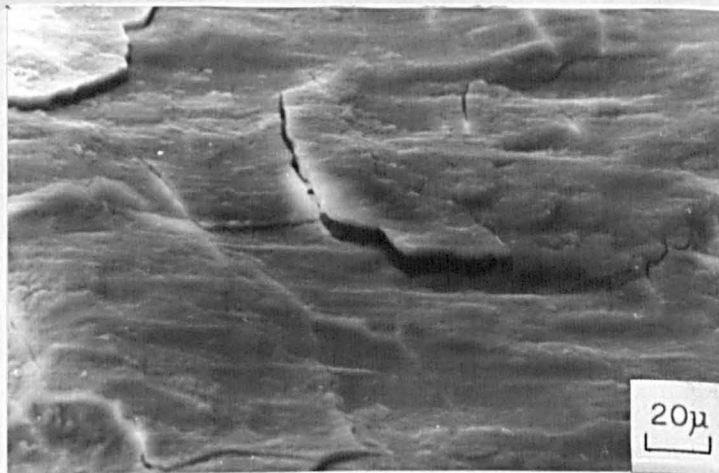
Scanning electron micrographs of the plain
fretting damage on a shot peened (smooth)
AH specimen.



(a) wide view of the scar showing extensive
delamination



(b) oblique view clearly showing the
delaminated plates

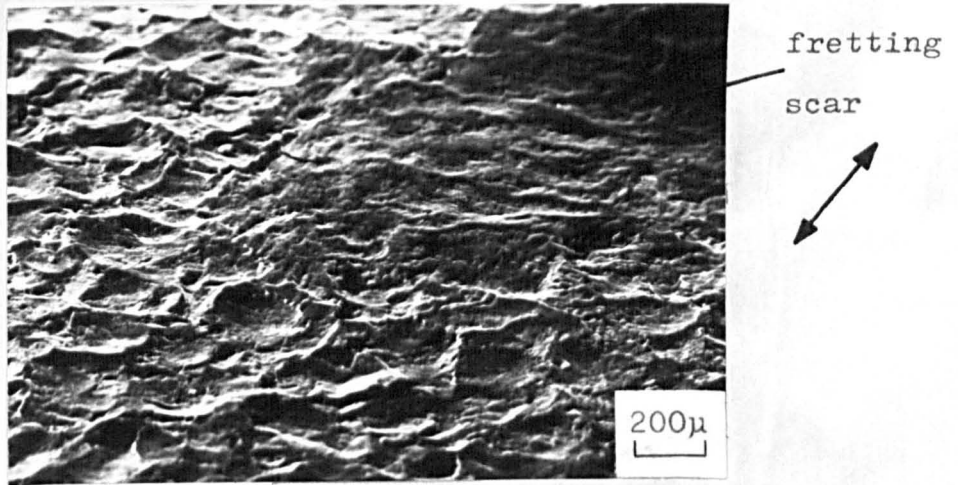


(c) higher magnification of above.

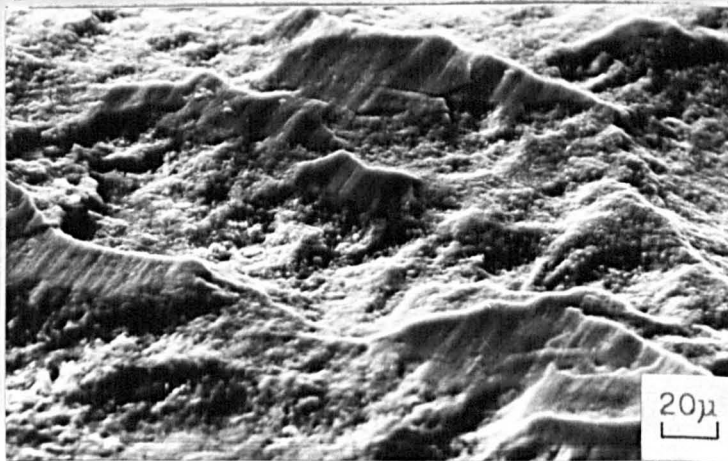


PLATE 28.

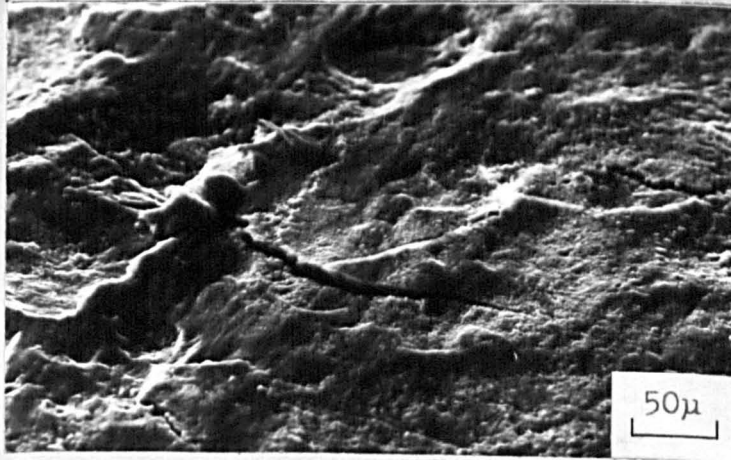
Scanning electron micrographs of the plain
fretting damage on a shot peened (rough)
NA specimen.



(a) wide view showing the levelling of the
dimples



(b) higher magnification of the levelled
dimples



(c) delamination on the levelled areas.